X-590-73-251
PREPRINT

NASA TM X- 70670

GRAVIMETRIC GEODESY AND SEA SURFACE TOPOGRAPHY STUDIES BY MEANS OF SATELLITE-TO-SATELLITE TRACKING AND SATELLITE ALTIMETRY

JOSEPH W. SIRY

AUGUST 1972

GSFC
GODDARD SPACE FLIGHT CENTER
GREENBELT, MARYLAND

Presented at the 9th International Symposium on Geophysical Theory and Computers Sponsored by the Committee for Mathematical Geophysics of the International Union of Geodesy and Geophysics . . . Banff, Canada . . . August, 1972

For information concerning availability
of this document contact:

Technical Information Division, Code 250
Goddard Space Flight Center
Greenbelt, Maryland 20771

(Telephone 301-982-4488)

X-550-73-19

GRAVIMETRIC GEODESY AND SEA SURFACE TOPOGRAPHY STUDIES BY MEANS OF SATELLITE-TO-SATELLITE TRACKING AND SATELLITE ALTIMETRY*

Joseph W. Siry

August 1972

*Presented at the 9th International Symposium on Geophysical Theory and Computers sponsored by the Committee for Mathematical Geophysics of the International Union of Geodesy and Geophysics, Banff, Canada, August, 1972.

GODDARD SPACE FLIGHT CENTER

Greenbelt, Maryland

GRAVIMETRIC GEODESY AND SEA SURFACE TOPOGRAPHY STUDIES BY MEANS OF SATELLITE-TO-SATELLITE TRACKING AND SATELLITE ALTIMETRY

Joseph W. Siry

ABSTRACT

The present knowledge of the earth's gravitational field is based upon a combination of satellite data and surface gravimetry. Satellite solutions employing precise optical observations and Doppler data have been obtained by a number of investigators over the past several years. More recently, surface gravimetric data have been added to the solutions. Fields complete to degree and order 16 have been obtained in this way. It is estimated that the satellite data contribute significantly to about degree and order 10. This corresponds to a half wave length of 18°, or about 2000 km. The uncertainty in the geoid height which is associated with the satellite contribution to this field is estimated to be on the order of 10 meters. This corresponds to an acceleration resolution of about 2-1/2 milligals.

It is planned to conduct a satellite-to-satellite tracking experiment between ATS-F and GEOS-C with a range accuracy of 2 meters and a range rate accuracy of 0.035 centimeters per second for a ten-second integration time. This experiment is now planned for 1974. It is anticipated that it will improve the spatial resolution of the satellite geoid by half an order of magnitude to about 6°. Longer

integration times should also permit a modest increase in the acceleration resolution to about a couple of milligals.

Satellite altimeter data will also be obtained by means of GEOS-C. An overall accuracy of five meters in altitude is the goal. The altimeter, per se, is expected to have an instrumental precision of about 2 meters, and an additional capability to observe with a precision of about 0.2 meters for limited periods. The ability to interpret such measurements in terms of the sea surface topography and the gravity field is dependent upon the ability to represent the satellite's motion in altitude, to analyze the altimeter signal return in terms of sea state, and to model appropriately the departures of the sea level surface from the geoid due to tides, currents, the general circulation of the oceans, and atmospheric effects. Lasers with accuracies of about a decimeter are expected to be available in time to track GEOS-C. Three such lasers located at sites such as Antigua, Key West and the Canal Zone, for example, could yield satellite altitude determination uncertainties of the order of a meter over most of the triangular region defined by these locations. It is estimated that satellite-to-satellite tracking can be used to extend the coverage over distances of oceanic scale with altitude uncertainties of less than 5 meters. Departures of the ocean surface from the geoid of up to one or two meters can be expected. Uncertainties associated with these increments are usually less than a meter over wide areas of the ocean. New information about the gravity field and the geoid with uncertainties in the range of a few meters should accordingly be derivable from the

GEOS-C altimeter data. This will represent an improvement in accuracy of a factor of two or so over many regions of the earth's surface.

The detailed analysis of the satellite-to-satellite tracking and satellite altimeter data will involve the simultaneous use of detailed mathematical models of the earth's gravitational field and figure, the tides, current systems such as the Gulf Stream, the general circulation of the oceans and, ultimately, factors associated with the ocean-atmosphere interface. Detailed analysis of the structure and evolution of a tsunami will also involve ray tracing and modelling of the ocean's wave propagation characteristics and bottom topography. The development of mathematical models for geophysics promises to increase markedly in complexity as the satellite Earth Physics Program unfolds.

CONTENTS

CONTENTS (Continued)

CONTENTS (Continued)

CONTENTS (Continued)

GRAVIMETRIC GEODESY AND SEA SURFACE TOPOGRAPHY STUDIES BY MEANS OF SATELLITE-TO-SATELLITE TRACKING AND SATELLITE ALTIMETRY

I. INTRODUCTION

The study of the earth's gravitational field by means of data from satellite-to-satellite tracking and satellite altimeter systems will take place in the context of the current knowledge of the subject. The consideration of these fundamentally new types of data will accordingly begin with a discussion of techniques which are already in use for probing the geopotential. The special nature of the approaches offered by the new tracking capabilities will be the more clear as they are contrasted with the older, more conventional methods.

The capability for studying sea surface topography opened up by the satellite altimeter is a two-edged one. The sea surface topography can be identified with the geoid, to within uncertainties associated with oceanographic effects and, conversely, it can be viewed in terms of features of interest to the oceanographer, to within the errors associated with the gravity field representation.

The actual positions of the sea surfaces are affected by a number of oceanographic factors including, in addition to the geoid, the tides, the general circulation, currents and their meanders, sea-state, winds, storm surges and tsunamis. Hence, for example, in order to conduct the gravimetric investigations

properly, it is necessary to represent these oceanographic effects on the sea surface heights appropriately. Similarly, existing knowledge of the gravity field will play an important role in the investigation of oceanographic effects. Thus, gravimetric and oceanographic investigations relying upon altimeter data are interrelated. This point is discussed further later.

The following discussion deals, in particular, with the potential contributions of the altimeter and satellite-to-satellite tracking systems associated with the GEOS-C spacecraft which is scheduled to be launched in mid-1974. The discussion begins, actually, with consideration of studies which are either ongoing or getting underway and which should be completed by the time the data begin to flow from GEOS-C. These analyses will involve the use of the additional satellite tracking data, including especially the laser data, which will become available in the intervening years. This aspect of the investigation will involve the simultaneous determination of gravimetric quantities and other environmental parameters which contribute to the observational residuals. The aims of this part of the investigation will accordingly include the determination of tracking station locations, quantities such as the earth's radius, and coefficients representing atmospheric drag and radiation pressure effects. Consideration is being given, too, to the possibility of equipping other spacecraft with the capability for satellite-to-satellite tracking through ATS-F. The potential contributions of such capabilities to the gravimetric geodesy investigations are also discussed. (1-4).

II. THE EXPLOITATION OF EXISTING DATA IN PREPARATION FOR THE ANALYSIS OF ALTIMETER AND SATELLITE-TO-SATELLITE TRACKING DATA FROM GEOS-C

A. General Considerations

The basic strategy is to derive the greatest benefit from the altimeter and satellite-to-satellite tracking data from GEOS-C by analyzing it together with all of the related data which can contribute to the determination of the earth's gravitational field. The determination of the characteristics of the gravitational field will be based upon the existing stores of geodetic data as well as the additional observational material which will become available in time for use in the analyses of the new types of data to be furnished by GEOS-C. The fundamental body of data upon which our current knowledge of the gravitational field is based consists of over a hundred thousand precisely reduced optical observations of some two dozen satellites, more than a hundred thousand electronic observations including both Doppler measures and range and range rate data, the beginnings of a supply of laser range measurements, as well as the gravimetric and survey results of classical geodesy. It is anticipated that, by the time the analysis of the new data types from GEOS-C commences, this store will be enriched through the addition of considerable numbers of laser observations obtained in programs following the ISAGEX campaign such as the San Andreas Fault Experiment (SAFE).

It is contemplated that the interpretation of these collections of data will involve general determinations of the gravitational field, resonance determinations

of geopotential coefficients, and studies involving representations in terms of mass anomalies.

Recent activity in the field of geopotential analysis at several institutions including Goddard is indicated in Tables I and II and discussed in references 28 and 29 which include bibliographies. Results of comparisons of some of the geopotential models listed in Tables I and II are indicated in Table III and in Figure 1. These findings give some idea of the effective accuracies associated with some of the models. Improvements obtained by the modeling of resonant terms are also seen in Table III.

Table I

General Determinations of Geopotential Coefficients

Author or Designation	Year	Reference Number	Basis			Field Characteristics	
			Satellite Data		Other Information		
			Number of Satellites	Tracking Systems		Last term in Complete Portion	Number of Coefficients
1. NWL 5E-6	1965	1	3	Doppler		7, 6	64
2. APL 3.5	1965	2	5	Doppler		8, 8	84
3. SAO M-1	1966	3	16	Optical		8, 8	122
4. Kaula K-8	1966	4	12	Optical, Doppler		7, 5	99
5. Kaula C	1966	4			Determinations 1-4	7, 2	
6. Rapp	1967	5	16	Optical	Gravimetry	14, 14	219
7. Köhnlein	1967	6	16	Optical	Gravimetry	15, 15	250
8. Kaula UCLA	1967	7	9	Optical, Doppler	Gravimetry	8, 8	
9. Rapp	1968	8	16	Optical	Gravimetry	14, 14	
10. SAO COSPAR	1969	9	24	Optical, Range, Range Rate		14, 14	280
11. SAO B6.1	1969	10	24	Optical, Range, Range Rate		16, 16	
12. SAO B 13.1	1969	11	24	Optical, Range, Range Rate	Gravimetry	16, 16	314
13. SAO SF	1969	12	24	Optical, Range, Range Rate	Gravimetry	16, 16	316
14. GSFC 1.70 C	1970	13			Determinations 1-9, 11, 12	15, 15	249
15. SAO 69 (II)	1970	14	21	Optical, Range, Range Rate	Gravimetry	16, 16	316

Table II

Resonance Determinations of Geopotential Coefficients

Author or Designation	Year	Reference Number	Basis		Field Characteristics
			Numbers and Types Satellites	Reference Coefficients	Coefficients Determined
1. Wagner	1967	15	3 24-hour		(2,2), (3,1), (3,3)
2. Gaposchkin and Veis	1967	16	3 12th order	SAO M-1	(13,12), (14,12), (15,12)
3. Murphy and Victor	1967	17	2 12-hour		(2,2), (4,4)
4. Yionoulis	1968	18	3 13th order		(13,13), (15,13), (17,13)
5. Wagner	1968	19	2 12-hour		(3,2), (4,4)
6. Murphy and Cole	1968	20	1 12th order		(14,12), (15,12)
7. Wagner	1968	21	3 24-hour 2 12-hour		(2,2), (3,1), (3,2) (3,3), (4,4)
8. Douglas and Marsh	1969	22	1 13th Order	Yionoulis, 1968	(14,13)
9. Wagner	1969	23	4 24-hour 4 12-hour	SAO B13.1	(2,2), (3,2), (3,3), (4,4)

Table III

Satellite Position Differences Associated with Various Gravity Models

SAO M-1 (modified*) vs.	Position (meters)							
	GEOS I				GEOS II			
	Radial	Cross Track	Along Track	Total	Radial	Cross Track	Along Track	Total
SAO M-1 (unmodified)	30.0	17.1	286.4	288.5	22.3	10.3	232.2	234.2
SAO COSPAR (no. 11th)	8.9	12.8	29.5	33.4	24.7	18.2	92.8	97.8
SAO 1969	8.3	13.5	26.9	31.2	16.6	19.3	59.2	64.4
Köhnlein	16.4	16.1	213.0	214.2	20.1	16.9	129.1	131.7
Köhnlein (modified)	9.2	10.9	28.0	31.4	11.8	15.1	41.9	46.1
Rapp	48.3	29.5	129.4	141.2	38.8	37.7	157.6	166.6
Rapp (modified)	46.4	33.2	99.9	115.0	36.2	39.1	84.8	100.1
APL 3.5	46.1	46.8	175.7	187.1	71.8	55.2	674.3	680.4
APL 3.5 (modified)	42.5	41.6	90.1	107.9	34.7	45.4	88.1	105.2
NWL 5E-6	16.3	16.6	204.0	205.3	46.4	80.9	374.6	386.1
NWL 5E-6 (modified)	16.7	12.9	49.1	53.4	26.3	80.0	82.9	118.2
Kaula	32.5	42.2	114.1	125.9	47.6	43.5	232.8	241.4
Kaula (modified)	32.1	42.5	110.2	122.4	48.7	42.0	140.5	154.6

*Gaposchkin & Veis (1967) 12th order terms for GEOS-I and Yionoulis (1968) and Douglas & Marsh (1968) 13th order terms for GEOS-II.

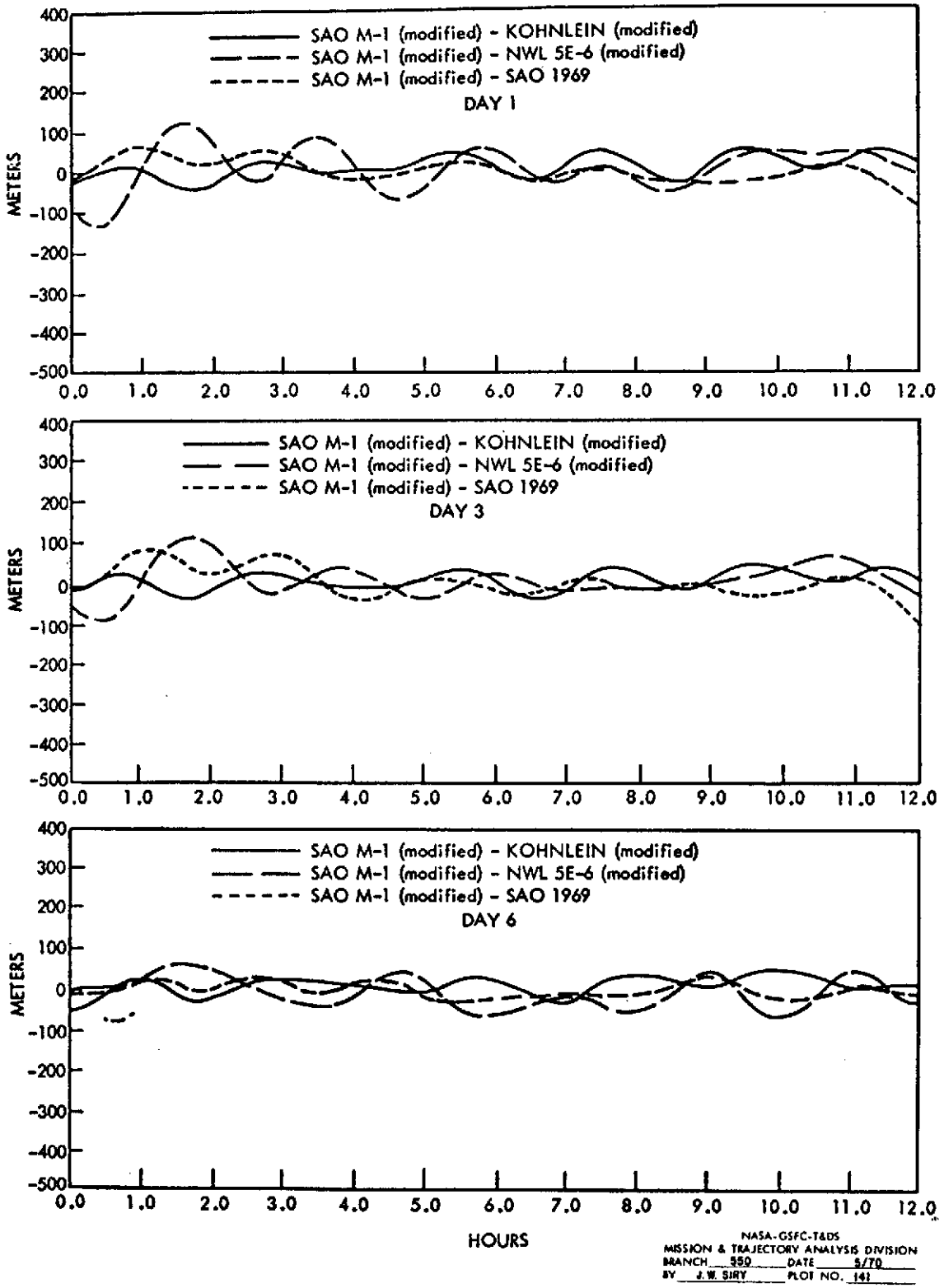

Figure 1. Along Track Position Differences GEOS-I July 11-16, 1966

The program for the study of earth's gravitational field at the Goddard Space Flight Center has several major aspects. These come together in a program for a general determination of both the zonal and tesseral harmonics of the geopotential, the locations of tracking stations, and fundamental parameters such as the earth's radius. These quantities are determined simultaneously in this portion of the program. In addition, the overall Goddard program includes specialized research efforts directed toward the determination of zonal harmonic coefficients, resonant tesseral terms both individually and in sets, tracking stations locations and the geoid.

B. The Goddard Earth Models

The program for the general determination of the gravitational field has thus far generated four earth models.[30] These are referred to as elements of the Goddard Earth Model (GEM) series, individual solutions being designated GEM-1, GEM-2, etc. A broad view of the four GEM results obtained so far is seen in Table IV. More details about the GEM-1 and GEM-2 solutions are summarized in Table V. The body of optical satellite tracking data which constitute the principal basis of these results is described in the listings of Table VI. The surface gravity data which permit the filling in of fine structure detail in many areas are portrayed summarily in Figure 2. Information related to the uncertainties associated with these two types of data is seen in Figure 3. The relative weighting of the satellite and gravimetric data in the combined solution was based largely upon this type of information.

Table IV

Description of Goddard Earth Models (GEM) Geopotential Solutions

Solution	Spher. Harm. Field	Satellite Data	Gravimetry Data
GEM 1	12 x 12 Satellite	120,000 Optical Obs. on 25 Satellites	
GEM 2	16 x 16 Combined	GEM 1 Data	1707 5° x 5° Mean Gravity Anomalies
GEM 3	12 x 12 Satellite	300,000 Optical and Electronic Obs. on 27 Satellites	
GEM 4	16 x 16 Combined	GEM 3 Data	1707 5° x 5° Mean Gravity Anomalies

- 61 center of mass tracking station locations
- Two low inclination satellites SAS 3°, PEOLE 15° 25 satellites in previous solution all have inclination > 28°
- 5° x 5° mean gravity anomalies based upon

  19,000 1° x 1° Anomalies from ACIC

  2,000 1° x 1° Anomalies from other sources

Table V

Summary of Solution, Data, and Results

A. SOLUTION

Geopotential solution in spherical harmonic series (degree n, order m).

Type Solution	Complete (n x m)	Zonals Complete	Resonant Coefficients
Satellite (GEM 1)	12 x 12	21	m = 12, 13, 14, n = m to 22 m = 9, n = 9 to 16
Satellite & Gravimetry (GEM 2)	16 x 16	21	m = 11, n = 11, 12, 14 Complete as above

46 Center of mass tracking station locations (see tracking systems below)

B. DATA

Satellite Data

Tracking Systems	25 Satellites (Data Processed)
13 Baker-Nunn Cameras	300 weekly arcs of optical data
23 MOTS Cameras	15 weekly arcs of electronic/laser data
3 GRARR (range/range-rate)	66 one/two-day arcs of GEOS-I and II flashing light data
2 LASERS	
5 DOPPLER	20 weekly arcs of Minitrack data

Gravimetry Data

19,000 1° x 1° mean gravity anomalies of ACIC data, and
2,000 1° x 1° mean gravity anomalies from other sources, used to form
1,705 4° x 5° means, providing 70% world coverage

C. RESULTS

1. Station heights indicate a_e = 6378145 meters.
2. Mean value of gravity ($\Delta\bar{g}_0$ = 3.28 mgal) indicates a_e = 6378142 (m).
3. Solution for 327 zonal and tesseral coefficients including $\Delta\bar{g}_0$ from satellite and gravimetry data.
4. Solution using optical and electronic tracking data for location of 46 tracking stations.

Table VI

Satellite Data

300 Weekly Satellite Arcs Opt. Data (Primarily SAO Baker-Nunn)

Satellite Name	A (Meters)	E	I (Deg)	Perigee Height (km)	Period (Rev./Day)	No. Arcs	No. Obs.	Avg. No. Obs./Arc	Avg. RMS (Weighted)
TELSTAR-1	9669530.1	0.2421	44.79	951.3	9.13	16	1946	121	2.70
TIROS-9	8020761.2	0.1167	96.42	706.7	12.09	14	1525*	109	1.16
GEOS-1	8067353.6	0.0725	59.37	1107.5	11.98	35	45555**	1301	1.28
SECOR-5	8154869.9	0.0801	69.23	1140.1	11.79	4	290	72	2.38
OVI-2	8314700.2	0.1835	144.27	414.8	11.45	4	910	227	1.93
ALOU-2	8097474.4	0.1508	79.83	502.0	11.91	6	590*	98	0.89
ECHO-1RB	7968879.1	0.0121	47.22	1501.0	12.20	18	2240	124	2.24
DI-D	7614681.9	0.0842	39.45	589.0	13.07	9	6386	709	1.86
BE-C	7503563.5	0.0252	41.17	941.9	13.36	22	4947	224	1.59
DI-C	7344163.4	0.0526	40.00	586.6	13.79	4	902	225	2.53
ANNA-1B	7504950.8	0.0070	50.13	1075.8	13.35	40	4183	104	1.51
GEOS-2	7710306.6	0.0308	105.79	1114.2	12.82	24	25315**	1054	1.75
OSCAR-7	7404041.3	0.0242	89.70	847.7	13.63	4	1780	445	2.34
SBN-2	7463226.9	0.0058	89.95	1062.5	13.47	5	355	71	5.17
COURIER-1B	7473289.0	0.0174	28.34	988.5	13.44	12	3375	281	1.66
GRS	7228289.3	0.0604	49.72	421.3	14.13	5	369	73	3.06
TRANSIT-4A	7321521.7	0.0079	66.83	806.0	13.86	14	1316	94	1.92
BE-B	7364785.0	0.0143	79.70	901.8	13.74	4	469	117	1.87
OGO-2	7345633.6	0.0739	87.37	424.8	13.79	7	461	65	3.47
INJUN-1	7312542.4	0.0076	66.81	895.0	13.88	9	768	85	2.15
AGENA-R	7297251.5	0.0010	69.91	920.2	13.93	7	1005	143	2.86
MIDAS-4	9995760.5	0.0121	95.84	1504.8	8.69	20	14879	743	1.20
VANGUARD-2	8306759.8	0.1645	32.89	566.7	11.47	11	379	34	1.13
VANGUARD-2S	8309120.5	0.1648	32.87	562.2	11.46	5	615	123	2.29
VANGUARD-3S	8511504.6	0.1906	33.35	517.9	11.06	15	996	66	2.89
					Summary Totals	314	121336	388	3.4*

*Minitrack
**MOTS
48,000 obs.
GEOS I & II

The Goddard Earth Models were determined by means of the method of numerical integration. The program system used is based on the one described by Velez et. al.[31] The special perturbation method employed here is fundamentally different from the general perturbation technique used by SAO in generating the 1969 Smithsonian Standard Earth (II)[18]. Sharper insights are provided by the latter, analytical, approach. Increased accuracy is usually more readily achievable by means of the former, numerical method.

The actual values determined in the GEM-4 solution are seen in Table VII which contains a listing of both zonal and tesseral geopotential coefficients, and Table VIII which lists the tracking station locations. The geoid heights corresponding to the values of Table VII are portrayed in Figure 4. The corresponding

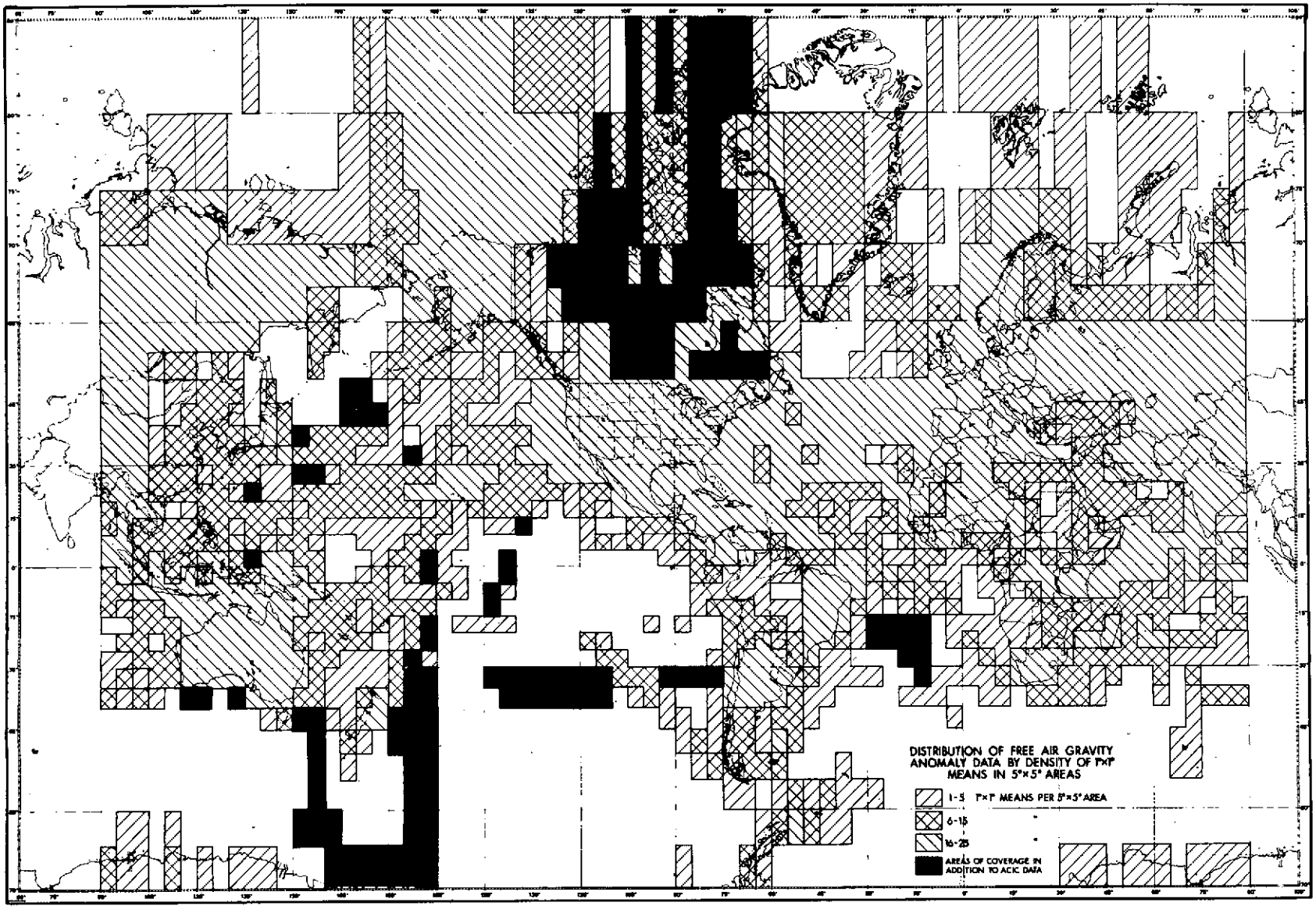

Figure 2. Surface Gravity Data 5° x 5° Mean Gravity Anomalies

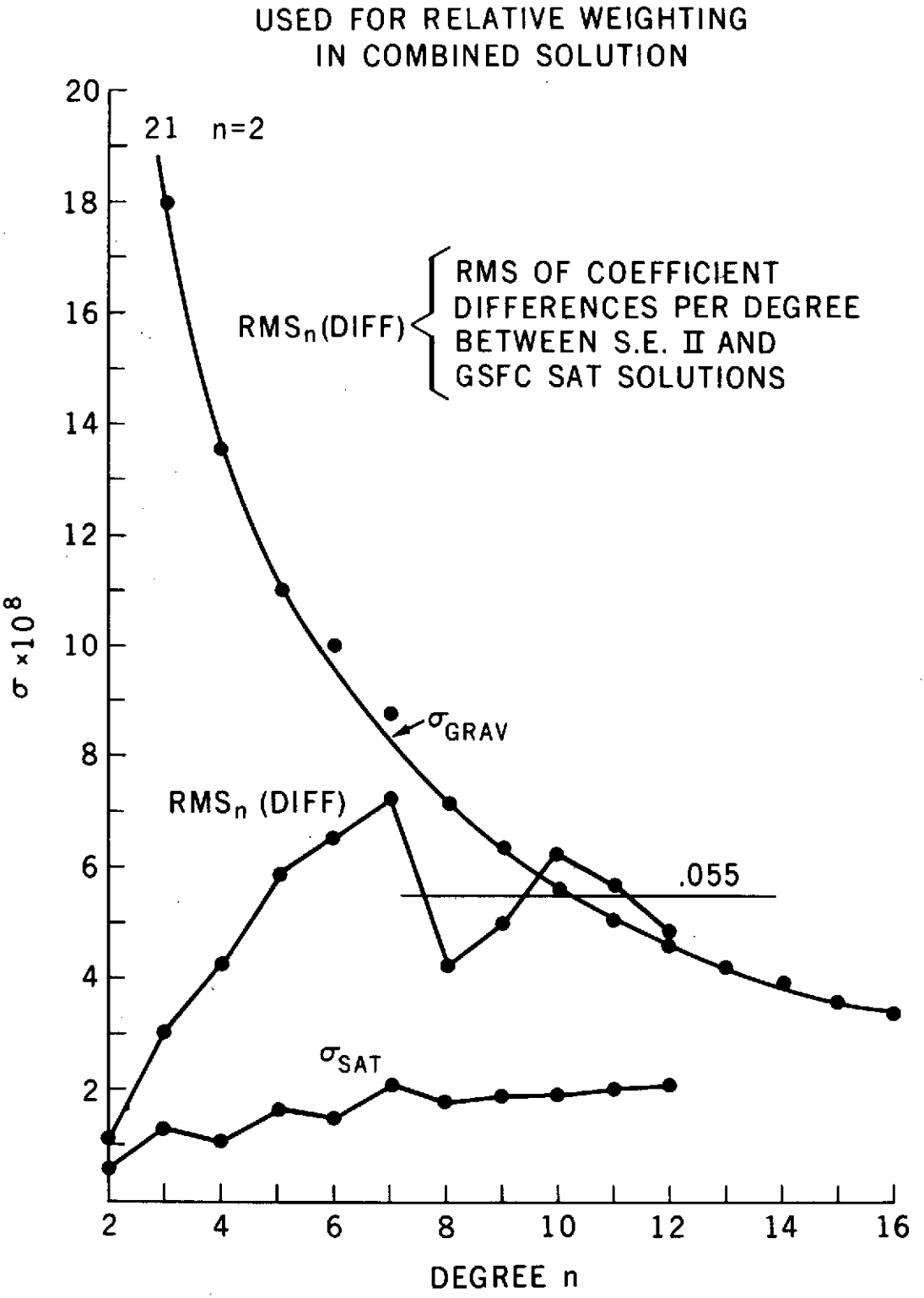

Figure 3. Average Standard Deviation of Coefficients per Degree n of Satellite and Gravimetry Solutions

Table VII

GSFC Geopotential Solutions (Normalized Coefficients x 10^8) 1

	L	M	GEM 4	GEM 3		L	M	GEM 4	GEM 3		L	M	GEM 4	GEM 3		L	M	GEM 4	GEM 3		L	M	GEM 4	GEM 3
C	2	0	-484.1690	-484.1718	C	21	0	-0.0076	-0.0075	C	4	2	0.3511	0.3542	C	9	3	-0.1700	-0.1493	C	15	4	0.0099	0.0
S	2	0	0.0	0.0	S	21	0	0.0	0.0	S	4	2	0.6652	0.6637	S	9	3	-0.1049	-0.1518	S	15	4	-0.0254	0.0
C	3	0	0.9570	0.9577	C	22	0	-0.0038	-0.0015	C	5	2	0.6620	0.6570	C	10	3	-0.0483	-0.0409	C	16	4	0.0308	0.0
S	3	0	0.0	0.0	S	22	0	0.0	0.0	S	5	2	-0.3145	-0.3188	S	10	3	-0.0976	-0.1206	S	16	4	0.0733	0.0
C	4	0	0.5412	0.5470	C	2	1	-0.0076	-0.0078	C	6	2	0.0679	0.0675	C	11	3	-0.0205	-0.0111	C	5	5	0.1700	0.1481
S	4	0	0.0	0.0	S	2	1	-0.0004	-0.0068	S	6	2	-0.3795	-0.3697	S	11	3	-0.0887	-0.1193	S	5	5	-0.6845	-0.6782
C	5	0	0.0692	0.0681	C	3	1	2.0164	2.0174	C	7	2	0.3395	0.3355	C	12	3	0.1389	0.1120	C	6	5	-0.2964	-0.3033
S	5	0	0.0	0.0	S	3	1	0.2498	0.2508	S	7	2	0.0746	0.0795	S	12	3	0.0429	0.0859	S	6	5	-0.5115	-0.5091
C	6	0	-0.1528	-0.1617	C	4	1	-0.5336	-0.5322	C	8	2	0.0511	0.0482	C	13	3	-0.0335	0.0	C	7	5	0.0035	-0.0102
S	6	0	0.0	0.0	S	4	1	-0.4614	-0.4444	S	8	2	0.0739	0.0659	S	13	3	0.0371	0.0	S	7	5	0.0321	0.0561
C	7	0	0.0910	0.0924	C	5	1	-0.0741	-0.0687	C	9	2	0.1534	0.0238	C	14	3	0.0386	0.0	C	8	5	-0.0884	-0.0957
S	7	0	0.0	0.0	S	5	1	-0.0786	-0.0817	S	9	2	-0.0171	-0.0176	S	14	3	-0.0157	0.0	S	8	5	0.0846	0.0858
C	8	0	0.0515	0.0619	C	6	1	-0.0905	-0.0889	C	10	2	-0.0457	-0.0471	C	15	3	0.0150	0.0	C	9	5	-0.0320	-0.0203
S	8	0	0.0	0.0	S	6	1	0.0084	-0.0209	S	10	2	-0.0667	-0.0498	S	15	3	0.0552	0.0	S	9	5	-0.0548	-0.0678
C	9	0	0.0312	0.0302	C	7	1	0.2553	0.2524	C	11	2	0.1158	0.0363	C	16	3	0.0306	0.0	C	10	5	-0.0682	-0.1102
S	9	0	0.0	0.0	S	7	1	0.1334	0.1308	S	11	2	-0.1256	-0.1130	S	16	3	-0.0160	0.0	S	10	5	-0.0076	-0.0133
C	10	0	0.0502	0.0469	C	8	1	0.0257	0.0276	C	12	2	-0.0449	-0.0458	C	4	4	-0.1811	-0.1815	C	11	5	0.0736	0.0270
S	10	0	0.0	0.0	S	8	1	0.0578	0.0544	S	12	2	0.0532	0.0373	S	4	4	0.3153	0.3123	S	11	5	0.0332	0.0252
C	11	0	-0.0561	-0.0560	C	9	1	0.1536	0.1609	C	13	2	0.0194	0.0	C	5	4	-0.3167	-0.3213	C	12	5	0.0399	0.0298
S	11	0	0.0	0.0	S	9	1	0.0588	0.0622	S	13	2	-0.1477	0.0	S	5	4	0.0321	0.0253	S	12	5	-0.0048	-0.0095
C	12	0	0.0389	0.0463	C	10	1	0.0757	0.0761	C	14	2	-0.0370	0.0	C	6	4	-0.1665	-0.1694	C	13	5	0.0418	0.0
S	12	0	0.0	0.0	S	10	1	-0.1434	-0.1798	S	14	2	0.1169	0.0	S	6	4	-0.4601	-0.4576	S	13	5	0.0548	0.0
C	13	0	0.0477	0.0495	C	11	1	-0.0199	-0.0155	C	15	2	0.0168	0.0	C	7	4	-0.2939	-0.3131	C	14	5	0.0426	0.0
S	13	0	0.0	0.0	S	11	1	0.0371	0.0326	S	15	2	-0.1410	0.0	S	7	4	-0.1064	-0.0869	S	14	5	-0.0311	0.0
C	14	0	-0.0260	-0.0296	C	12	1	-0.0592	-0.0650	C	16	2	0.0168	0.0	C	8	4	-0.2486	-0.2531	C	15	5	0.0237	0.0
S	14	0	0.0	0.0	S	12	1	-0.0466	-0.0152	S	16	2	0.0217	0.0	S	8	4	0.0466	0.0693	S	15	5	-0.0175	0.0
C	15	0	-0.0050	-0.0073	C	13	1	0.0183	0.0	C	3	3	0.7063	0.7203	C	9	4	0.0212	0.0026	C	16	5	0.0160	0.0
S	15	0	0.0	0.0	S	13	1	-0.0793	0.0	S	3	3	1.4231	1.4197	S	9	4	0.0139	0.0338	S	16	5	0.0334	0.0
C	16	0	-0.0053	-0.0116	C	14	1	-0.0453	-0.0151	C	4	3	0.4713	0.4755	C	10	4	-0.0934	-0.0981	C	6	6	0.0313	0.0406
S	16	0	0.0	0.0	S	14	1	0.0371	0.0053	S	4	3	-0.2187	-0.2196	S	10	4	-0.1177	-0.1101	S	6	6	-0.2348	-0.2278
C	17	0	0.0174	0.0196	C	15	1	0.1043	0.0	C	5	3	-0.4701	-0.4674	C	11	4	0.0027	0.0191	C	7	6	-0.3230	-0.3323
S	17	0	0.0	0.0	S	15	1	0.0419	0.0	S	5	3	-0.2566	-0.2778	S	11	4	-0.0937	-0.0770	S	7	6	0.1664	0.1563
C	18	0	0.0113	0.0163	C	16	1	-0.0314	0.0	C	6	3	0.0164	0.0226	C	12	4	-0.0423	-0.0195	C	8	6	-0.0476	-0.0346
S	18	0	0.0	0.0	S	16	1	0.0082	0.0	S	6	3	-0.0127	-0.0259	S	12	4	-0.0168	-0.0131	S	8	6	0.2841	0.3067
C	19	0	0.0190	0.0177	C	2	2	2.4237	2.4255	C	7	3	0.2558	0.2655	C	13	4	-0.0543	0.0	C	9	6	0.0651	0.0897
S	19	0	0.0	0.0	S	2	2	-1.3855	-1.3856	S	7	3	-0.2281	-0.2224	S	13	4	-0.0737	0.0	S	9	6	0.2216	0.2286
C	20	0	0.0060	0.0032	C	3	2	0.9164	0.9141	C	8	3	-0.0262	-0.0238	C	14	4	0.0366	0.0	C	10	6	-0.0178	0.0039
S	20	0	0.0	0.0	S	3	2	-0.6322	-0.6260	S	8	3	-0.0809	-0.0831	S	14	4	0.0064	0.0	S	10	6	-0.1220	-0.1227

Table VII

GSFC Geopotential Solutions (Normalized Coefficients x 10^8) 2

	L	M	GEM 4	GEM 3
C	11	6	-0.0211	-0.0342
S	11	6	0.0443	0.0605
C	12	6	0.0034	0.0610
S	12	6	-0.0282	-0.0193
C	13	6	-0.1284	0.0
S	13	6	0.0376	0.0
C	14	6	0.0534	0.0
S	14	6	-0.0323	0.0
C	15	6	-0.0174	0.0
S	15	6	-0.0481	0.0
C	16	6	-0.0407	0.0
S	16	6	-0.0189	0.0
C	7	7	-0.0752	0.0646
S	7	7	0.0131	0.0381
C	8	7	0.0464	0.0519
S	8	7	0.0679	0.0714
C	9	7	-0.0665	-0.0570
S	9	7	-0.0212	-0.0276
C	10	7	0.0117	-0.0191
S	10	7	-0.0337	-0.0371
C	11	7	0.0223	0.0113
S	11	7	-0.1164	-0.1156
C	12	7	-0.0335	-0.0223
S	12	7	0.0015	0.0108
C	13	7	-0.0526	0.0
S	13	7	0.1473	0.0
C	14	7	0.1313	0.0
S	14	7	-0.0797	0.0
C	15	7	-0.0214	0.0
S	15	7	0.0988	0.0
C	16	7	0.0256	0.0
S	16	7	-0.0462	0.0
C	8	8	-0.1075	-0.0926
S	8	8	0.1158	0.0974
C	9	8	0.2182	0.1812
S	9	8	0.0052	-0.0296
C	10	8	0.0418	0.0479
S	10	8	-0.1256	-0.1364
C	11	8	0.0011	-0.0269
S	11	8	0.0639	0.0336
C	12	8	-0.0317	-0.0342
S	12	8	0.0060	-0.0274
C	13	8	0.0412	0.0
S	13	8	-0.0192	0.0
C	14	8	0.0007	0.0
S	14	8	-0.0605	0.0
C	15	8	-0.1600	0.0
S	15	8	0.0295	0.0
C	16	8	-0.0381	0.0
S	16	8	-0.0248	0.0
C	9	9	-0.0273	-0.0347
S	9	9	0.0861	0.0760
C	10	9	0.1062	0.1157
S	10	9	-0.0724	-0.0657
C	11	9	-0.0505	-0.0138
S	11	9	0.0857	0.0469
C	12	9	0.0081	0.0343
S	12	9	0.0208	0.0331
C	13	9	0.0137	0.0531
S	13	9	0.1198	0.0707
C	14	9	0.0116	0.0476
S	14	9	0.0401	0.0602
C	15	9	0.0066	0.0389
S	15	9	0.0769	0.0855
C	16	9	0.0479	0.0
S	16	9	-0.0606	0.0
C	10	10	0.0766	0.0641
S	10	10	-0.0232	-0.0094
C	11	10	-0.0727	-0.0188
S	11	10	-0.0063	0.0047
C	12	10	-0.0257	-0.0215
S	12	10	0.0312	0.0569
C	13	10	-0.0128	0.0
S	13	10	0.0171	0.0
C	14	10	0.0273	0.0
S	14	10	-0.1311	0.0
C	11	11	0.0900	0.0848
S	11	11	-0.0255	-0.0221
C	12	11	0.0052	0.0093
S	12	11	0.0305	0.0337
C	13	11	-0.0443	0.0
S	13	11	-0.0215	0.0
C	14	11	0.0980	0.0
S	14	11	-0.0331	0.0
C	15	11	-0.0567	0.0
S	15	11	0.0568	0.0
C	16	11	0.0046	0.0
S	16	11	-0.0064	0.0
C	12	12	-0.0117	-0.0120
S	12	12	0.0049	0.0052
C	13	12	-0.0306	-0.0300
S	13	12	0.0994	0.0991
C	14	12	0.0068	0.0090
S	14	12	-0.0268	-0.0241
C	15	12	-0.0341	-0.0327
S	15	12	0.0153	0.0151
C	16	12	0.0256	0.0235
S	16	12	-0.0076	-0.0019
C	17	12	0.0261	0.0283
S	17	12	-0.0011	-0.0103
C	18	12	-0.0568	-0.0572
S	18	12	-0.0229	-0.0182
C	19	12	-0.0256	-0.0244
S	19	12	-0.0203	-0.0201
C	20	12	0.0121	0.0092
S	20	12	-0.0023	0.0066
C	21	12	0.0072	0.0113
S	21	12	-0.0347	-0.0326
C	22	12	-0.0537	-0.0531
S	22	12	-0.0333	-0.0315
C	13	13	-0.0274	-0.0282
S	13	13	0.0930	0.0951
C	14	13	0.0318	0.0302
S	14	13	0.0087	0.0045
C	15	13	-0.0023	-0.0014
S	15	13	0.0107	0.0120
C	16	13	0.0064	0.0044
S	16	13	-0.0213	-0.0219
C	17	13	0.0319	0.0324
S	17	13	0.0423	0.0436
C	18	13	-0.0027	-0.0039
S	18	13	-0.0834	-0.0897
C	19	13	-0.0068	-0.0062
S	19	13	-0.0012	-0.0003
C	20	13	0.0312	0.0277
S	20	13	-0.0637	-0.0725
C	21	13	-0.0196	-0.0188
S	21	13	0.0257	0.0263
C	22	13	-0.0137	-0.0180
S	22	13	-0.0348	-0.0398
C	14	14	-0.0521	-0.0519
S	14	14	-0.0074	-0.0081
C	15	14	0.0025	0.0026
S	15	14	-0.0216	-0.0212
C	16	14	-0.0108	-0.0139
S	16	14	-0.0374	-0.0374
C	17	14	-0.0155	-0.0159
S	17	14	0.0060	0.0051
C	18	14	-0.0234	-0.0218
S	18	14	-0.0043	-0.0048
C	19	14	0.0005	0.0008
S	19	14	-0.0109	-0.0102
C	20	14	0.0117	0.0127
S	20	14	-0.0035	-0.0024
C	21	14	0.0042	0.0045
S	21	14	0.0134	0.0138
C	22	14	0.0215	0.0206
S	22	14	0.0071	0.0079
C	15	15	-0.0788	0.0
S	15	15	0.0308	0.0
C	16	15	-0.0544	0.0
S	16	15	0.0090	0.0
C	16	16	-0.0048	0.0
S	16	16	-0.0036	0.0

Table VIII

GEM 4 Station Coordinate Solution

TYPE	STATION NAME	STATION NUMBER	LATITUDE DEG	LATITUDE MIN	LATITUDE SEC	LONGITUDE DEG	LONGITUDE MIN	LONGITUDE SEC	HEIGHT M	MSL M	GRAVITY M	RES M
M	1HPOIN	1021	38	25	49.920	282	54	48.543	-42.3	5.8	-42.3	-5.8
M	1FTMYR	1022	26	32	53.408	278	8	4.219	-32.3	4.8	-29.8	-7.3
M	1OKEE	1024	-31	23	25.122	136	52	15.442	129.5	132.8	-3.0	-0.3
M	1SATAG	1028	-33	8	58.371	289	19	53.674	707.9	693.4	23.7	-9.2
M	1MOJAV	1030	35	19	47.898	243	5	59.184	889.5	929.1	-28.9	-10.7
M	1JOBUR	1031	-25	53	0.742	27	42	26.375	1537.3	1522.0	22.3	-7.0
M	1NEWFL	1032	47	44	29.861	307	16	46.193	63.2	69.0	12.0	-17.8
M	1GFORK	1034	48	1	21.333	262	59	19.474	215.2	252.6	-33.1	-7.3
M	1WNKFL	1035	51	26	46.074	359	18	8.307	104.4	67.4	45.3	-8.3
M	1ROSMN	1037	35	12	7.395	277	7	41.380	867.3	909.3	-37.9	-4.1
M	1ORORL	1038	-35	37	32.109	148	57	14.881	944.4	931.6	15.0	-3.2
M	1ROSMA	1042	35	12	7.398	277	7	41.169	867.5	909.4	-37.9	-4.0
M	1TANAN	1043	-19	0	31.629	47	17	59.444	1362.6	1378.0	-5.1	-9.3
M	1UNDAK	7034	48	1	21.403	267	59	19.464	216.7	252.6	-30.1	-5.8
M	1CDINB	7036	26	22	46.796	261	40	7.504	21.3	59.6	-18.9	-19.4
M	1COLBA	7037	38	53	36.235	267	47	40.934	227.6	272.7	-32.3	-12.8
M	1PERMD	7039	32	21	49.897	295	20	35.029	-17.1	31.2	-43.4	-4.9
M	1PURIO	7040	18	15	28.918	294	8	23.629	-7.4	43.7	-47.5	-9.6
M	1GSFCP	7043	39	1	15.736	283	10	20.326	3.0	53.5	-41.9	-8.6
M	1DENVR	7045	39	38	48.057	255	23	38.668	1758.2	1790.0	-21.5	-10.3
M	1JUMAO	7072	27	1	14.408	279	53	12.876	-33.6	14.2	-34.2	-13.6
M	1SUDAR	7075	46	27	21.244	279	3	10.410	236.0	281.9	-39.0	-6.9
M	1JAMAC	7076	18	4	34.762	283	11	27.073	419.6	445.9	-25.2	-1.1
B	1ORGAN	9001	32	25	24.986	253	26	49.004	1617.3	1651.0	-23.9	-9.8
B	1OLEAN	9002	-25	57	36.338	29	14	52.527	1561.3	1544.0	21.6	-4.6
B	1OOMER	9005	-31	6	2.109	136	47	3.350	153.7	162.5	-2.7	-6.1
B	1SPAIN	9004	36	27	46.734	353	47	36.956	57.3	25.9	50.0	-18.6
B	1TOKYO	9005	35	40	22.975	139	32	16.555	83.9	59.8	38.2	-14.1
B	1NATOL	9006	29	21	34.687	79	27	27.520	1869.4	1927.0	-50.2	-7.4
B	1QUITA	9007	-16	27	56.824	288	33	24.631	2484.7	2452.0	29.6	3.1
B	1SHRAZ	9008	29	38	13.743	52	31	11.369	1578.7	1596.0	-9.0	-8.3
B	1CURAC	9009	12	5	25.356	291	3	44.547	-26.4	9.7	-29.3	-3.8
B	1JUPTR	9010	27	1	14.020	279	53	13.375	-24.9	15.1	-36.2	-5.6
B	1VILOO	9011	-31	56	34.719	296	53	36.626	626.6	598.4	24.6	3.6
B	1MAUIO	9012	20	42	26.051	203	44	33.964	3040.4	3034.0	4.5	1.9
B	HOPKIN	9021	31	41	3.174	249	7	18.592	2337.2	2382.0	-26.7	-18.1
B	AUSBAK	9023	-31	23	25.874	136	52	43.675	136.6	141.2	-3.0	-1.6
B	DEZELT	9026	8	44	51.106	38	57	33.366	1900.8	1924.0	-6.7	-16.5
B	COMRIV	9031	-45	53	17.419	292	23	9.422	195.3	186.5	11.2	-2.4
* B	GREECE	9091	38	4	44.736	23	55	58.650	483.2	467.0	32.1	-15.9
* B	EDWARD	9425	34	57	50.520	242	5	7.455	747.3	784.2	-30.9	-6.0
* B	JOHNST	9427	16	44	38.733	190	29	9.342	17.3	5.0	10.9	1.4
G	MADGAR	1123	-19	1	14.228	47	18	11.362	1386.9	1399.0	-6.1	-6.0
G	ROSRAN	1126	35	11	45.641	277	7	24.252	927.0	873.9	-37.9	-9.0
G	ULASKA	1128	64	58	19.069	212	29	12.706	341.4	346.6	10.5	-15.7
G	CARVON	1152	-24	54	10.766	113	42	59.736	6.1	37.9	-20.6	-11.2
L	GODLAS	7050	39	1	14.539	283	10	18.736	13.4	54.8	-41.9	0.5
L	WALLAS	7057	37	51	36.235	284	29	23.889	-42.9	8.6	-43.1	-8.4
L	ORMLAS	7054	-24	54	14.794	113	42	58.262	-6.6	31.4	-20.6	-17.4
* D	ANCHOR	2014	61	17	0.152	210	10	28.960	64.0	68.0	15.0	-19.0
D	TAFUNA	2017	-14	19	50.005	189	17	3.159	27.5	6.1	25.5	-5.1
* D	WAHIWA	2100	21	31	15.577	202	0	10.408	396.2	388.0	7.6	0.6
* D	LACRES	2103	32	16	44.544	253	14	45.439	1151.6	1203.0	-26.0	-27.6
* D	LASHAM	2106	51	11	9.359	359	58	25.632	218.5	190.3	45.7	-17.5
* D	APLMND	2111	39	9	48.639	283	6	11.907	95.7	145.0	-41.8	-7.5
* D	THOLFG	2116	76	32	20.076	291	13	52.867	50.7	43.0	13.8	-6.1
* D	PRETOR	2115	-25	56	48.233	28	20	52.072	1581.0	1580.0	21.4	-20.4
* D	ASAMOA	2117	-14	19	50.099	189	17	2.960	38.5	6.0	26.5	6.0
D	MESMED	2817	36	14	26.605	53	37	44.419	953.1	994.6	-19.9	-21.6
D	FRTLMY	2822	12	7	54.040	15	2	6.939	299.1	298.4	13.0	-12.3
D	NBRZIL	2937	-5	54	57.855	324	49	55.940	6.2	41.0	-11.2	-23.6

*MEAN SEA LEVEL HEIGHTS, MSL, FOR THESE SITES MAY NOT BE RELIABLE.
M—MOTS, B—BAKER-NUNN, G—GRARR, L—LASER, D—NWL DOPPLER.

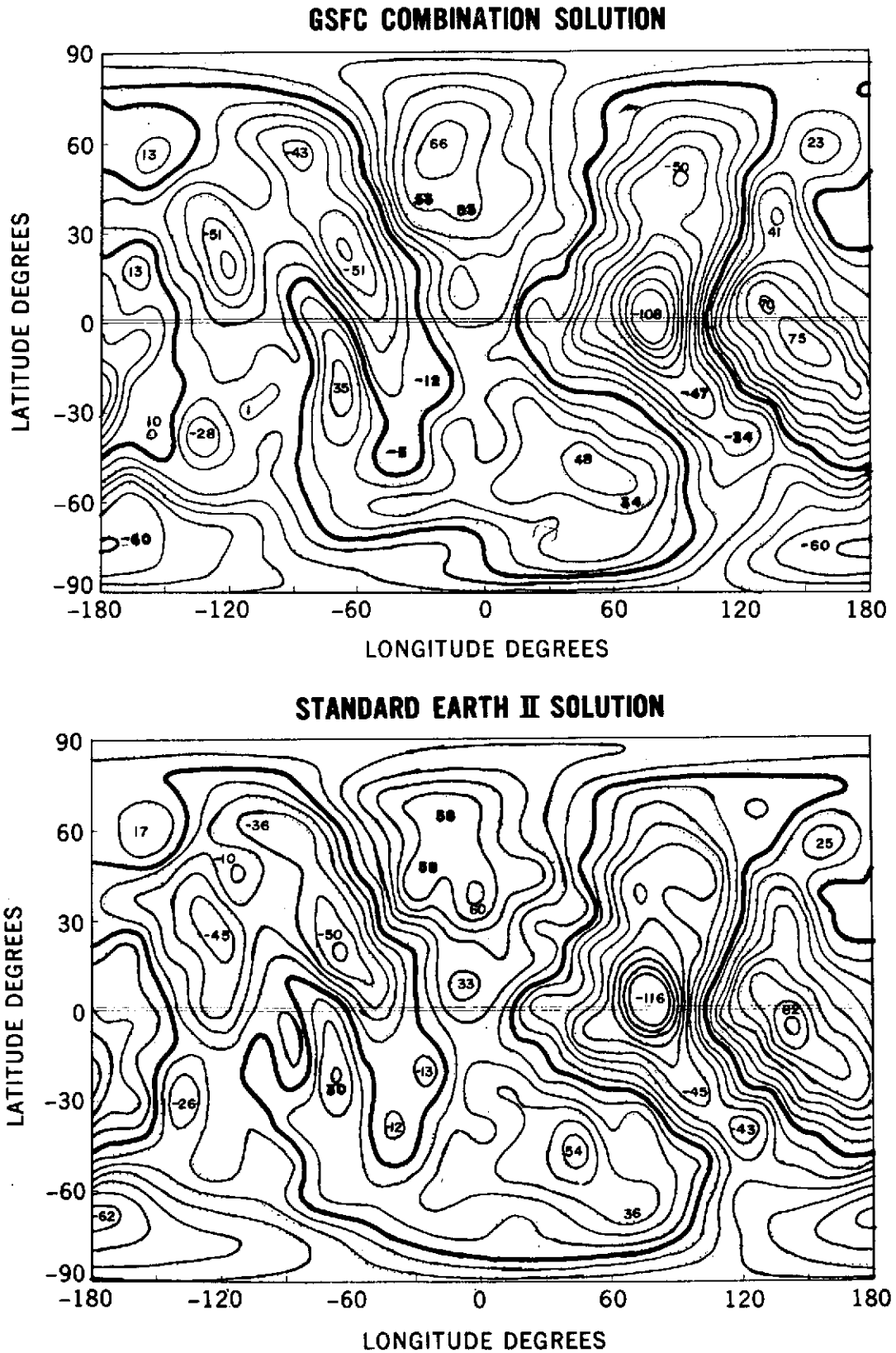

Figure 4. Geoid Heights (Meters)

contours derived from the SAO 1969 (II) solution are also shown there. Some feel for the accuracy of the GEM-4 solution can be had by inspecting Figure 5. The closures of the tracking station heights have a scatter of the order of ten meters about a mean which corresponds to the value of 6378145 meters for the earth's equatorial radius.

C. Zonal Harmonics

Zonal harmonic coefficients obtained simultaneously with the tesseral harmonic coefficients in the GEM solutions are based on arcs a week in length. In the past zonal harmonics have been derived separately and, in fact, are often used as fixed reference quantities in the determination of the tesseral harmonic coefficients [32, 13] . Zonal Harmonic coefficients have secular and long period effects on all the elements except the semi-major axis. Collections of elements spanning at least a complete revolution of the perigee accordingly provide a good basis for zonal harmonic solutions. The earth's pear-shape was discovered in this way through examination of the eccentricity perturbations of the Vanguard I satellite. Kozai and King-Hele have extended this process using theoretical approaches which are primarily analytical in nature. Cazenave, et. al., using a similar approach, derived an extension of Kozai's field by adding data for three low inclination satellites.[33] Wagner has recently derived a solution using a method of numerical integration of the orbital elements.[34] It is of special interest to compare Wagner's results derived by the classical approach, which relies on long arcs whose lengths spans a full revolution of perigee, with the

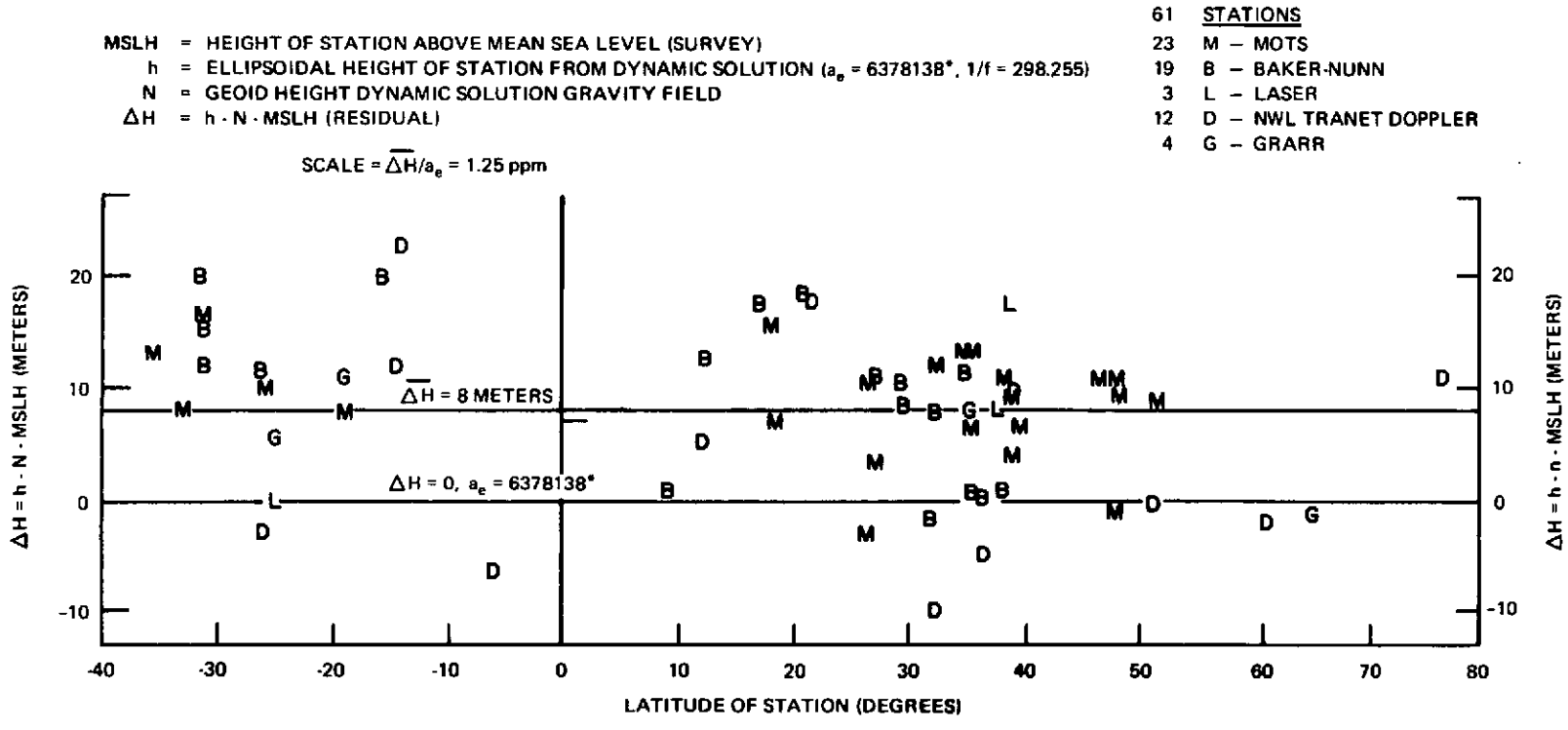

*REFERENCE a_e IS BASED UPON RECENT VALUES FOR g_e AND 6M.

g_e = 978032.2 MGALS OBTAINED FROM SURFACE GRAVITY DATA IN GEM 4 MODEL
6M = 3.98600.8 km^3/sec^2 OBTAINED BY JPL FROM MARINER 9 DATA.

Figure 5. Dynamic Station Height Above Geoid vs. Survey

GEM-2 results which are based on arcs an order of magnitude shorter, i.e., about a week in length. This is done in Figures 7 and 8. The field derived by Cazenave, et. al.,[33] is also indicated in the comparisons in these figures where it is designated FR 71. The basis for each of these three solutions is tabulated in Table IX and depicted graphically in Figure 6. Results and estimates of uncertainties are indicated in Table X and XI.

The SAO field listed in Table X was obtained using orbits and a method similar to those employed in deriving the FR 71 set of coefficients. Comparisons of Wagner's field with GEM-2 and FR 71 results in terms of secular rates and eccentricity oscillation amplitudes are seen in Figures 8 and 8. Finally, zonal geoid profile information is given in Figures 9 and 10.

D. Resonant Tesseral Harmonics

Resonant tesseral harmonics also can be studied very effectively through the analysis of longer arcs.

Some of the results obtained by Wagner, Murphy, and Victor are contained in references 19, 21, 23-25, 27, and 34A, summarized in references 28 and 29, and indicated in Figures 11 through 14 and Tables XII through XIV.

The possibilities for obtaining an improved geopotential solution through the more extensive use of synchronous and semi-synchronous satellite data are indicated in Table XIV where it is seen that relatively small changes in the coefficients result in a significant improvement in the fits to the orbital data. A

Table IX

Satellites Used in Recent Zonal Solutions

SATELLITE	ZONAL SOLUTIONS			SATELLITE/ORBIT CHARACTERISTICS						
	GEM 2	WAG 72	FR 71	I°	h_p (Km)	h_a (Km)	e	A/M (cm^2/gm)	C_D (2.3)	C_R (1.5)
SAS-1		X	X	3.0	530	560	0.002	0.11	2.2	1.4
DIAL (1970-17A)			X	5.4	310	1600	0.09			
PEOLE (1970-109A)		X	X	15.0	530	760	0.02	0.20	1.7	1.4
COURRIER 1B (1960-7A)	X		X	28.3						
EXPLORER II (1961-7A)		X		28.8	490	1800	0.086	0.10	1.6	1.1
PEGASUS 3 (1965-60A)		X		28.9	510	550	0.002	0.11	2.2	1.2
OSO 3 (1967-20A)		X		32.9	910	950	0.002	0.05	1.6	2.0
VANGUARD 2 (1959-1A)	X	X	X	32.9	550	3280	0.165	0.21	1.2	1.1
VANGUARD 3 (1959-5A)	X			33.4						
OVI-2	X			35.7(144.3)						
DI-D	X			39.5						
DI-C	X			40.0						
BE-C (EX-27) (1965-32A)	X	X		41.2	940	1320	0.025	0.17	2.4	1.3
TELSTAR-I (1962-29A)	X	X	X	44.8	950	5630	0.242	0.08	2.7	1.3
ECHO-I ROCKET (1960-9B)	X	X	X	47.2	1500	1670	0.011	0.21	2.6	1.0
GRS (1963-26A)	X		X	49.7						
ANNA-1B (1962-60A)	X	X	X	50.1	1080	1200	0.008	0.06	2.3	1.9
TIROS 5 (1962-25A)		X		58.1	590	960	0.026	0.06	2.1	2.3
TIROS 7 (1963-24A)				58.2						
GEOS 1 (1965-89A)	X	X	X	59.4	1110	2380	0.072	0.07	2.7	1.4
TRANSIT 4A (1961-15A)	X	X	X	66.8	880	980	0.008	0.11	2.7	1.3
SECOR 5 (1965-63A)	X			69.2						
AGENA ROCKET (1964-1A)	X		X	69.9						
EGRS-3 (1965-16E)		X		70.1	900	940	0.003	0.10?	3.3	-0.2
GEOS 2 (1968-2A)	X	X		74.2(105.8)	1080	1580	0.032	0.04	3.1	1.3
FR-1 (1965-101A)		X		75.9	740	750	0.001	0.11	2.8	1.2
BE-B (1964-64A)	X	X	X	79.7	890	1080	0.013	0.18	2.8	1.4
ALOUETTE 2 (1965-98A)	X			79.8						
ESSA I (1966-8A)		X		82.1(97.9)	710	850	0.010	0.06	2.3	1.3
TIROS 9 (1965-4A)	X	X		83.6(96.4)	690	2560	0.117	0.05	1.4	0.3
MIDAS 4 (1961-28A)	X	X	X	84.2(95.8)	3500	3740	0.012	0.06	1.9	1.6
OGO-2 (1965-81A)	X		X	87.4						
ISIS-I (1969-9A)		X		88.4	580	3520	0.175	0.10	1.0	1.8
OSCAR 7	X			89.7						
5-BN2 (1965-48C)	X			90.0						
TOTALS	23	21	15							

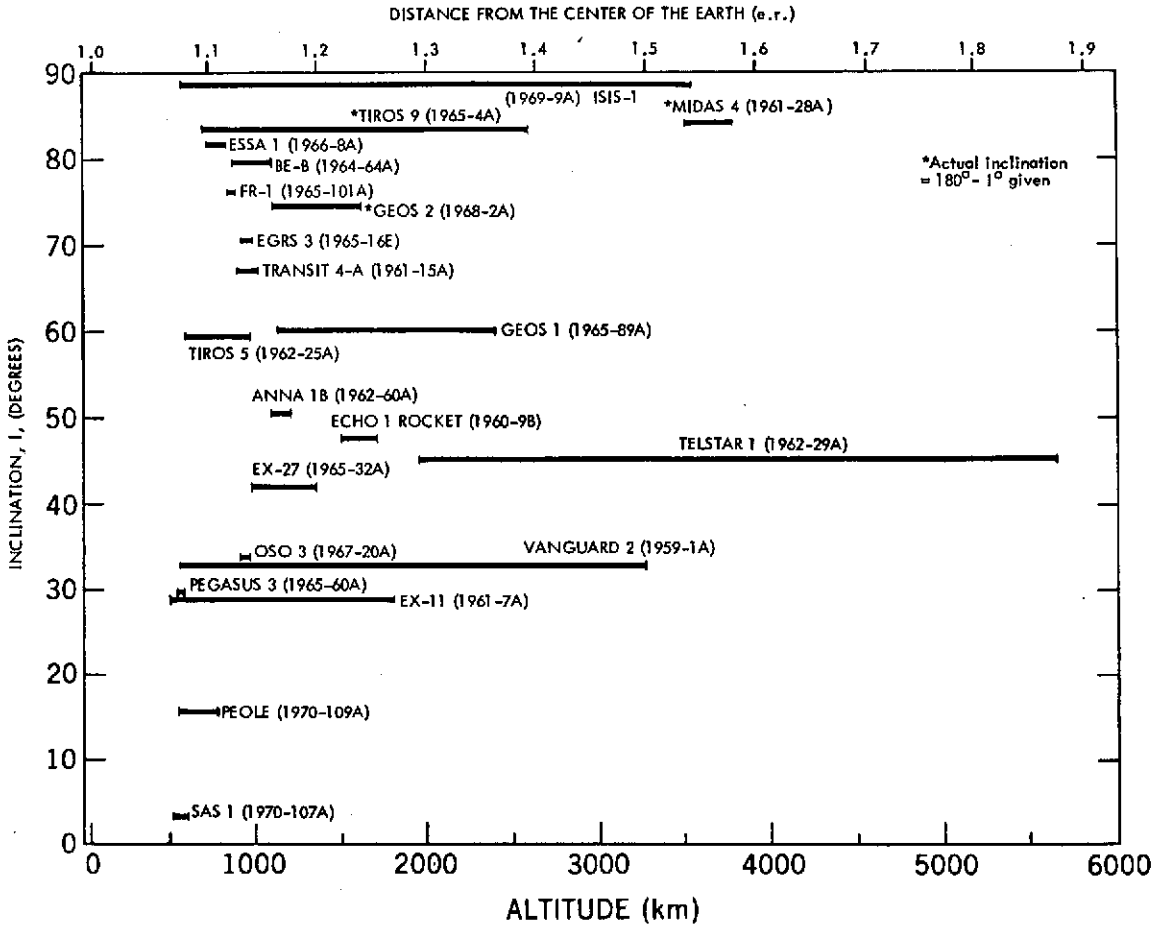

Figure 6. Satellites Used in Present Solution

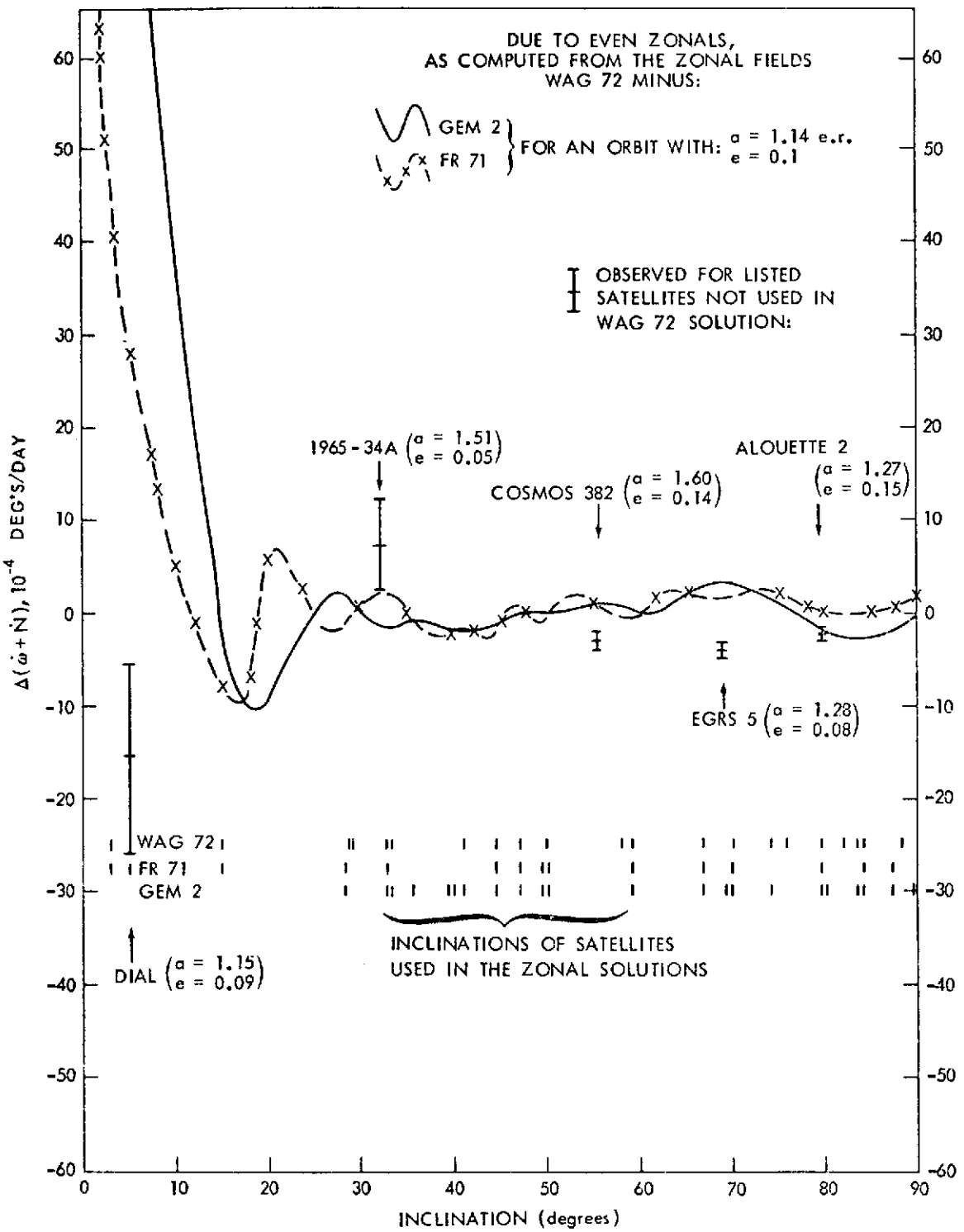

Figure 7. Differences in Secular Rates

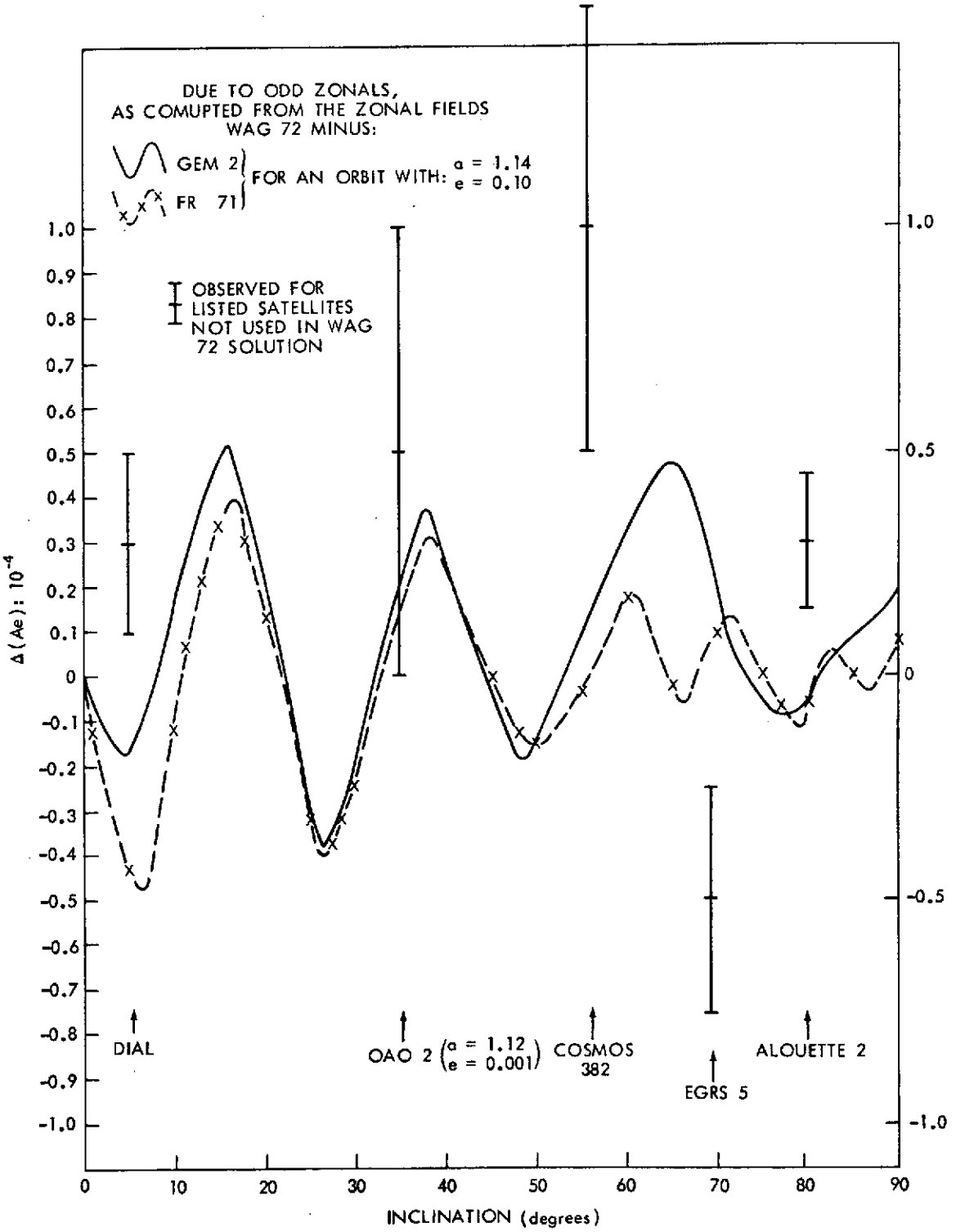

Figure 8. Differences in Amplitudes of Eccentricity Oscillation

Table X

Zonal Coefficients from Recent Solutions
(unnormalized in units of 10^{-6} except as noted)

J_ℓ	FR 71	SAO 71	GEM 2	WAG 72	FORMAL S.D. WAG 72 (10^{-9})	LIKELY SYSTEMATIC ERRORS IN WAG 72 FROM VARIOUS SOURCES (10^{-9})				TOTAL RSS S.D. ESTIMATE FOR WAG 72 (10^{-9})	ABS. VALUE WAG 72 −FR 71 Δ (10^{-9})	ABS. VALUE WAG−FR 71: Δ(NORMALIZED), (10^{-9})
						TRUNCATION	UNCERTAIN START. ELEM.	USE OF M. ANOM.	INTEGRATOR ERROR & S.P. LUNAR EFFECTS			
2	1082.637	1082.638	1082.631	1082.635	3	4	9	1	3	11	2	1
3	-2.543	-2.547	-2.526	-2.541	4	6	3	8	4	12	2	1
4	-1.619	-1.623	-1.610	-1.600	4	10	3	4	1	12	19	6
5	-0.226	-0.222	-0.241	-0.230	8	7	7	2	1	13	4	1
6	0.558	0.567	0.524	0.530	5	19	14	7	6	26	28	8
7	-0.365	-0.350	-0.337	-0.364	13	2	8	3	1	16	1	0
8	-0.209	-0.220	-0.164	-0.200	5	11	23	11	6	29	9	2
9	-0.118	-0.155	-0.144	-0.081	18	1	6	11	5	23	37	8
10	-0.233	-0.213	-0.297	-0.224	6	38	19	13	5	45	9	2
11	0.236	0.335	0.264	0.137	26	4	10	18	5	34	99	21
12	-0.188	-0.208	-0.106	-0.208	5	7	12	4	7	17	20	4
13	-0.202	-0.340	-0.225	-0.101	36	28	11	18	3	50	101	19
14	0.085	0.105	0.048	0.166	8	23	3	5	0	25	81	15
15	-0.081	0.139	-0.022	-0.072	40	31	8	30	2	59	9	2
16	0.048	0.022	0.149	0.003	7	47	7	26	8	55	45	8
17	-0.027	-0.252	-0.043	-0.204	41	1	29	51	8	72	177	30
18	-0.137	-0.118	-0.139	-0.086	13	11	14	50	12	56	51	8
19	-0.112	0.081	-0.096	0.047	42	13	15	26	2	53	159	25
20	-0.087	-0.087	0.004	-0.085	14	50	15	27	9	61	2	0
21	0.106	-0.040	0.077	0.015	29	50	8	20	8	62	91	14
												12 RMS

Table XI
Total Weighted RMS Residuals in Road Solutions
for Long Satellite Arcs

21 SATELLITES USED IN PRESENT SOLUTION	WITH FIELD USED		
	PRESENT SOLUTION (WAG 72)	FR 71	GEM 2
VANG. 2	1.52	1.39	1.39
TRAN. 4A	2.90	3.01	7.40
MIDAS 4	1.63	2.18	2.30
BE-B	3.25	3.63	3.62
GEOS 1	0.62	0.56	0.56
ECHO 1 ROCKET	0.84	1.34	1.35
PEOLE	1.00	1.73	1.19
SAS 1	1.05	15.94	45.52
EXPLORER I	1.11	1.51	1.48
ANNA 1B	1.23	1.27	1.27
TELSTAR I	2.49	2.63	2.63
GEOS 2	3.34	7.99	9.77
EGRS 3	2.45	5.25	4.45
PEGASUS 3	1.45	1.80	1.91
FR-1	1.49	3.10	1.61
OSO 3	1.33	1.80	1.47
EXPLORER 27	1.47	4.09	4.02
ESSA 1	1.67	2.91	2.33
TIROS 5	1.27	3.53	3.32
TIROS 9	1.00	0.95	1.00
ISIS 1	1.44	2.26	2.16
AVG. RMS IN 21 ARCS	1.65	3.28	4.80
6 SATELLITES NOT USED IN PRESENT SOLUTION			
CAO 2 (a = 1.12 e = 0.001)	0.82	0.81	0.85
1965-34A (a = 1.51 e = 0.05)	1.44	1.46	1.45
ALOUETTE 2 (a = 1.27 e = 0.15)	1.37	1.32	1.47
COSMOS 382 (a = 1.60 e = 0.14)	2.95	2.97	3.00
DIAL (a = 1.15 e = 0.09)	1.79	3.09	7.59
EGRS 5 (SECOR 5) (a = 1.28 e = 0.08)	2.40	2.36	2.49

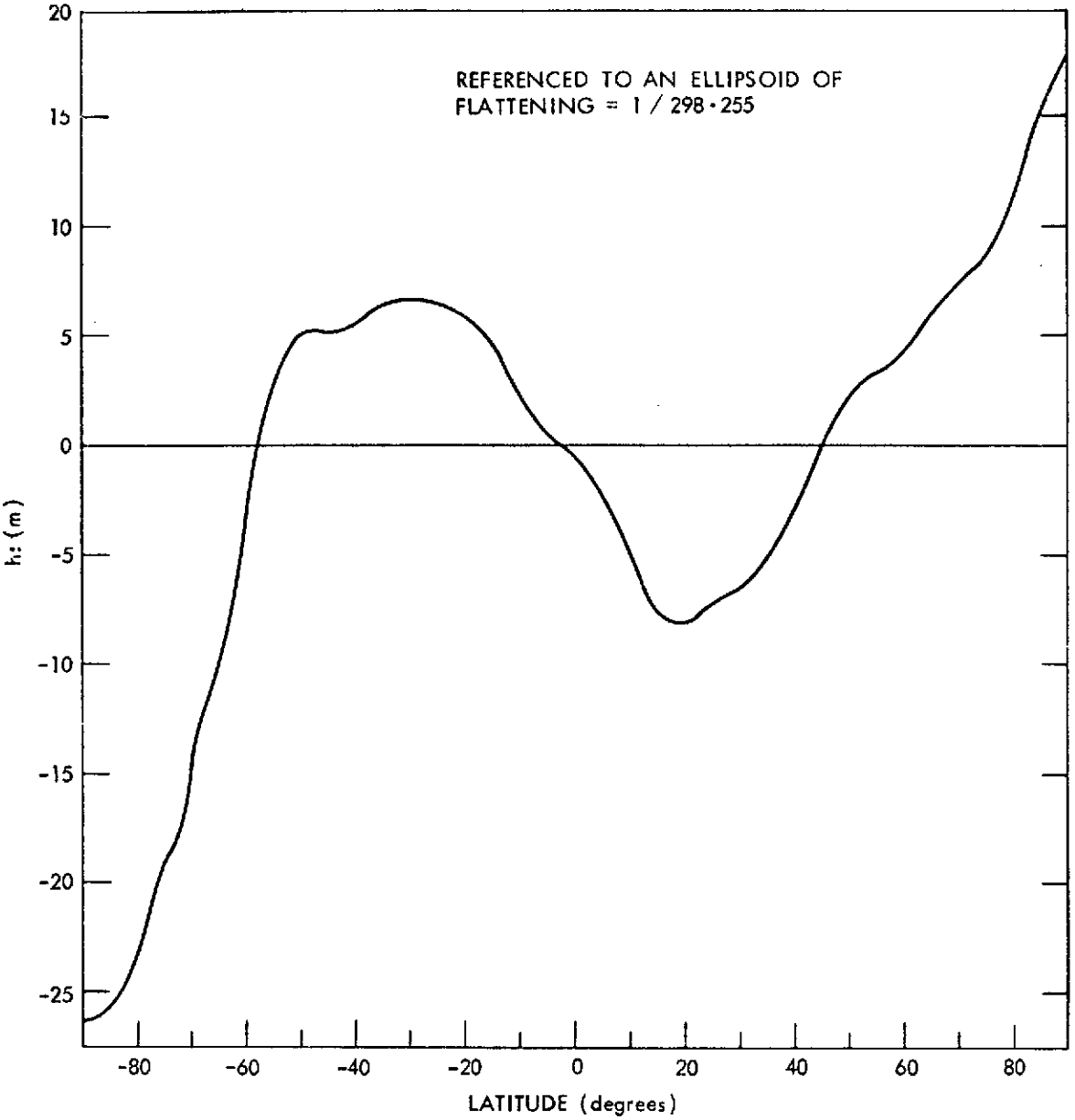

Figure 9. Zonal Geoid Profile for WAG 72

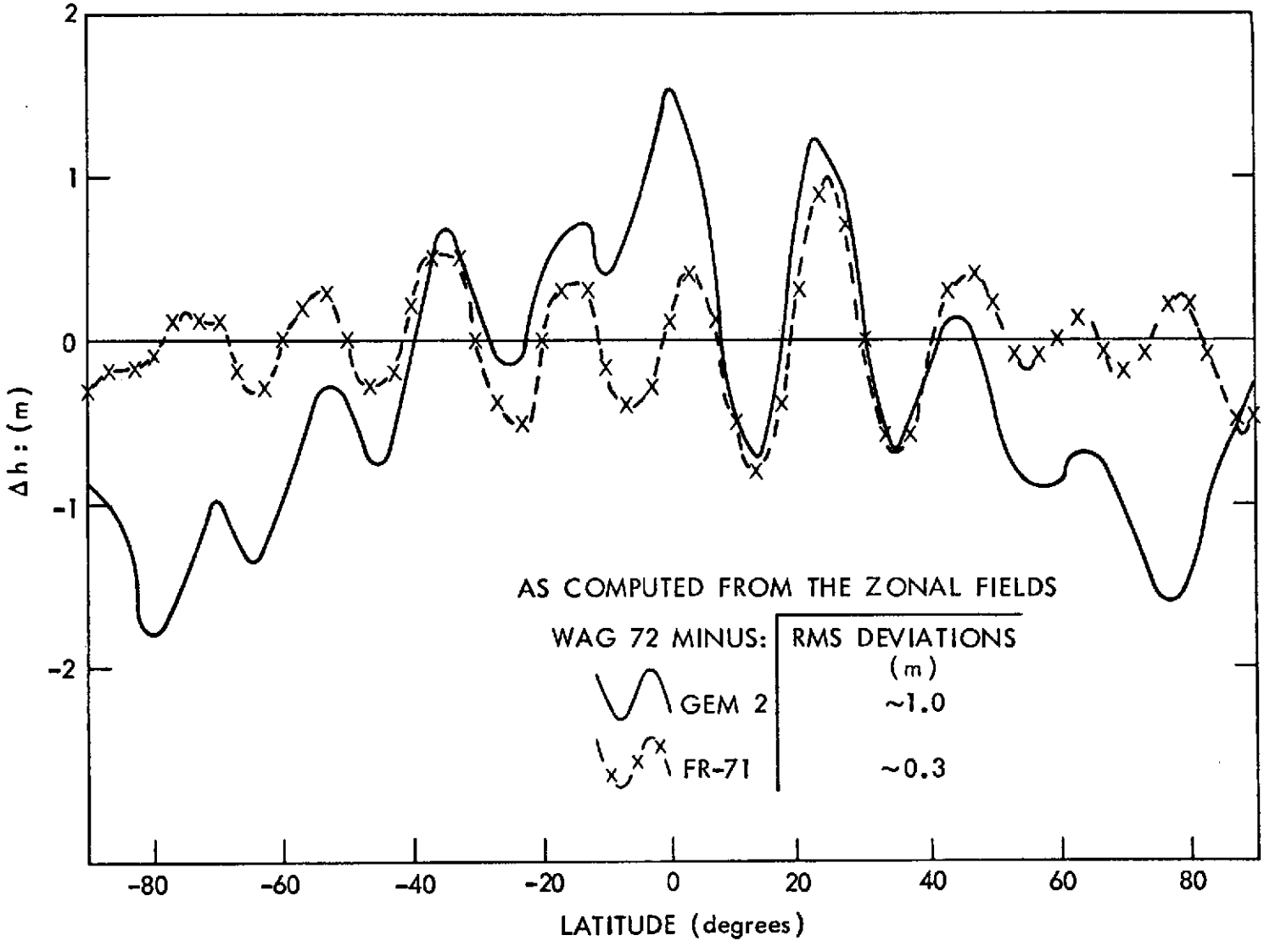

Figure 10. Differences in Zonal Geoid Profiles

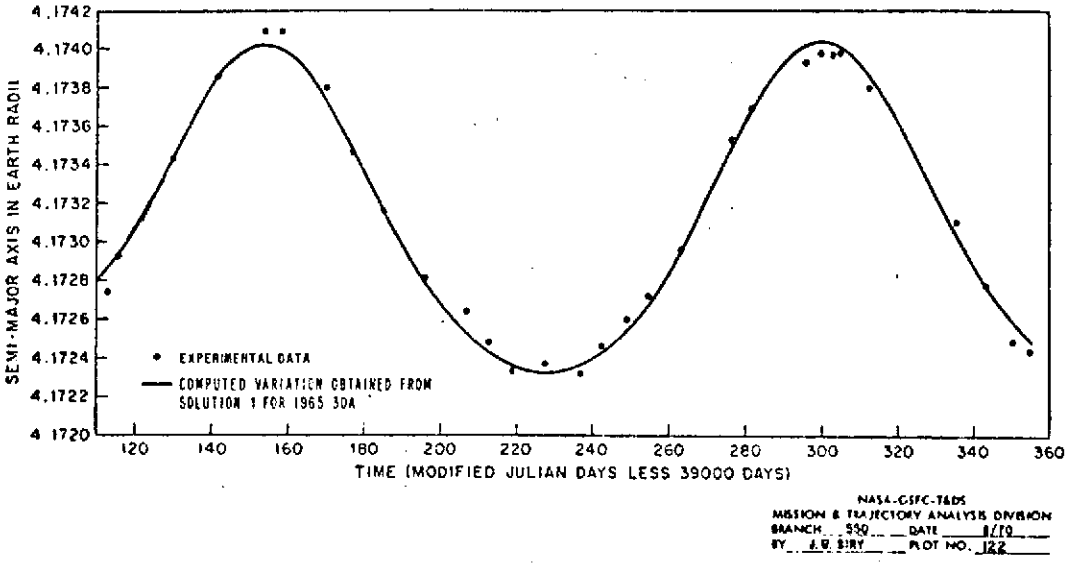

Figure 11. Semi-Major Axis of 1965 30A [Molniya] vs. Time

substantial improvement is obtained in residuals for synchronous and semi-synchronous satellites by solving for five pairs of tesseral harmonic coefficients in the context of a recent SAO general field. Improved values for low order harmonics which represent these features, and for the general field as a whole, can accordingly be expected to result from the inclusion of these added data in subsequent solutions in the GEM series.

Higher order resonances have been studied by somewhat different methods. Use has been made, for example, of general perturbation approaches such as those discussed in references 21, 24, 28 and 25 through 37.

An example of results of such a determination of resonant harmonic coefficients based on Minitrack data is indicated in Figure 15. The influence of this satellite is also reflected in overall general solutions in the GEM series.

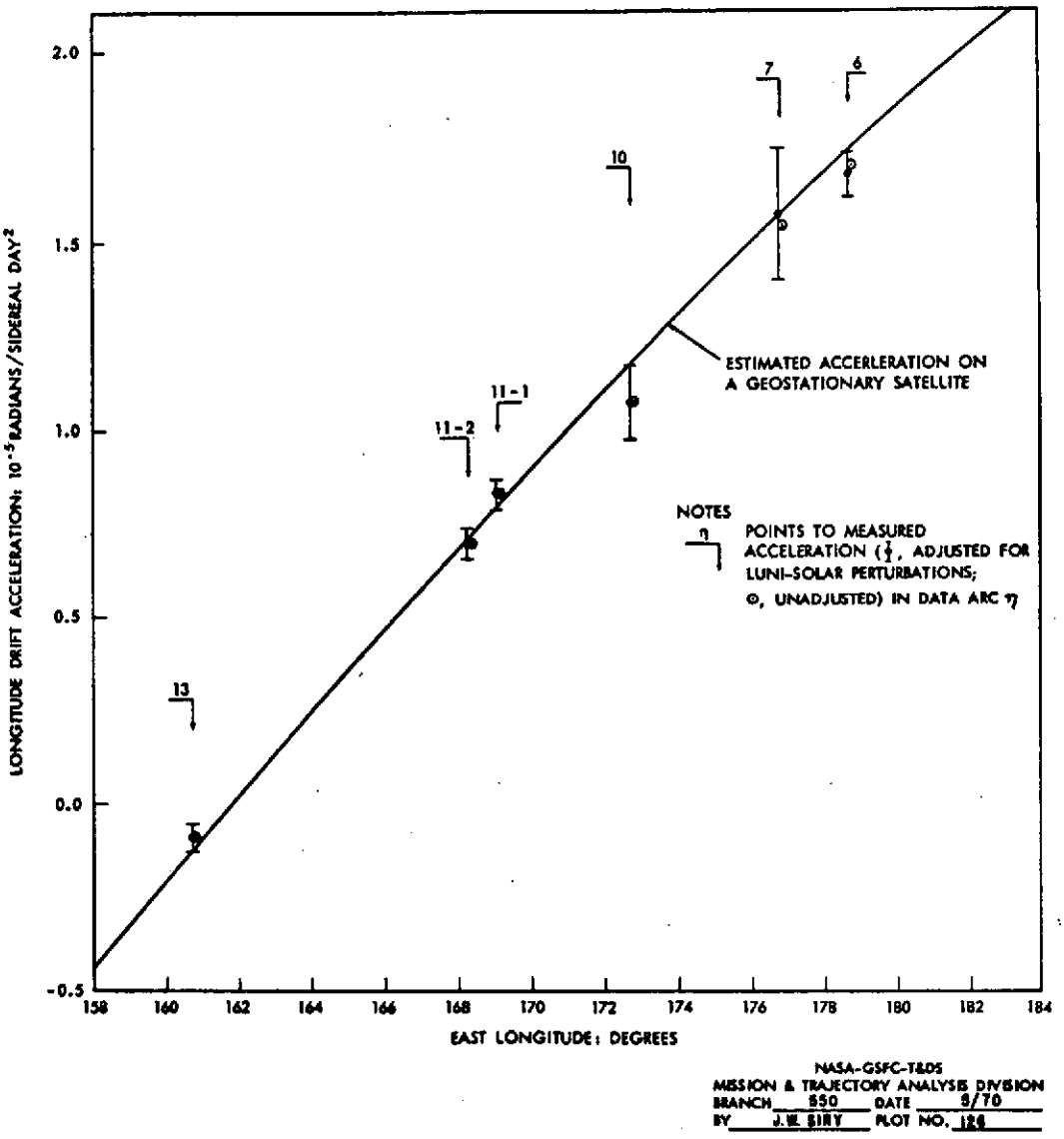

Figure 12. Drift Acceleration in Syncom 3 Arcs 6, 7, 10, 11 and 13

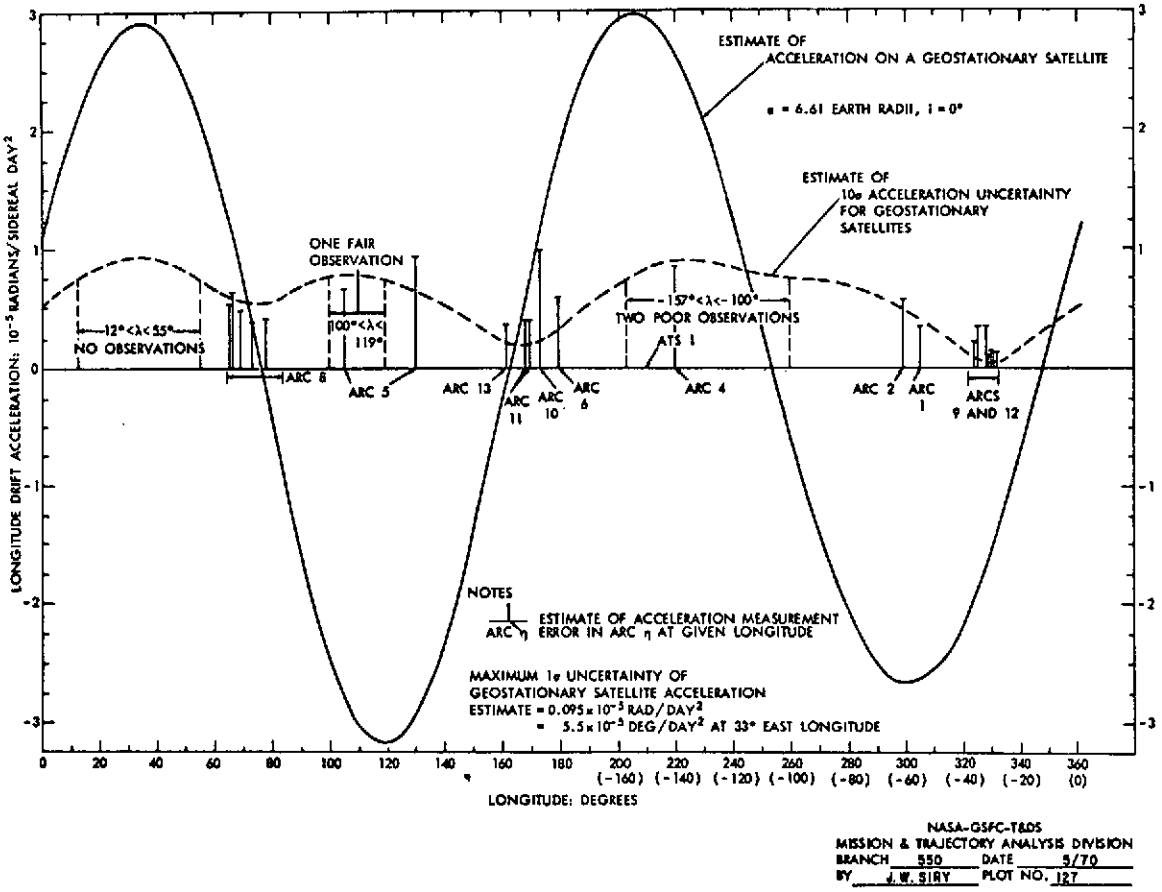

Figure 13. Drift Acceleration and Estimate of Acceleration Uncertainties on 24 Hour Satellites

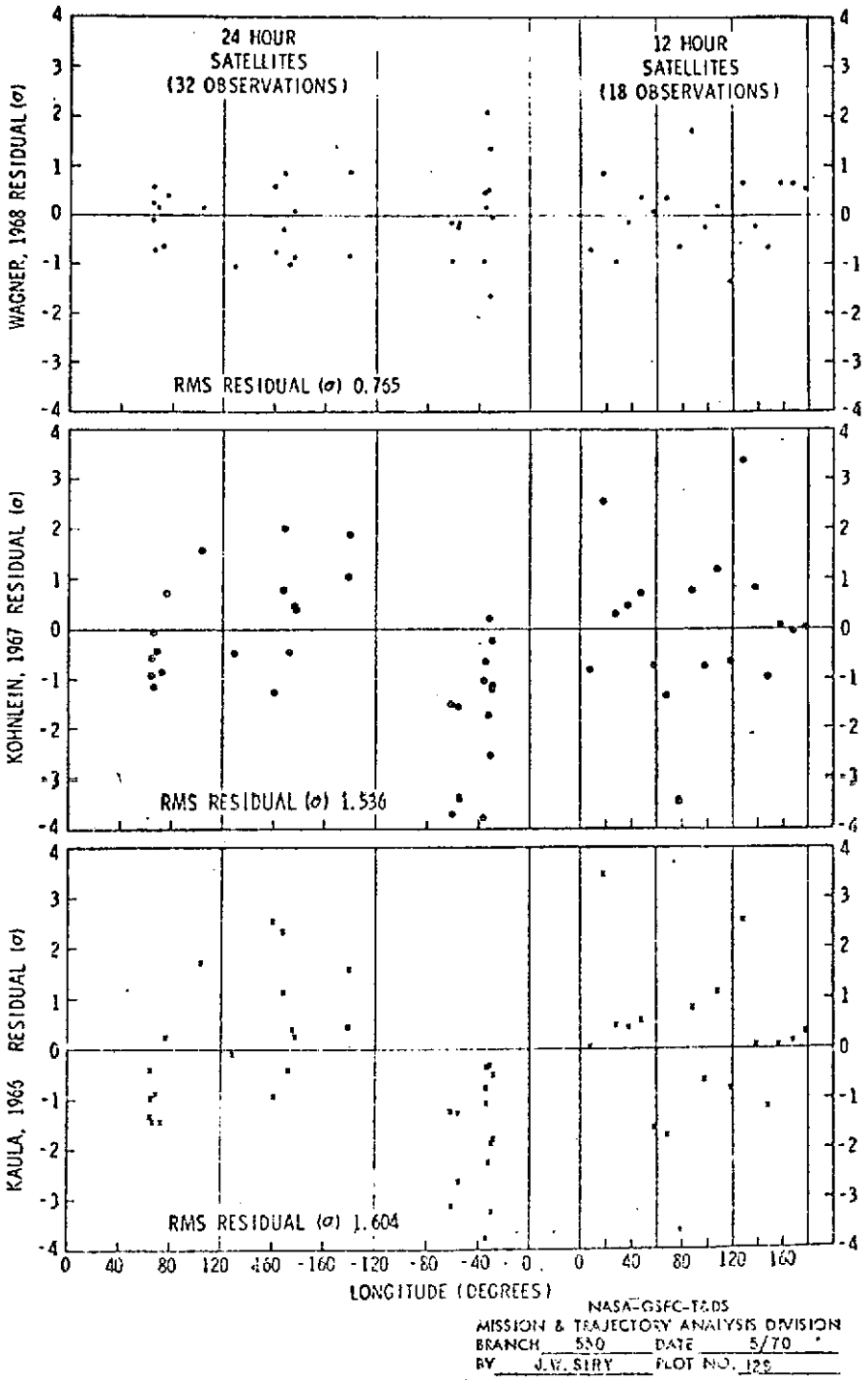

Figure 14. Observation Residuals for 12- and 24-Hour Satellite Accelerations from Recent Geoids

Table XII

Resonant Longitude Gravity Coefficients* from Recent Studies

Geoid	C_{22} (10^{-6})	S_{22} (10^{-6})	C_{31} (10^{-6})	S_{31} (10^{-6})	C_{32} (10^{-6})	S_{32} (10^{-6})	C_{33} (10^{-6})	S_{33} (10^{-6})	C_{42} (10^{-6})	S_{42} (10^{-6})	C_{44} (10^{-6})	S_{44} (10^{-6})
Köhnlein	2.38	-1.35	1.71	0.23	0.84	-0.51	0.66	1.43	0.35	0.48	0.04	0.30
Kaula [1966]	2.42	-1.36	1.79	0.18	0.78	0.75	0.57	1.42	0.30	0.60	-0.06	0.32
Wagner	2.40 ± .03	-1.43 ± .03	-0.42	-1.58	0.69 ± .20	-0.53 ± .20	0.16	1.10	0.0	0.0	0.02	0.70

*Fully normalized coefficients.

Resonances have also been determined by means of a numerical integration approach. Results of this kind are indicated in Figures 16 and 17 in reference 26.

E. Tracking Station Locations

Dynamical determinations of tracking station locations were carried out in the Goddard Space Flight Center prior to the derivation of the GEM solutions.[38-41] Some indications of the coverage provided by the thirty thousand observations employed in a recent determination is indicated in Table XV and XVI and Figure 18. Results are presented in reference 41.

F. Geoid Studies

A detailed gravimetric geoid from North America to Eurasia has been derived by Vincent, Strange and Marsh by combining information resulting from both satellites and surface gravity studies.[42] A comparison of this result with the geoid based on the SAO 69 (II) field is seen in Figure 19.

Table XIII

24 Hour Satellite Arcs in 1970 Resonant Geopotential Solutions

SATELLITE	ARC	NUMBER OF KEPLER ELEMENT SETS USED	SPAN OF DATA (modified Julian Days)	GEOGRAPHIC LONGITUDE SPAN IN ARC (degrees)	ORBIT INCLINATION (degrees)	ESTIMATE OF QUALITY OF DETERMINATION OF THE GEOGRAPHIC LONGITUDE, σ (λ), IN ARC, FROM INDIVIDUAL ARC ANALYSES (degrees)	RMS RESIDUALS IN LONGITUDE FROM COMBINED ARC SOLUTIONS (degrees)		
							WITH 24 HOUR SATELLITES ALONE, SOLVING FREELY FOR 6 RESONANT COEFFICIENTS	WITH 24 HOUR SATELLITES COMBINED WITH SAO 1969 COSPAR DATA, IN CONSTRAINED SOLUTION FOR 10 RESONANT COEFFICIENTS	WITH SAO 1969 COSPAR FIELD ALONE
SYNCOM 2	1	16	38263-38351	302-305	33.0	0.025	0.013	0.013	0.013
SYNCOM 2	2	11	38361-38443	296-301	32.8	0.025	0.034	0.034	0.035
SYNCOM 2	4	9	38510-38570	196-243	32.5	0.020	0.015	0.014	0.014
SYNCOM 2	5	24	38580-38807	72-189	32.3	0.035	0.039	0.038	0.035
SYNCOM 2	8	15	38816-38918	65-68	31.8	0.020	0.018	0.018	0.018
SYNCOM 2	DoD	42	38816-40104	65-86	29-32.0	0.040	0.037	0.038	0.103
SYNCOM 3	6	9	38699-38750	178-180	0.0	0.015	0.014	0.015	0.013
SYNCOM 3	7	10	38775-38835	174-181	0.0	0.055	0.054	0.055	0.052
SYNCOM 3	11	16	39075-39262	165-172	0.5	0.020	0.012	0.014	0.013
SYNCOM 3	13	4	39385-39491	160-161	1.3	0.015	0.005	0.006	0.010
SYNCOM 3	14	15	39663-40175	146-160	2-3.0	0.045	0.061	0.061	0.110
ATS 1	1	12	40204-40248	210-211	1.2	0.005	0.001	0.001	0.001
ATS 3	1	12	40197-40241	288-312	0.6	0.005	0.002	0.003	0.003
ATS 3	2	13	40267-40337	287-288	0.3	0.005	0.004	0.003	0.002
ATS 3	3	10	40524-40577	313-315	0.3	0.005	0.002	0.003	0.003
INTELSAT 2-F3	1	12	39607-39905	349-352	1.0	0.025	0.028	0.028	0.030
INTELSAT 2-F3	2	10	40406-40642	346-349	1.0	0.020	0.011	0.012	0.015
INTELSAT 2-F4	1	8	40323-40608	179-194	1.0	0.040	0.043	0.046	0.062
EARLY BIRD	1	11	38897-39080	324-332	0.5	0.025	0.025	0.026	0.026
EARLY BIRD	2	6	39096-39219	321-331	0.8	0.010	0.007	0.009	0.009
ATS 5	1	14	40476-40556	253-256	2.6	0.005	0.004	0.006	0.009

NASA-GSFC-T & DS

Table XIV

Resonant Geopotential Coefficients for 24 Hour Satellites and RMS Fits to 21 Arcs

:UNNORMALIZED COEFFICIENTS IN UNITS OF 10^{-6}:

Field	Overall Weighted RMS Residual in 21 Arc Solution	2,2		3,1		3,3		4,2		4,4	
		C	S	C	S	C	S	C	S	C	S
SAO STANDARD EARTH II (1970)	2.46	1.558	-0.881	2.128	0.281	0.096	0.199	0.074	0.158	-0.0017	0.0072
SAO COSPAR (1969)	1.38	1.566	-0.896	2.040	0.262	0.096	0.198	0.073	0.148	-0.0028	0.0078
WAGNER (UNCONSTRAINED) 2,2–3,1–3,3 (1970)	0.849	1.568	-0.907	1.687	0.483	0.103	0.204	0.074	0.158	-0.0017	0.0072
WAGNER–SAO COSPAR (CONSTRAINED) (1970)	0.896	1.570	-0.908	2.029	0.267	0.098	0.205	0.075	0.150	-0.0029	0.0079

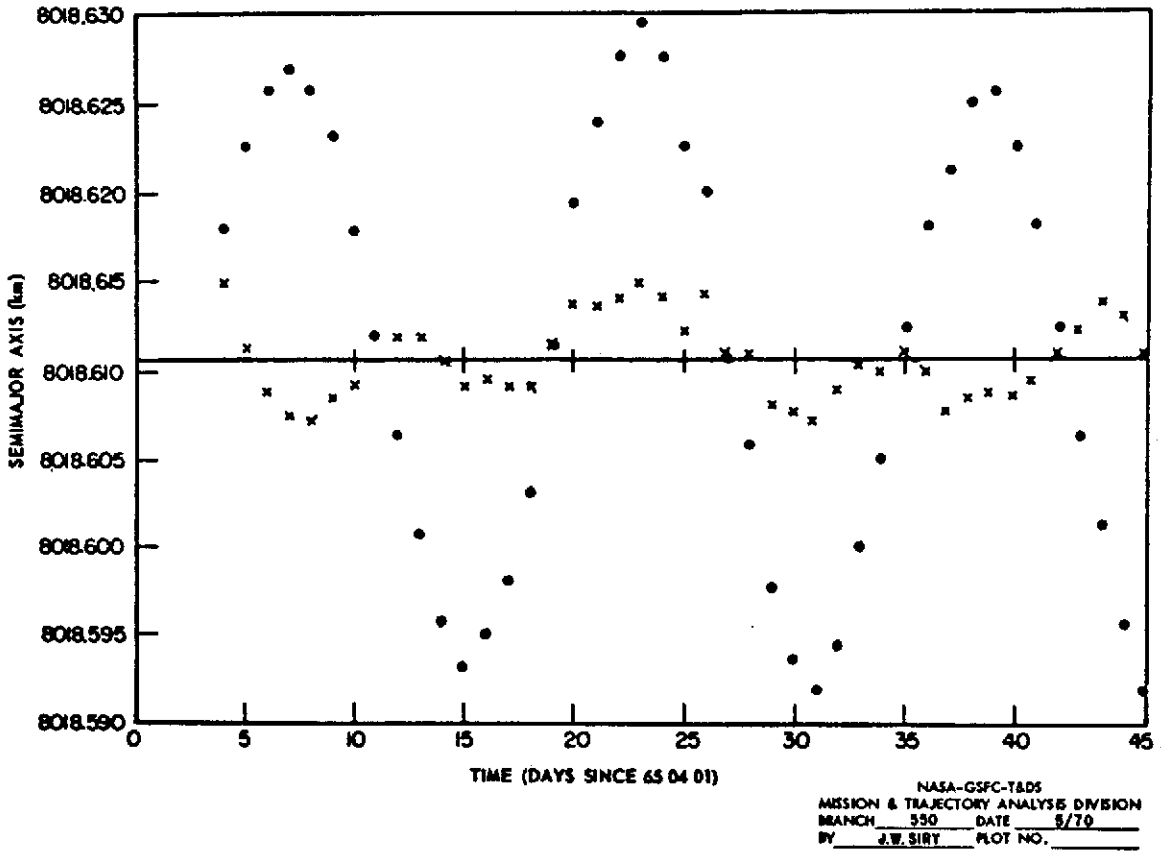

Figure 15. Semimajor Axis of Tiros IX

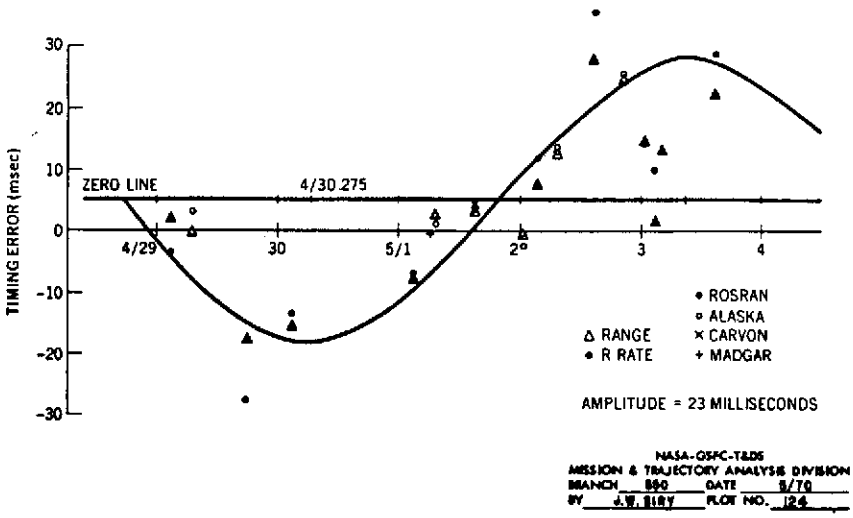

Figure 16. Apparent GEOS-II GRARR Timing Errors SAO M1 Gravity + APL 13th-Order Terms 4/29/68-5/4/68

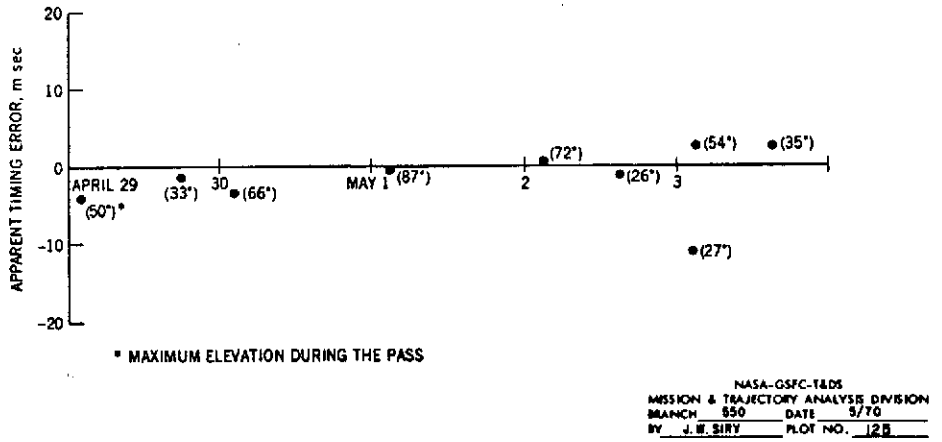

Figure 17. Apparent Rosman Range Timing Errors with SAO M1 Gravity, APL 13th-Order Coefficients and $C_{14,13} = 0.57 \times 10^{-21}$, $S_{14,13} = 6.5 \times 10^{-21}$, 4/29/68 to 5/4/68

III. THE ANALYSIS OF GEOS-C DATA

A. Satellite-to-Satellite Tracking Data

1. The Satellite-to-Satellite Tracking System

The satellite-to-satellite tracking experiment involving a geodetic satellite calls for the tracking of GEOS-C via ATS-F and, later ATS-G. The quantities to be observed are the range from a ground station through ATS-F to GEOS-C, and the corresponding range difference over a small time interval which is often referred to as range rate. The use of these data involves the analysis of the motions of both the GEOS-C and the ATS-F spacecraft. It will be possible to make independent measurements of the range and range rate from the ground tracking station to ATS-F using the basic ATS tracking system. It is anticipated that the ATS-G spacecraft may also be fitted with laser corner reflectors, and hence that this accurate tracking system can also be used to obtain

Table XV

Number of Optical Observations Per Station Used in Dynamical Estimation

Station		Observations
Blossom Point, Md.	(1021)	650
Ft. Myers, Fla.	(1022)	680
Woomera, Australia	(1024)	152
Santiago, Chile	(1028)	264
Mojave, Cal.	(1030)	932
Johannesburg, Un. of So. Afr.	(1031)	623
St. Johns, Newfoundland	(1032)	179
E. Grand Forks, Minn.	(1034)	542
Winkfield, England	(1035)	400
Rosman, N. C.	(1037, 1042)	1015
Orroral, Australia	(1038)	482
Tananarive, Madagascar	(1043)	339
Univ. of N. Dakota, N. D.	(7034)	548
Edinburg, Texas	(7036)	1109
Columbia, Mo.	(7037)	1540
Bermuda	(7039)	448
San Juan, P. R.	(7040)	475
Greenbelt, Md.	(7043)	158
Denver, Colo.	(7045)	573
Jupiter, Fla.	(7072)	516
Sudbury, Ontario	(7075)	699
Kingston, Jamaica	(7076)	388

Table XVI

GRARR and Laser Arcs Used in Solutions

1968 ARCS

Date	ULASKR			MAYGAR			ROSRAN			WALLAS		GODLAS	
	No. of Obs.			No. of Obs.			No. of Obs.			No. of Obs.		No. of Obs.	
	Range	Range Rate	No. of Passes	Range	Range Rate	No. of Passes	Range	Range Rate	No. of Passes	Range	No. of Passes	Range	No. of Passes
4/2-3/68	215	149	3				180	180	3	495	2		
4/26-27/68	136	84	3				313	313	4	119	1		
5/7-8/68	172	172	2				102	102	1	460	2		
5/21-22/68	132	132	2				167	166	4	492	2		
6/9-10/68	262	252	3				277	277	4				
6/11-12/68	182	182	3				456	456	5	588	3		
6/14-15/68	252	252	4				196	197	3				
6/16-17/68	136	136	2				193	194	3				
6/21-22/68	271	271	5				263	279	4	422	3		
6/23-24/68	285	285	5				229	229	4				
9/24-25/68				111	112	2						69	1
9/27-28/68	193	193	3		57	2						38	1
10/4-5/68	200	200	3	105	107	2						70	1
10/6-7/68	271	271	4	186	189	4							
10/8-9/68	67	67	1	177	188	4						318	2
10/21-22/68	132	132	2									312	2
10/23-24/68	202	202	3									437	2
TOTALS	3108	2990	48	579	653	14	2378	2393	34	2536	13	1247	9

1969 ARCS

Date	ULASKR*			CARVON			CRMLAS		GODLAS*	
	No. of Obs.			No. of Obs.			No. of Obs.		No. of Obs.	
	Range	Range Rate	No. of Passes	Range	Range Rate	No. of Passes	Range	No. of Passes	Range	No. of Passes
3/2-3/69	127	127	5	158	158	4	99	2	64	1
3/5-6/69	124	124	3	92	129	2	227	3	366	4
3/11-12/69	99	99	3	232	232	4	190	3	108	2
3/13-14/69	150	150	3	314	379	6	199	3	32	1
3/17-18/69	196	196	5	232	237	5	214	4	234	3
3/29-30/69	92	92	5	170	170	5				
3/31-4/1/69	164	163	4	192	206	1	101	2		
4/8-9/69	75	75	2	167	176	4	146	2	91	3
4/10-11/69	172	172	5	90	143	2	321	4	73	1
4/14-15/69	123	123	3	99	125	3	271	4		
4/24-25/69	199	199	5	150	179	3	251	2	159	1
5/5-6/69	163	163	4	219	280	4	216	4		
TOTALS	1684	1683	47	2115	2414	43	2235	33	1127	16

*Station coordinates held fixed.

SUMMARY

GRARR	No. of Obs.	GRARR Laser	No. of Obs.
range	9862		
range rate	10133	range	7205
number of passes	186	number of passes	71

NAME	LOCATION	INSTRUMENT
ULASKR	Fairbanks, Alaska	GRARR
MAYGAR	Tananarive, Madagascar	GRARR
ROSRAN	Rosman, N.C.	GRARR
CARVON	Carnarvon, Australia	GRARR
WALLAS	Wallops Island, Virginia	Laser
GODLAS	Greenbelt, Maryland	Laser
CRMLAS	Carnarvon, Australia	Laser

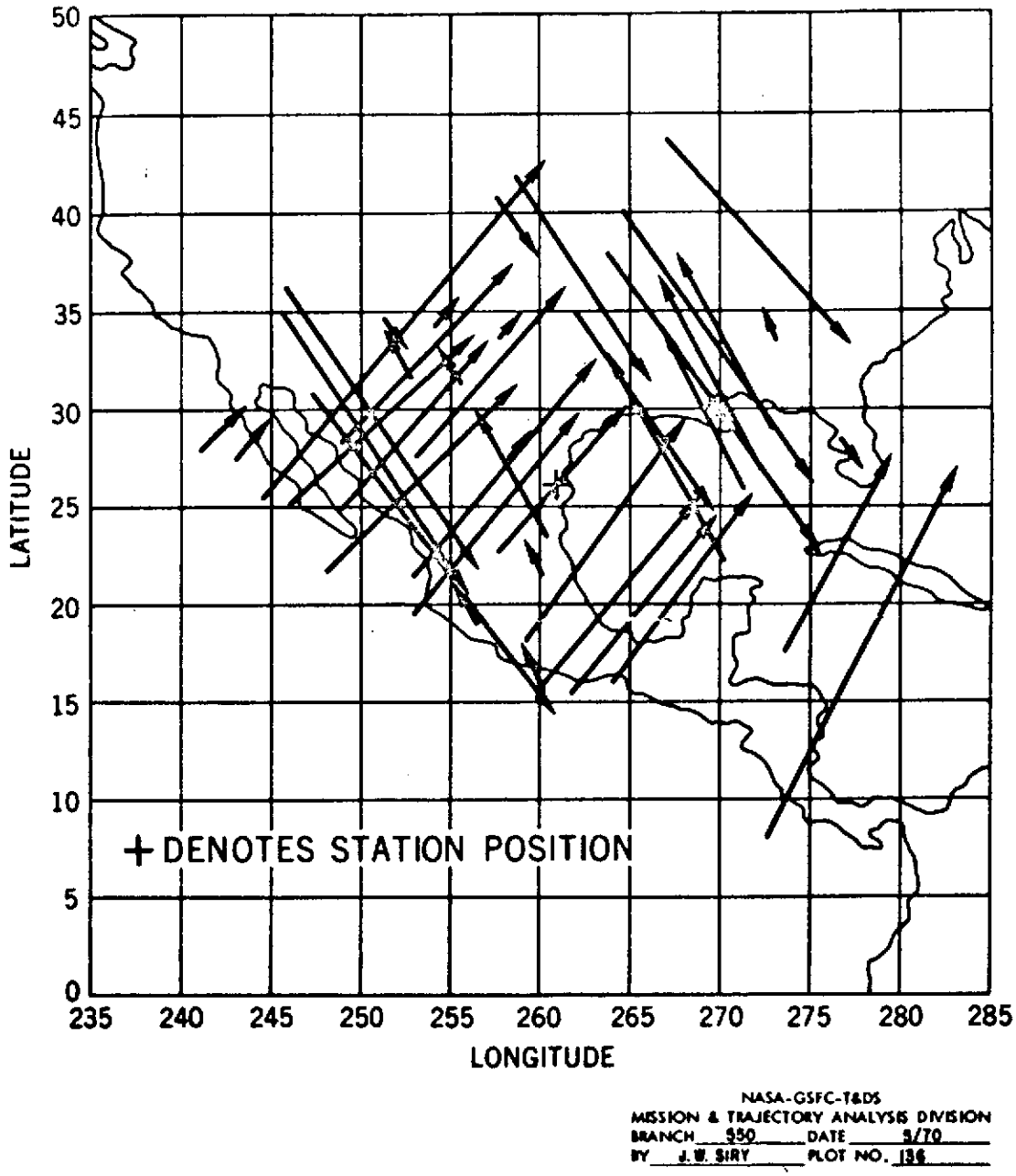

Figure 18. Subsatellite Plot of GEOS-I and GEOS-II Passes, Edinburg, Texas

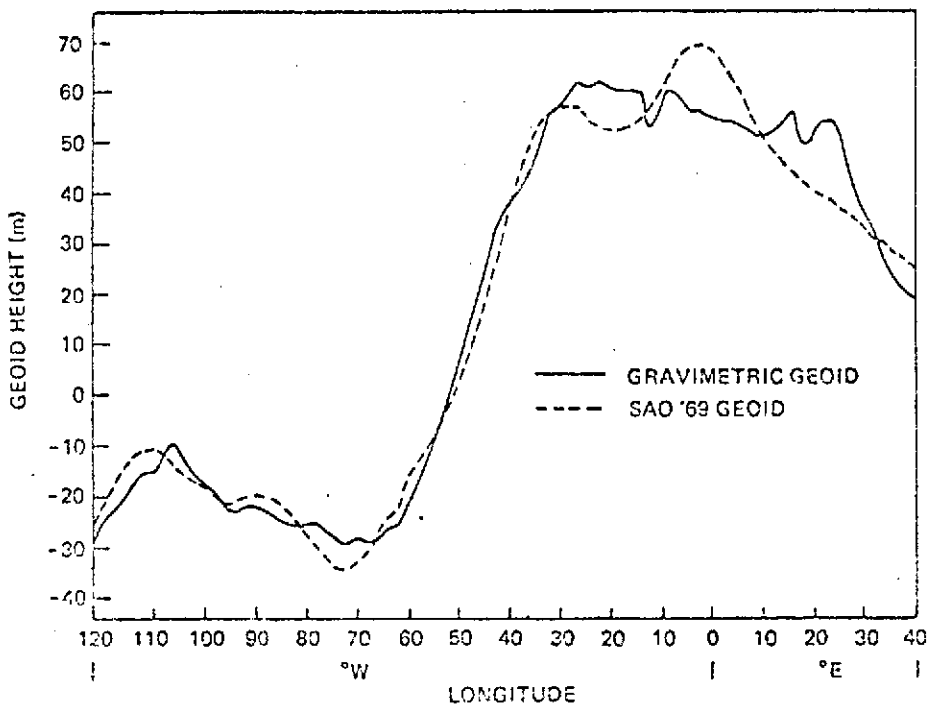

Figure 19. Detailed Gravimetric Geoid and SAO '69 Geoid (Gaposchkin and Lambeck, 1970) at 38° N Latitude

The tracking of GEOS-C from ATS will be analogous in many ways to the tracking of lunar satellites from stations on the earth. The data from lunar orbiters were originally analyzed in conventional ways in terms of spherical harmonic coefficients. It was realized after a time that many of the lunar satellite range rate tracking data residual anomalies correspond to mascons or surface density distributions. This interpretational approach is perhaps one of the most striking features of recent research relating to gravitational fields. (Cf. Figure 20). Both the traditional and the new approaches have been used at Goddard as is pointed out in reference 43 and 44.

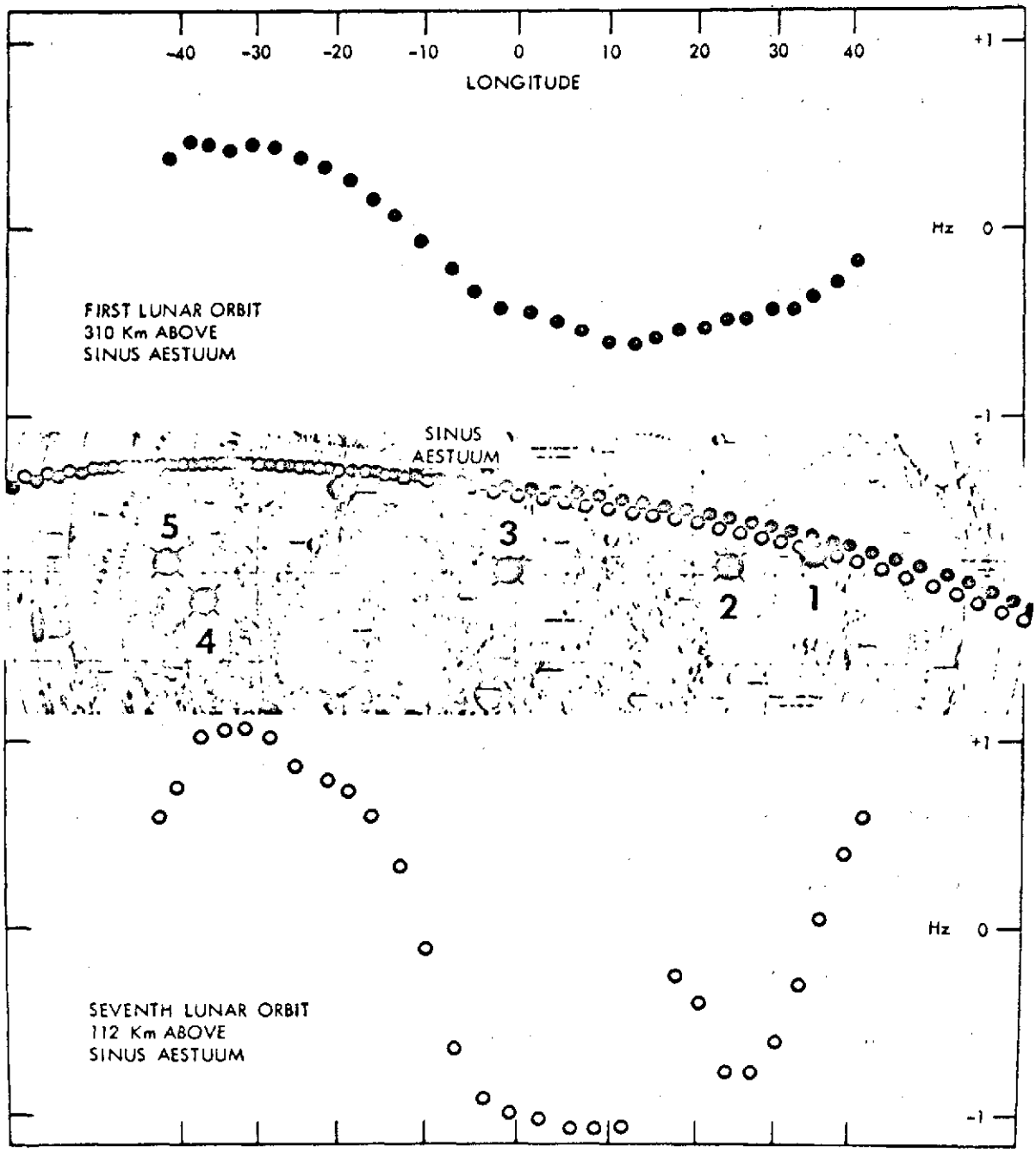

Figure 20. Doppler residuals from Lunar orbits of Apollo VIII on December 24, 1968. The upper and lower portions of the Fig. depict residuals obtained in the neighborhood of Sinus Aestuum during the first and seventh revolutions, respectively. The residuals are plotted vs. position along the retrograde orbit. The positions in the two revolutions are indicated by surface tracks which are correspondingly marked in the central portion of the Fig. The Apollo Lunar landing sites are also shown.

The tracking of a low altitude satellite such as GEOS-C from ATS-F is expected to yield information about the gravitational field which is more detailed in terms of space resolution than that obtainable from the existing sets of satellite data. The degree to which mean gravity anomalies in adjacent squares on the earth's surface can be separated on the basis of satellite-to-satellite tracking data of the ATS/GEOS-C type is a function of the altitude of the low satellite.

The dimension of such a square are roughly comparable to the altitude of the low satellite. This problem has been studied in some detail by Schwartz[45]. Figure 21 depicts the relationship he found between the satellite altitude and the size of the square in which gravity anomalies can be identified by means of satellite-to-satellite tracking techniques. Extrapolation of this result to the general altitude region now planned for GEOS-C, i.e., the neighborhood of 800 to 1000 kilometers, leads to an estimate of the order of six degrees for the spatial resolution capability of the GEOS-C/ATS-F experiment.

The magnitudes of the effects are indicated in Figure 22 for a satellite in a 700 km altitude orbit. It is presently estimated that the ATS-F/GEOS-C tracking system will have an accuracy of about 0.35 mm/sec for a twenty second integration time. The corresponding resolution capability in terms of a mean anomaly in a five-degree square for a satellite in a 700 kilometer altitude orbit is about 4.4 milligals. The implications of this for GEOS-C will be discussed further in Section IV.

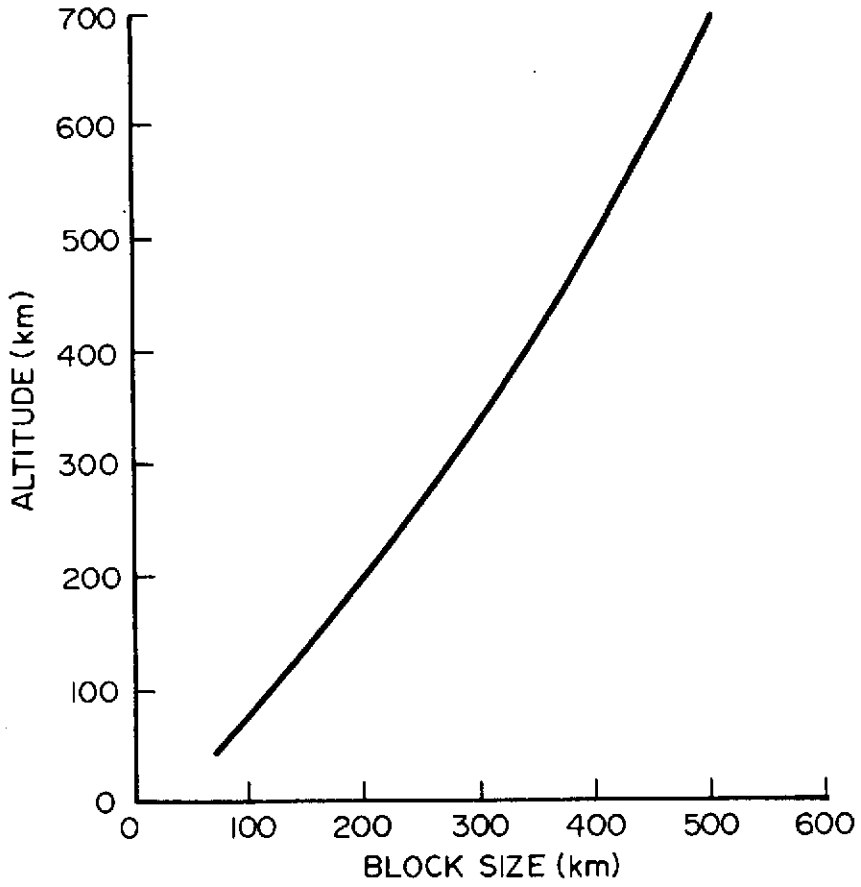

Figure 21.

2. GEOS-C Orbit Selection Considerations

The following discussion is intended to indicate the different kinds of scientific objectives which can be met with a particular selection of a GEOS-C orbit.

It is assumed for the purpose of the case considered here that the GEOS-C orbit will have an inclination of about 115°, i.e., 65° retrograde and a mean altitude in the neighborhood of 800 to 1000 kilometers. The eccentricity will be

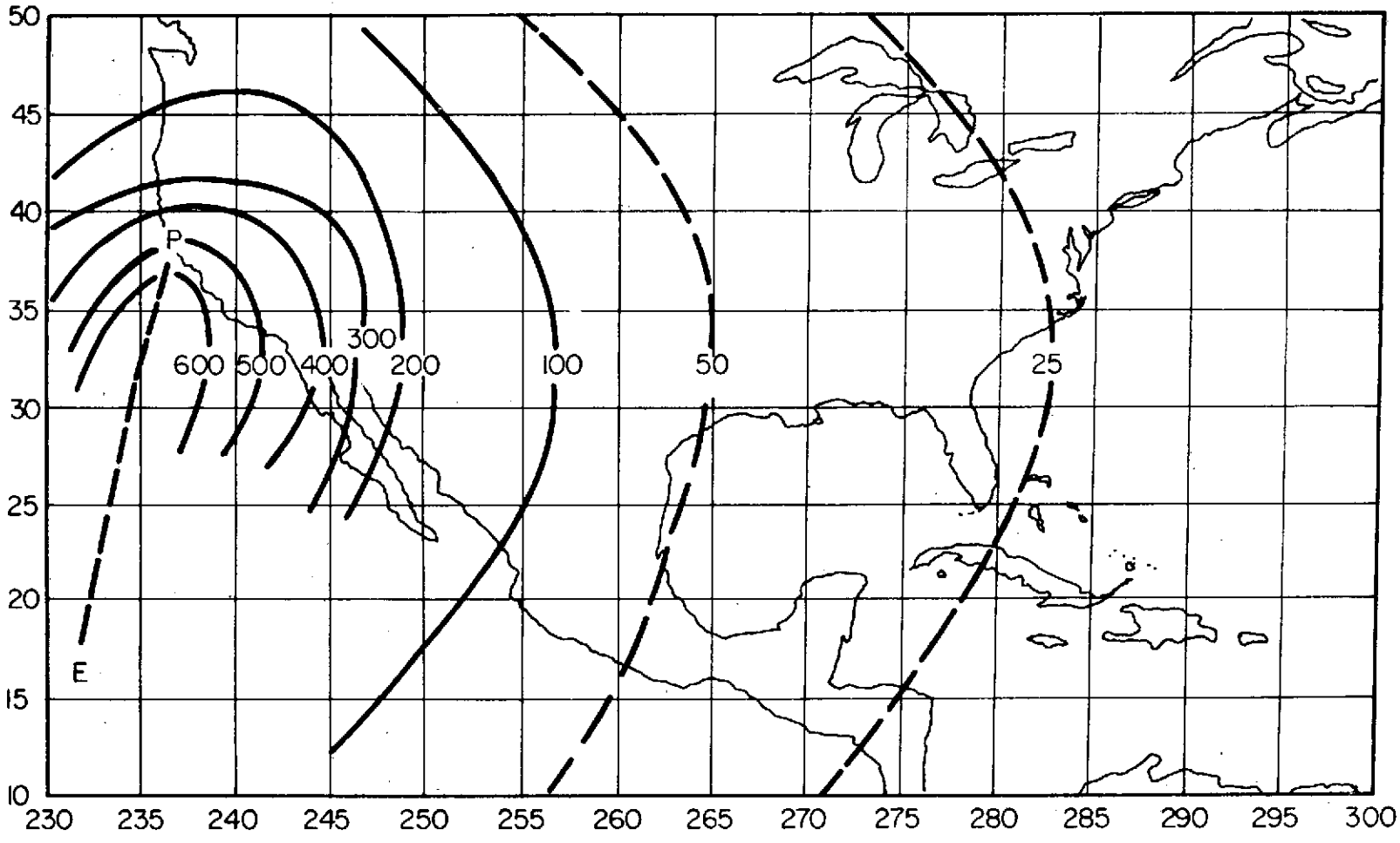

Figure 22. Sensitivities of $\dot{\rho}$ in thousandths of a millimeter per second to φ in milligals. One satellite in a 700 km high orbit is tracked by a very high geostationary satellite. E denotes the position of the low satellite at the initial epoch, and P denotes its position at the epoch for which the partial derivatives are evaluated.

taken to be 0.006 or less, a range which will simplify the altimeter design. One is at liberty to adjust the mean altitude or the period within certain limits in the attempt to achieve as many of the scientific goals as possible. The values finally selected will be governed partly by considerations brought out in the following discussions. They may be somewhat different than those indicated here, however it is not anticipated that the principles underlying the present discussion will be fundamentally changed.

The spatial resolution obtainable with the satellite-to-satellite tracking data in an experiment of the GEOS-C/ATS-F type is about 5.7 degrees for the case considered. Starting from this point, one can work out the following orbit parameters which will accommodate the objectives of a gravimetric geodesy investigation from the standpoints of the gathering of both the satellite-to-satellite tracking data dn altimeter tracking data. It will be seen later that a number of important oceanographic objectives can also be met with the orbit selection which is discussed here.

An orbit having a 65° retrograde inclination, a mean altitude of approximately 1000 km and a corresponding period of about 105 minutes will move westward in longitude by about 26.2° each revolution. This orbit has ground tracking equator crossings which shift to the west about 6.3 degrees per day. The resulting separation between the orbit traces, which is smaller by the factor sin i, is 5.7° which corresponds to the value indicated above. The desired 5.7° survey

pattern is thus approximately traversed in fifty-five revolutions of GEOS-C, on a bit more than four days. It includes a complete set of tracks, crossing the equator in both the ascending and descending directions separated by about 5.7 degrees.

At the beginning of the fifth day, the longitude of the ascending node of the 56th revolution is found to be displaced from that of the first revolution by about a degree, i.e., about a sixth of the daily shift. (Cf. Figure 23). This can be thought of as the beginning of the phase in which the fine, or one-degree, pattern is laid down. The process continues for a total of 344 revolutions, at the end of which the ground track repeats, i.e., the ground tracks of the first and the 345th revolutions would coincide. This, in fact, provides a precise defining criterion for the orbit in the context of the chosen inclination, i.e., 65° retrograde, and eccentricity, namely, about 0.006. Thus, in something over 25 days, such a GEOS-C orbit would provide for an altimeter survey with orbits separated by slightly less than a degree. Since the altimeter cannot operate continuously, due to power limitations, an actual survey of this type would take much longer, perhaps on the order of a year or more.[46]

Clearly other strategies are possible, e.g., by selecting patterns which would give spacings of about 3°,1.5°, etc. The example sketched here will suffice for the purposes of the present discussions, however. Resonances may be associated with some of these choices. A preliminary look at this point

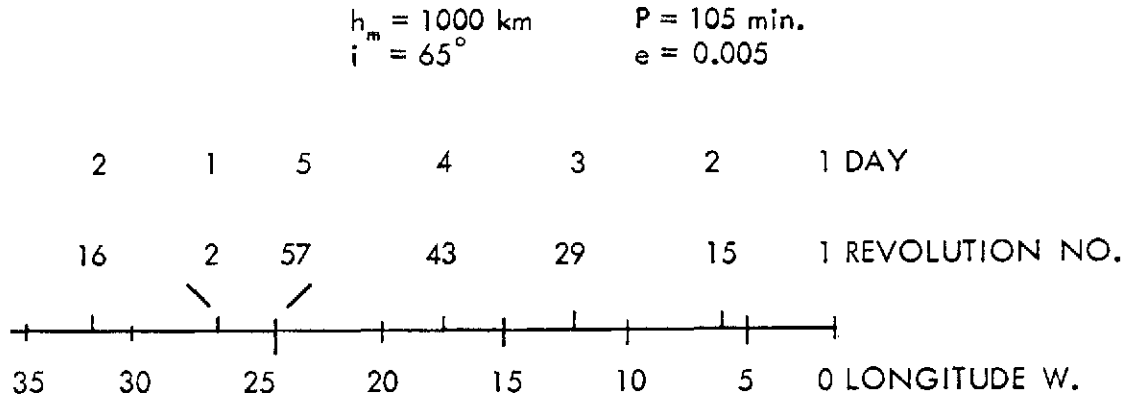

Figure 23. Equator Crossing Pattern for a Typical GEOS-C Orbit

indicates that these will not be unduly severe, however. The degree to which such a specific fine resolution can be realized depends upon the launch vehicle capabilities.

3. Satellite-to-Satellite Tracking Data Requirements

a. Gravimetric Geodesy Analyses

This information about the orbit furnishes the basis for estimating typical data taking requirements. The 6.3 degree separation at the equator implies that some 57 passes will be trackable from ATS while it is in a fixed position.

Half of these correspond to ascending nodes, half to descending nodes. Each pass will be about 58 minutes long. Hence, a total of some 56 hours of satellite-to-satellite tracking would complete such a six-degree survey. Redundant information would be obtained near the maximum latitudes since the tracks are less than 6 degrees apart. In an initial experiment, however, it would probably

be wise, even so, to plan on continuous satellite-to-satellite tracking which should aid considerably in the interpretation of the data.

ATS-F will be at 94° W longitude at first, and then at 35° E longitude. Thus some 112 hours in all would be required to complete the satellite-to-satellite tracking surveys in these two regions. Again, some redundant information will be obtained, since the coverage regions around 94° W and 35° E overlap somewhat. This will provide a valuable opportunity for checks and comparisons.

Some satellite-to-satellite tracking will also be done while ATS-F is enroute between these 2 locations. This will, again, permit correlative studies which will strengthen the overall results. Perhaps another 50 hours or so could be devoted to this pahse of the activity.

b. Orbit Determination Studies

A satellite-to-satellite tracking and orbit determination investigation can involve data taking patterns such as those indicated in Figures 24 and 25.

These data sequences could presumably be abstracted from those indicated above for the scientific investigations. Accordingly, they would not necessarily involve the additional use of the GEOS-C/ATS-F satellite-to-satellite tracking resources.

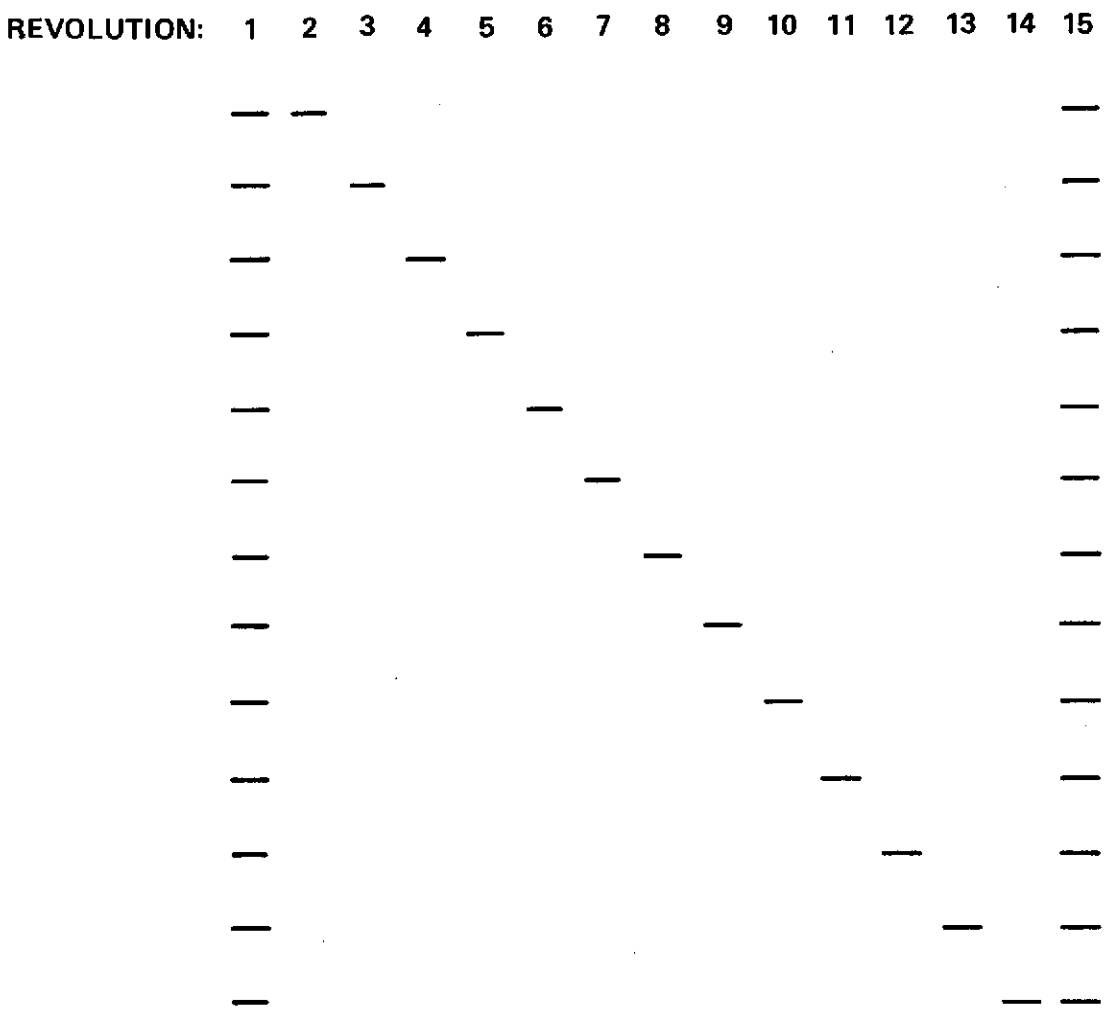

"–" ≡ ONE GEOS-C/ATS-F SATELLITE-TO-SATELLITE TRACKING PASS SPINNING HALF A REVOLUTION

Figure 24. Satellite-To-Satellite Tracking Data for Orbit Determination Analyses

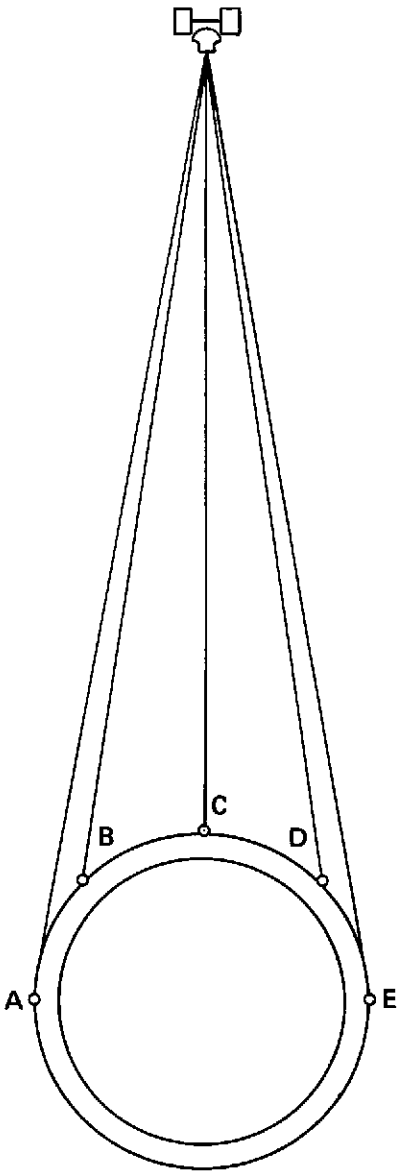

"o" ≡ A ONE-MINUTE GEOS-C/ATS-F SATELLITE-TO-SATELLITE TRACKING PASS. TRACKING PATTERNS SUCH AS THE FOLLOWING WOULD BE OF INTEREST: BD, BCD, ACE, & ABCDE.

Figure 25.

B. Altimeter Data

1. Introduction

It was pointed out above that the altimeter will be useful for both gravimetric and oceanographic investigations and that, to a certain extent, these studies may be inter-twined.

For example, the portion of the gravimetric geodesy investigation which is conducted with the aid of the altimeter will make use of the available knowledge of all of the factors which affect ocean height representation. These include, in addition to the gravitational field, the following oceanographic effects:

1. Tides
2. The General Circulation
3. Currents
4. Sea State
5. Storm Surges
6. Tsunamis

The following discussion is concerned partly with the representation of these oceanographic effects using available information. It is anticipated that each effect represented will also be investigated with the aid of the altimeter data. Thus the above list of oceanographic topics is both a list of effects to be represented, in connection with the gravimetric geodesy investigation, and a list of investigations to be conducted with the altimeter data. These various investigations are thus inter-related. In principle, with enough data, it should be

possible to separate the gravitational effects, which are nearly invariant over the lifetime of the experiment, from the oceanographic ones many of which vary with time in one way or another. In practice, however, it may be some time before enough data are available to make it feasible to effect such a separation without studying the data with both gravimetric and oceanographic thoughts in mind. In other words, it may be advisable that the gravimetric and oceanographic analyses be viewed as coordinated or joint undertakings in some sense. The observational as well as the analytical aspects of the gravimetric and oceanographic investigations may also be approached jointly.

This portion of the discussion is aimed primarily at the gravimetric investigation and the representation of those oceanographic effects which are necessary in order to conduct the gravimetric investigation properly. Portions of the discussion that seemed to be especially likely to involve the possibility of joint planning such as those concerned with the observational programs, for example, do include suggestive thoughts relating to certain aspects of possible oceanographic investigations.

2. Ocean Surface Altitude and Satellite Position Representation

The representation of ocean surface altitudes and satellite positions will be considered in terms of the theoretical formulation, the organization of the calculations, and the specification of physical features associated with gravitational and oceanographic aspects of the earth.

a. Theoretical Formulation

The theoretical formulation of the problem can be considered conveniently with the aid of the following definitions and relations:

$\underline{r}(t)$ ≡ spacecraft position vector

$\underline{h}_n(t)$ ≡ vector normal to reference ellipsoid extending from reference ellipsoid to spacecraft

h_g ≡ height of geoid above ellipsoid of reference

h_s ≡ height of sea surface above geoid

$\underline{R}_n(t) \equiv \underline{r}(t) - \underline{h}_n(t)$

$\underline{h}_g(t) \equiv h_g \underline{h}_n^*(t)$

$\underline{h}_s(t) \equiv h_s \underline{h}_n^*(t)$

$\underline{h}(t) \equiv \underline{h}_n(t) - \underline{h}_g(t) - \underline{h}_s(t)$

$h(t) \equiv |\underline{h}(t)|$

Functional dependences can be indicated further as follows, where the symbols have the meanings specified.

$$\underline{r}(t) = \underline{r}\Big\{t, \underline{e}_0, GM, C_{nm}, S_{nm},$$

$$\rho(h, \varphi, \lambda, t, \odot_a, B_a),$$

$$\odot, \mathbf{c}, \sigma, \pi, \gamma,$$

$$\text{p.m., UT1, } T_e\Big\},$$

where

$$\underline{e}_0 \equiv (a, e, i, \Omega, \omega, m_0),$$

or

$$\underline{e}_0 \sim \underline{r}_0, \underline{v}_0,$$

GM GM = product of gravitational constant and mass of earth,

C_{nm}, S_{nm} = cosine and sine coefficients of spherical harmonic potential terms.

ρ (h, φ, λ, t, $\odot_a$, B_a) = atmospheric density as a function of:

h: height

φ: latitude

λ: longitude

t: time

$\odot_a$: solar activity

B_a: magnetic activity

and where

$\odot$: solar gravitational field

c: lunar gravitational field

σ: radiation pressure

π: precession

ν: nutation

p.m.: polar motion

UT1: earth's rotational position

T_e: earth tides

$$h_g = h_g \left\{ C_{nm}, S_{nm}, g(\varphi_{ij}, \lambda_{ij}), \mu_k, g(\varphi_{pg}, \lambda_{pg}) \right\},$$

where the

$g(\varphi_{ij}, \lambda_{ij})$ denote gravitational anomalies specified in terms of latitude and

longitude regions, the μ_k denote gravitational anomalies specified in terms of mascon parameters, and the $g(\varphi_{pq}, \lambda_{pq})$ denote gravitational anomalies specified either directly or in terms of equivalent geoid heights at a number of latitude and longitude points.

Values at intermediate points are found by interpolation. A typical interval size would be specified as an integral multiple of a hundredth of a degree. The interval size may vary up to ten times over the range, and the interval patterns for latitude and longitude would be specified separately. Similar remarks apply to the specification of the order of interpolation. It is estimated that up to ten sets of the type $g(\varphi_{pq}, \lambda_{pq})$ containing a total of 10^5 functional values might be needed initially, and that each of these storage parameters might be an order of magnitude larger for more advanced studies.

The calculation of geoid height quantities, which are based on gravitational field expressions, could be implemented in more than one way. It could be done, for example, by evaluating these expressions at each point of interest. It could, alternatively, be done by evaluating these expressions at a specified set of times, e.g., at the times corresponding to those employed in the numerical integration processes, and by employing numerical procedures to calculate the geoid height quantities at the points of interest. The method could be optimized keeping in mind numerical analysis and computational efficiency considerations.

One or more specified sets of the quantities $g_m(\varphi_{pq}, \lambda_{pq})$, e.g., those associated with features such as trenches, say, would be multiplied by factors, k_m, respectively, which would initially have the value unity, but would be solved for as unknown parameters. Ten to a hundred such quantities could be of interest. Thus, e.g.,

$$h_g = h_g \left\{ C_{nm}, S_{nm}, g(\varphi_{ij}, \lambda_{ij}), \mu_k \right\} + \sum_{m=1}^{n} k_m g_m(\varphi_{pq}, \lambda_{pq}).$$

$$h_s = h_s \left\{ T_e, T_0, h_0(\varphi_{pq}, \lambda_{pq}) \right\},$$

where T_0 denotes ocean tides and the $h_0(\varphi_{pq}, \lambda_{pq})$ denote heights above the geoid of oceanographic and meteorological features, such as currents, tsunamis, and wind and pressure fields, specified at a number of latitude and longitude points. The remarks about interpolation, intervals, arrays and unknowns, k_m, made in connection with the functions $g(\varphi_{pq}, \lambda_{pq})$, etc., apply in analogous fashion to the functions $h_0(\varphi_{pq}, \lambda_{pq})$, etc. Other functions may also be used to represent oceanographic and meteorological phenomena. $\underline{R}_n(t) = \underline{R}_n(t, R_e, f)$, where R_e denotes the mean equatorial radius, and f denotes the flattening.

The quantities $\underline{r}$, h_g, h_s, and $\underline{R}_n$, will in general, be functions of unknown parameters which can be identified or associated with the indicated arguments. These unknown and any others involved, will be denoted here simply by x_i. The partial differential coefficients can be found with the aid of methods and expressions employed in systems such as the Goddard Trajectory Determination System

(GTDS), the Goddard General Orbit Determination System, Geostar, etc. That which is obtainable involves the use of numerical differentiation, numerical integration, or analytic theory, as appropriate.

$$\frac{\partial h}{\partial x_i} = \frac{\partial \underline{r}}{\partial x_i} \cdot \underline{h}^* - \frac{\partial \underline{R}_n}{\partial x_i} \cdot \underline{h}^* - \frac{\partial h_g}{\partial x_i} - \frac{\partial h_s}{\partial x_i}.$$

Here, for example,

$$\frac{\partial h_g}{\partial k_m} = g_m (\varphi_{pq}, \lambda_{pq}),$$

for $m = 1, 2, \ldots, n$.

$\partial \dot{h}/\partial x_i$ can be derived, for example, numerically by differencing over a suitable time interval, e.g., one which corresponds to the measurement interval. The determination of the time to be associated with the derived quantity can be made by an appropriate method. Alternatively, such a measure may be regarded directly as a height difference over a finite time interval and treated accordingly.

b. The Organization of the Calculations

The organization of the partial derivative calculations is indicated in Figure 26 and Table XVII. The notation of Figure 26 corresponds to that employed in reference 37.

c. The Specification of Physical Features

Analysis of the altimeter data involves the representation of the gravitational field and of the types of oceanographic effects which were listed above in the introduction to this section.

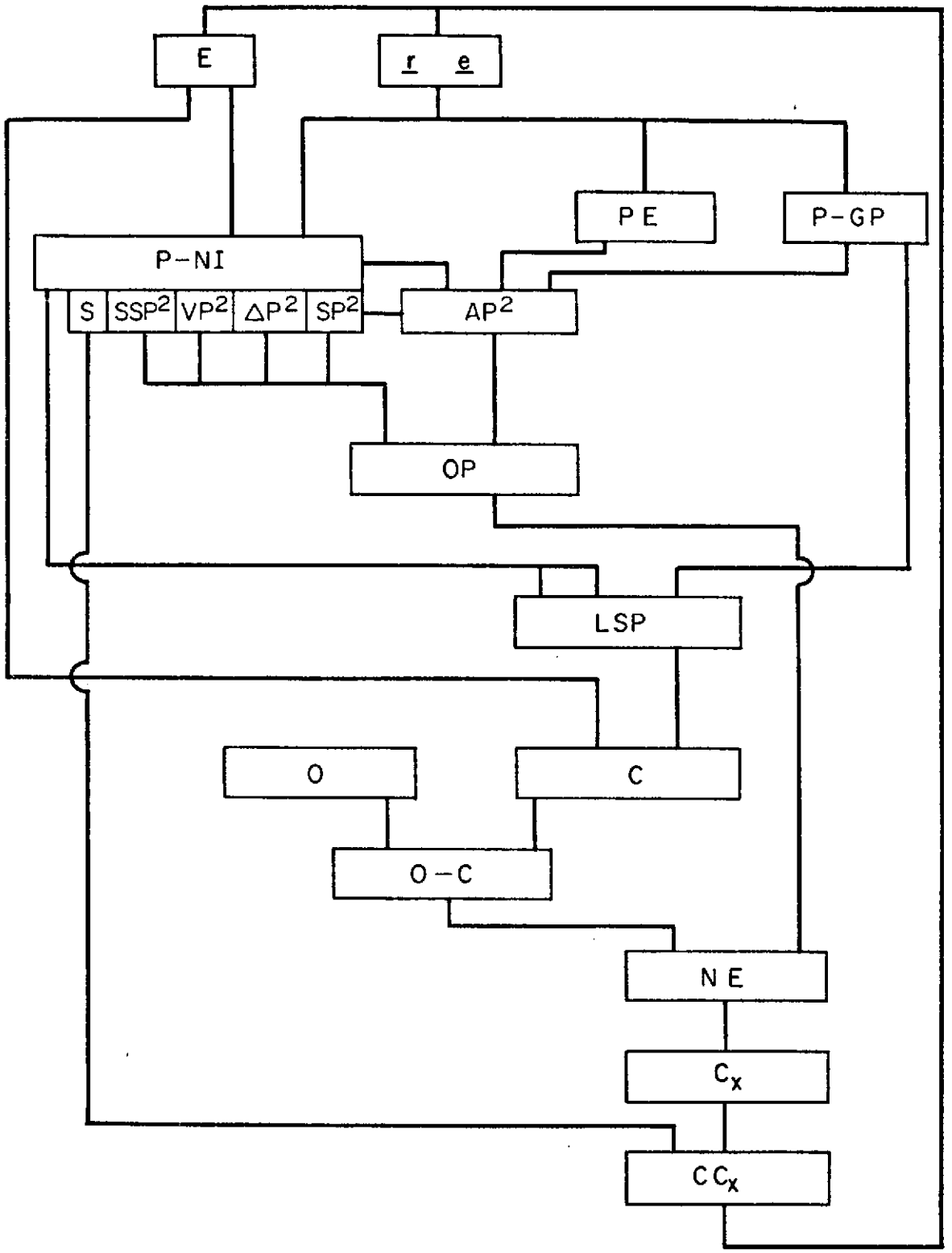

Figure 26.

Table XVII

	$\underline{r}$	$\underline{R}_n$	h_g	h_s
$aei\Omega\omega M_0$	√			
GM	√			
$C_{nm}\ S_{nm}$	√		√	
$\rho\ \sigma$	√			
○ **c**	√			
$\pi\ \nu$	√			
PM UT1	√			
Tides	√			√
Anomalies	√			
Regions	√		√	
Mascons	√		√	
Features	√		√	
Trenches	√		√	
Ref.		√		
Currents				√
Storm Surges				√
Tsunamis				√
Winds				√
Pressures				√

It will be assumed for the purposes of this portion of the discussion that the GEOS-C altimeter will be capable of instrumental resolution at the 2 meter level in a global mode and at the 0.5 meter level in a intensive or local mode.

i. The Geoid

The broad features of the geoid are given by satellite analysis. Typical representations are seen in Figure 4.

Detailed studies of the geoid in certain regions have been conducted by a number of investigators including Von Arx, Talwani, Uotila, Rapp, Strange, Vincent, Berry, and Marsh.[42, 47-51] An indication of the availability of results in several regions of interest off the East and Gulf Coasts of the United States is presented in Figure 27. An example of such a detailed geoid, and a satellite geoid for the same region, are seen in Figures 28 and 29.[52, 18]

ii. Tides

The departure of the ocean surface from the geoid can be thought of in terms of tidal phenomena and the features of the general circulation, including current patterns and more vaiable features associated with currents such as the meanders of the Gulf Stream.

Tidal phenomena have been studied by Hendershott, Munk and Zetler[53, 54]. Hendershott and Munk describe a model involving a number of amphidromic points which can be obtained by solving the Laplace Tidal Equations (LTE) in

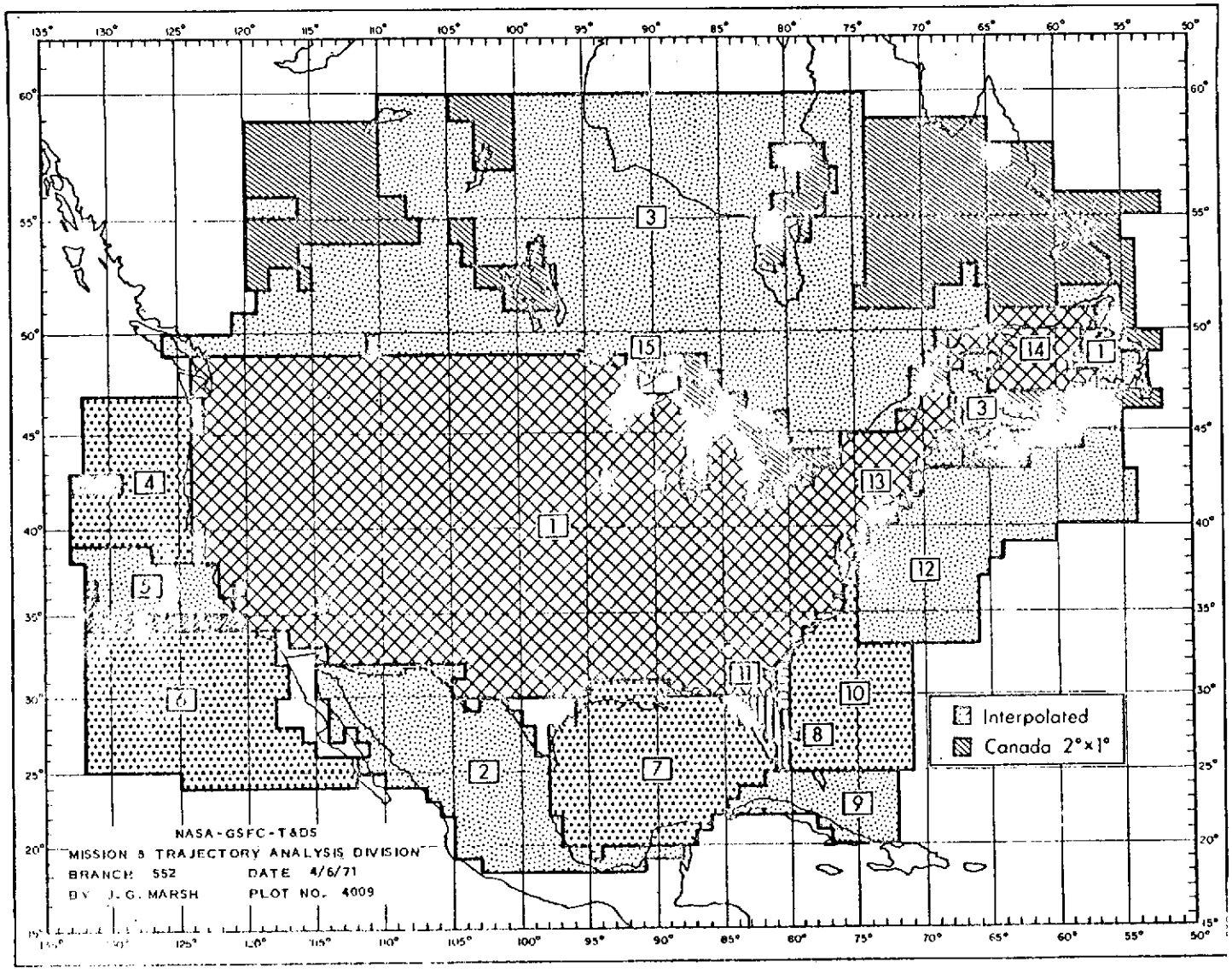

Figure 27. Area of Surface Gravity Coverages

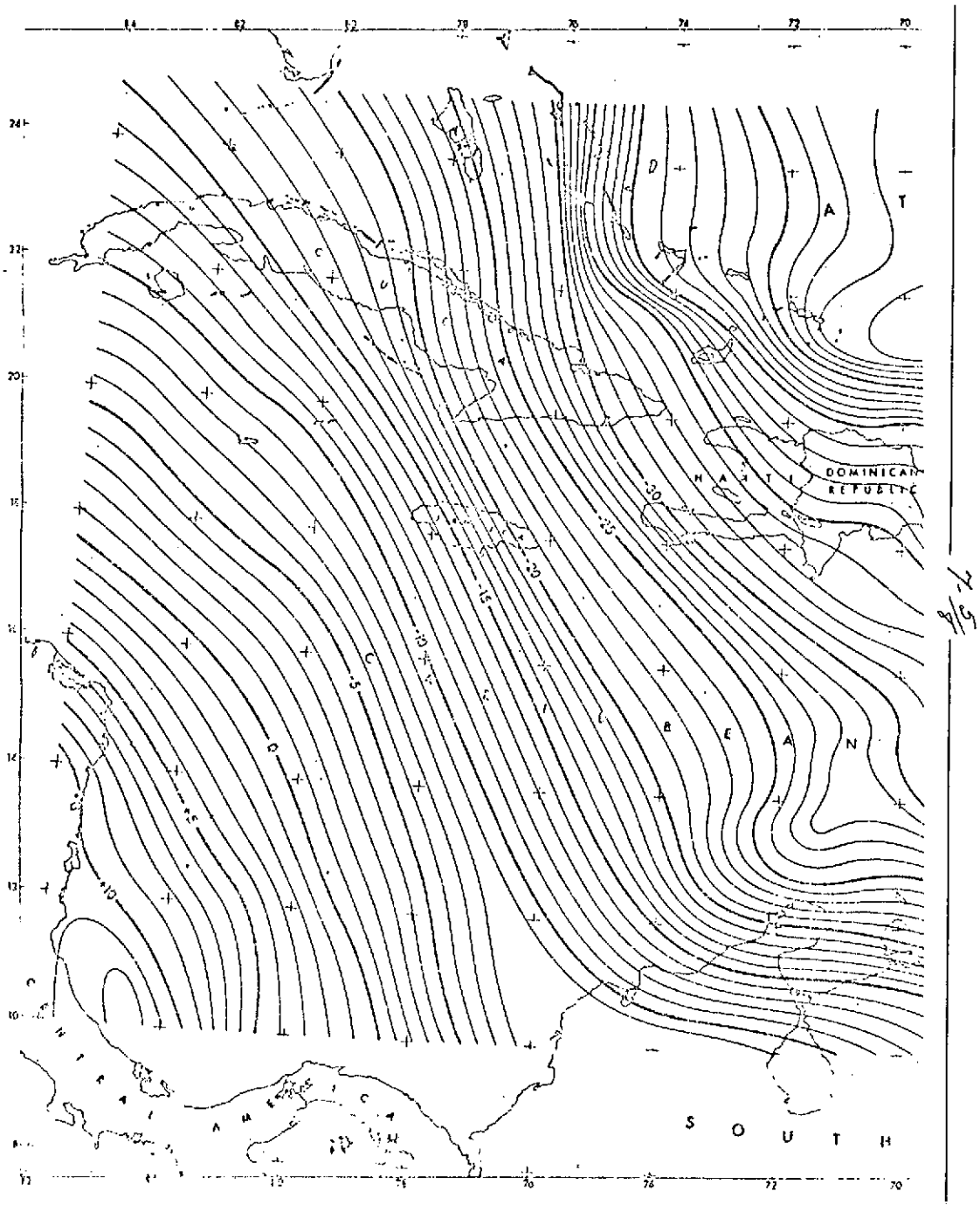

Figure 28a.

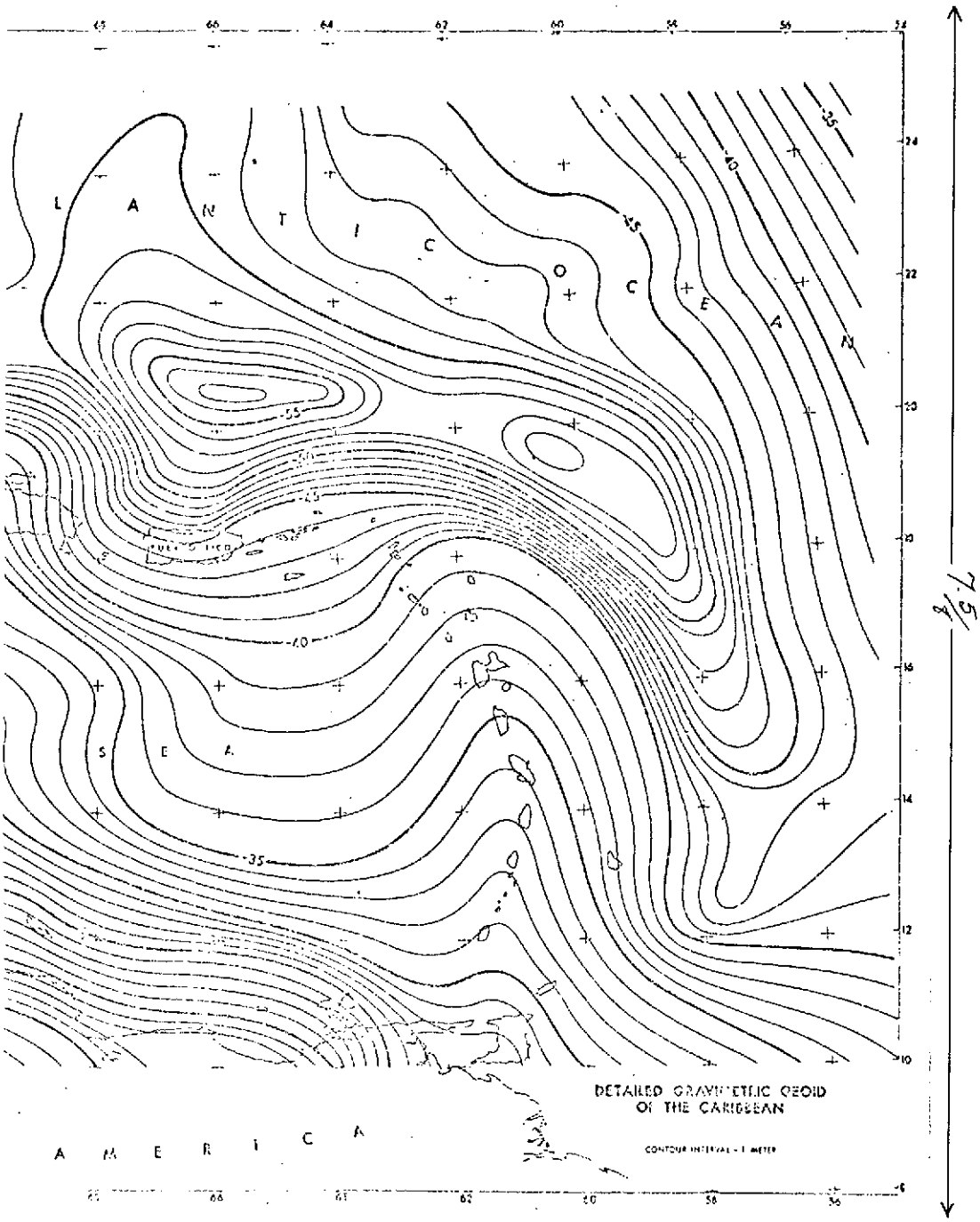
L A N T I C O C E A N
S E A
A M E R I C A
DETAILED GRAVIMETRIC GEOID
OF THE CARIBBEAN
CONTOUR INTERVAL = 5 METER
-35
-40
-45
-55
7.5"/°

Figure 28b.

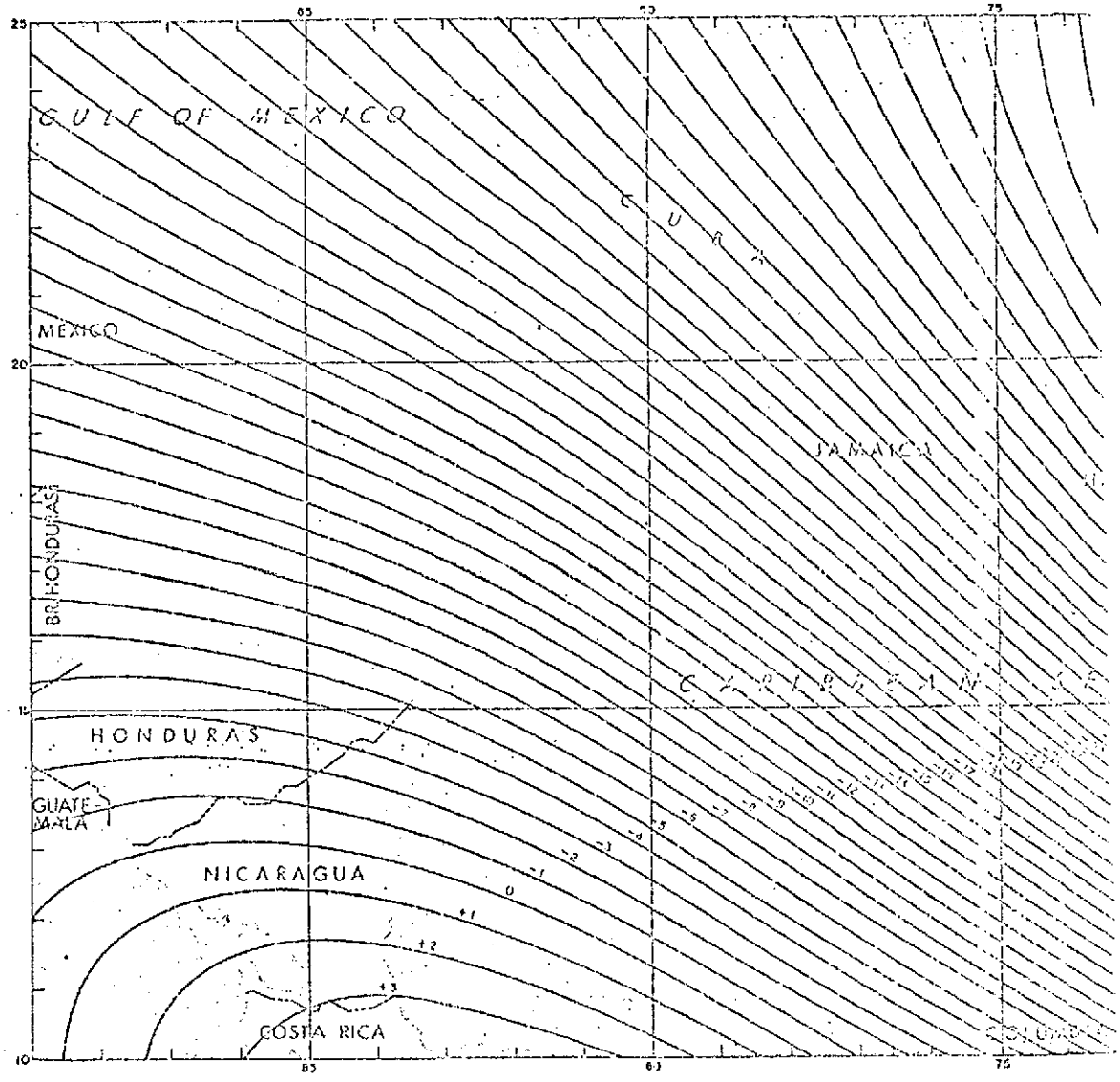
GULF OF MEXICO
CUBA
MEXICO
JAMAICA
BR. HONDURAS
HONDURAS
GUATE-
MALA
NICARAGUA
COSTA RICA
COLOMBIA
25
20
15
10
85
80
75

Figure 29a.

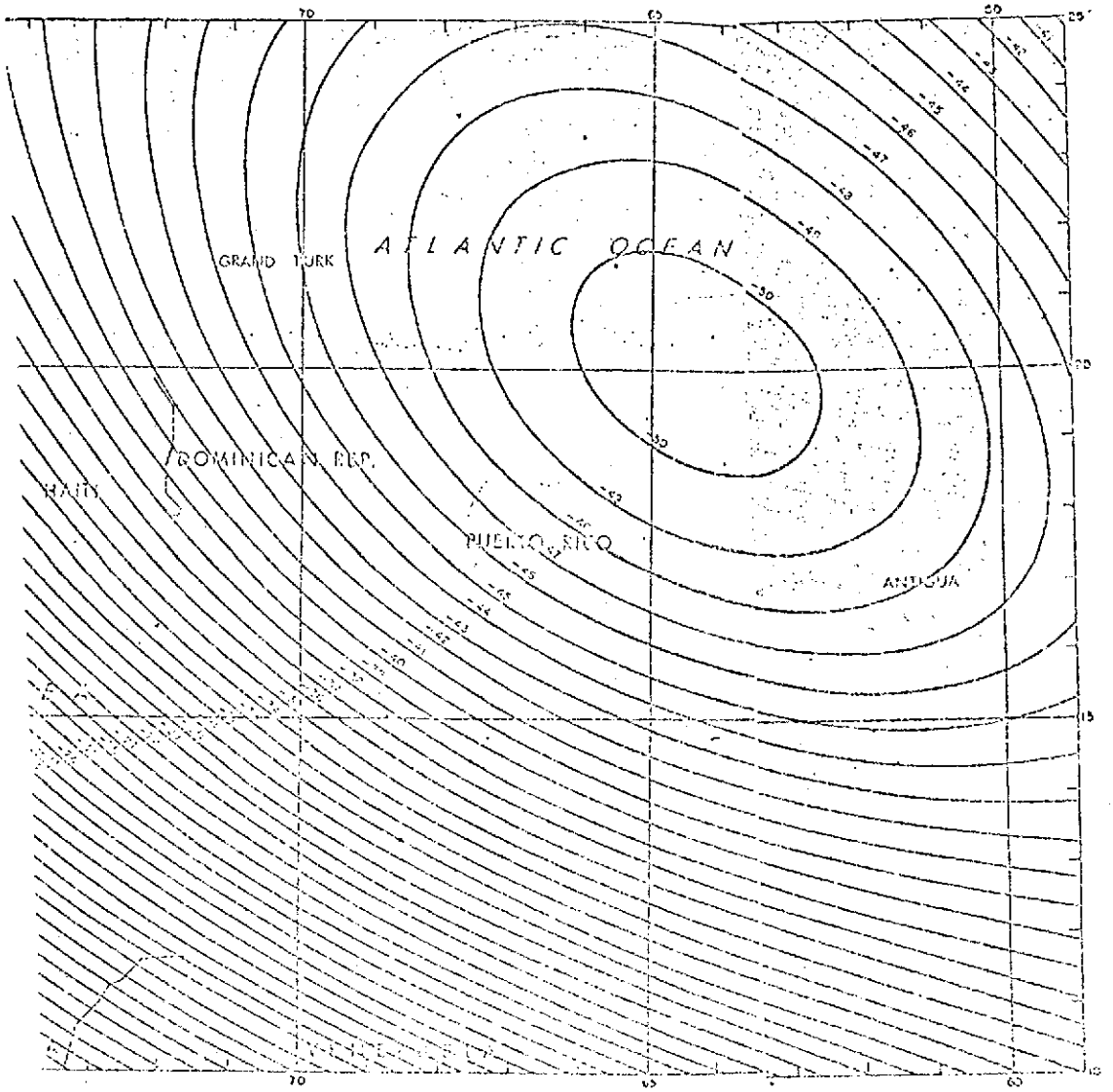
ATLANTIC OCEAN
GRAND TURK
DOMINICAN REP.
HAITI
PUERTO RICO
ANTIGUA
70
65
60
25
20
15
10
-30
-35
-40
-42
-43
-44
-45
-46
-47
-48

Figure 29b.

the case where coastal values are given. (Cf. Figure 30) Cotidal lines for the Atlantic Ocean are given in more detail in Figure 31 which is due to Hansen.[55]

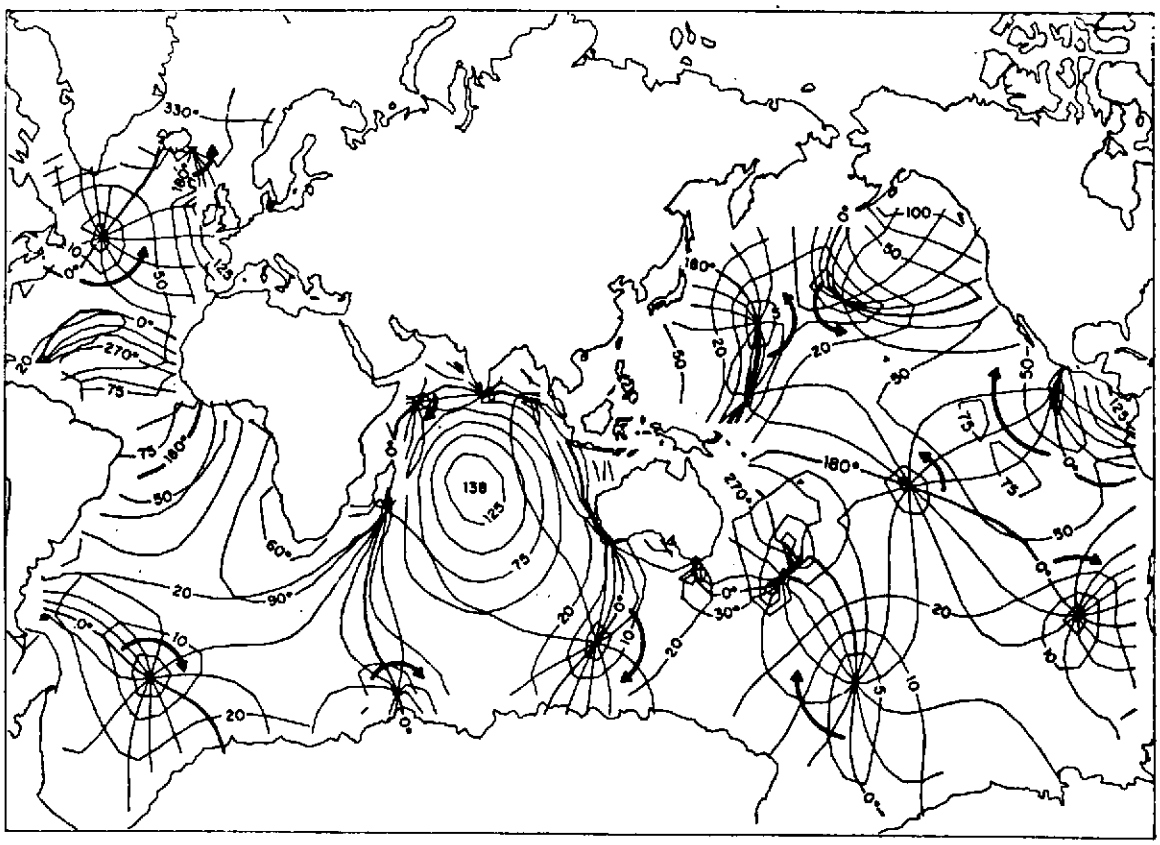

Figure 30. Cotidal and corange lines for the M_2 tide obtained by solving LTE with coastal values specified. Cotidal lines radiate from amphidromic points, corresponding to the progression of tidal crests in the sense indicated by the arrows around these points of vanishing tidal range (Section 5). High tide occurs along the cotidal lines labeled 0° just as the moon pases over Greenwich meridian. Successive cotidal lines delineate tidal crests at lunar hourly intervals. (For clarity, only selected cotidal lines are labeled, 30° corresponds to a dealy of one lunar hour.) Corange lines (5, 10, 20, 30, 75, 100, 125 cm) connect locations of equal tidal amplitude (not double amplitude). They surround amphidromic points (where range vanishes and phases very rapidly) and range maxima (where range is longest and phases nearly constant).

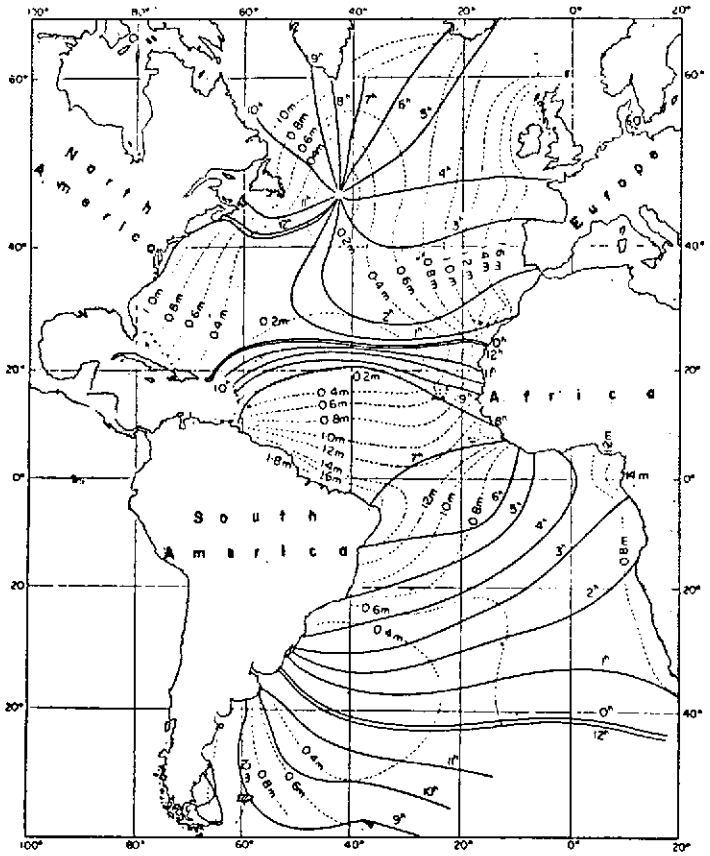

Theoretical tides of Atlantic Ocean. Full lines: co-tidal lines referred to moon-transition through meridian of Grw., dashed lines: co-range lines of the semi-diurnal tide M_2 in m (according to Hansen).

Figure 31.

The basic Laplace tidal equations are given by:

$$\frac{\partial u}{\partial t} - (2\Omega \sin\theta)\, v = \frac{-g}{a\cos\theta}\,\frac{\partial(\zeta - \zeta)}{\partial\phi},$$

$$\frac{\partial v}{\partial t} + (2\Omega \sin\theta)\, u = \frac{-g}{a}\,\frac{\partial(\zeta - \zeta)}{\partial\theta},$$

and

$$\frac{\partial \zeta}{\partial t} + \frac{1}{a\cos\theta}\left(\frac{\partial(uD)}{\partial\phi} + \frac{\partial(vD\cos\theta)}{\partial\theta}\right) = 0$$

They have been studied in a number of simplified forms.

Hendershott's recent research has extended them to include effects of solid earth tides which he found to be significant[56].

iii. The General Circulation of the Oceans

Problems associated with the general circulation have been discussed by H. Stommel and K. Bryan. (Cf. references 57 and 58.)

A model for the world-wide general circulation has been presented by Stommel. It appears in Figure 32. More detailed studies of particular regions such as the North Atlantic are being conducted by Bryan and Holland (cf. reference 77).

iv. Currents

The general circulation embraces a number of major current systems including the Gulf Stream, the Kuroshio Current near Japan, and the Antarctic circumpolar current.

The Gulf Stream is of special interest here for several reasons including the fact that it meanders.

a. The Gulf Stream Meanders

Considerable effort has been devoted to the study of the meanders of the Gulf Stream. This research is discussed by Hansen[59]. The Gulf Stream proper can be thought of as a Kelvin wave. Departures from this model are also of interest here.

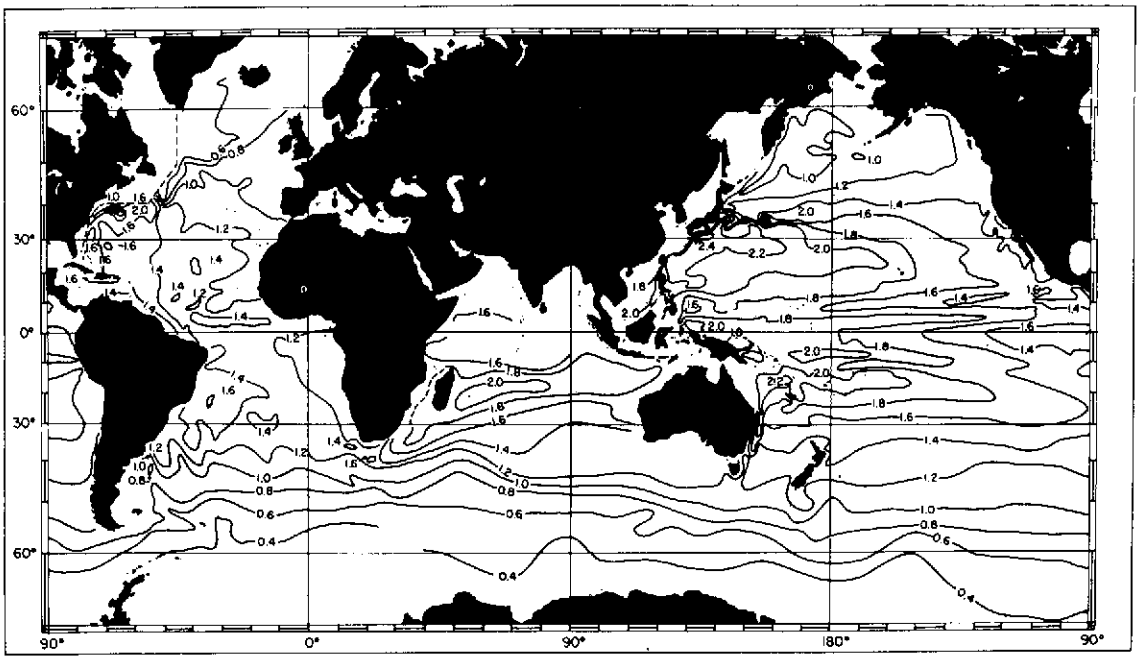

Figure 32. Dynamic Topography of the Sea Surface
Relative to the 1000-Decibar Surface

In the study described by Hansen, the position of the Gulf Stream between Cape Hatteras and approximately 60° west longitude was observed at intervals ranging from a few days to a month. The 15° isotherm was chosen as an index of the main thermal front at a depth of 200 meters, and hence as an indication of the Gulf Stream position 59.

Wavelike features having wavelengths of 200-400 km were observed. Hansen shows them in Figure 33. The evolution of the meanders in terms of phase progression as indicated in Figure 34. It is seen there that the meanders progress at a rate of the order of a mean wavelength, taken to be 300 km, each couple of months. This corresponds to about 5 km/day.

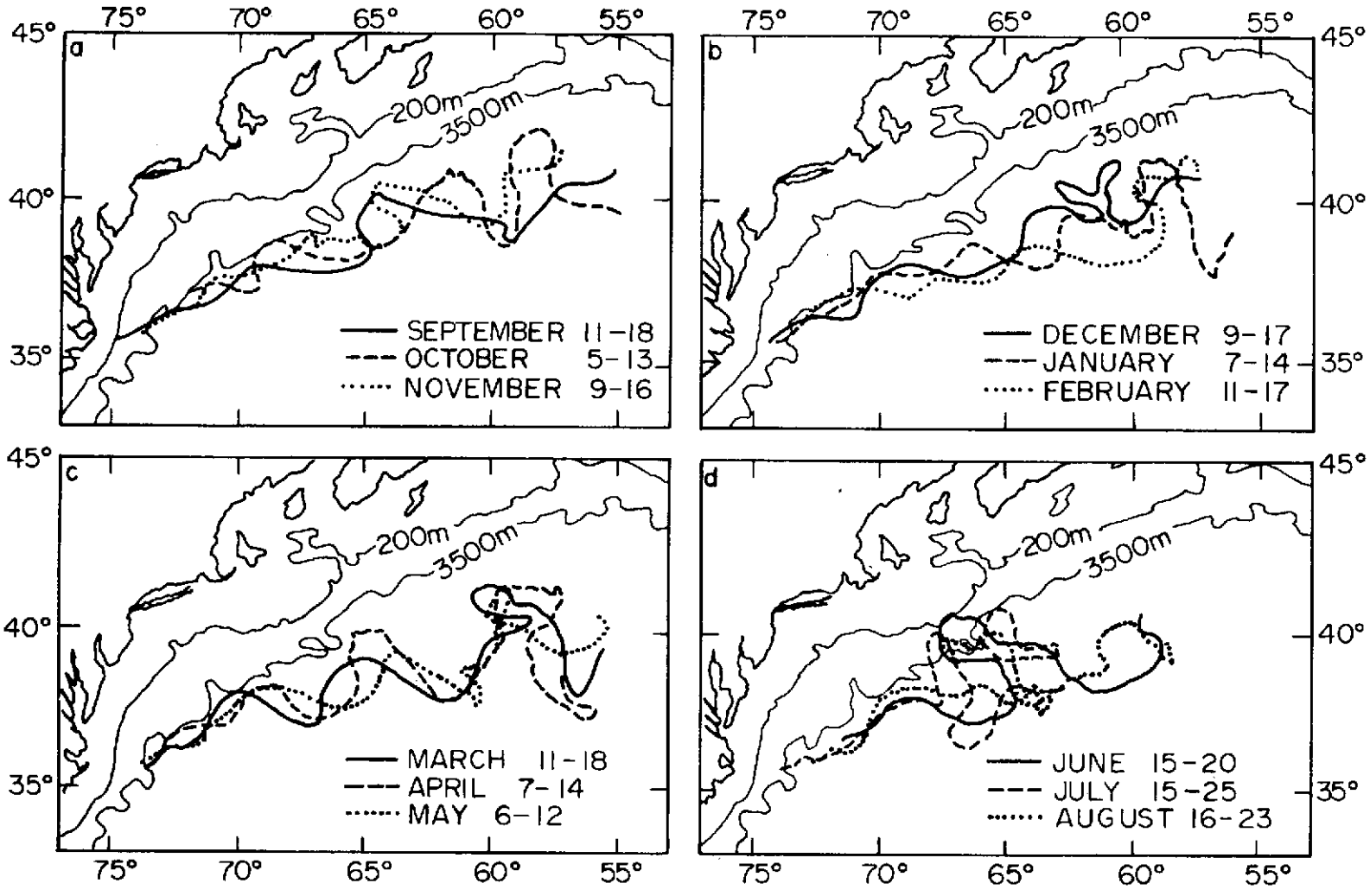
a
75°
70°
65°
60°
55°
45°
40°
35°
200m
3500m
SEPTEMBER 11-18
OCTOBER 5-13
NOVEMBER 9-16
b
DECEMBER 9-17
JANUARY 7-14
FEBRUARY 11-17
c
MARCH 11-18
APRIL 7-14
MAY 6-12
d
JUNE 15-20
JULY 15-25
AUGUST 16-23

Figure 33.

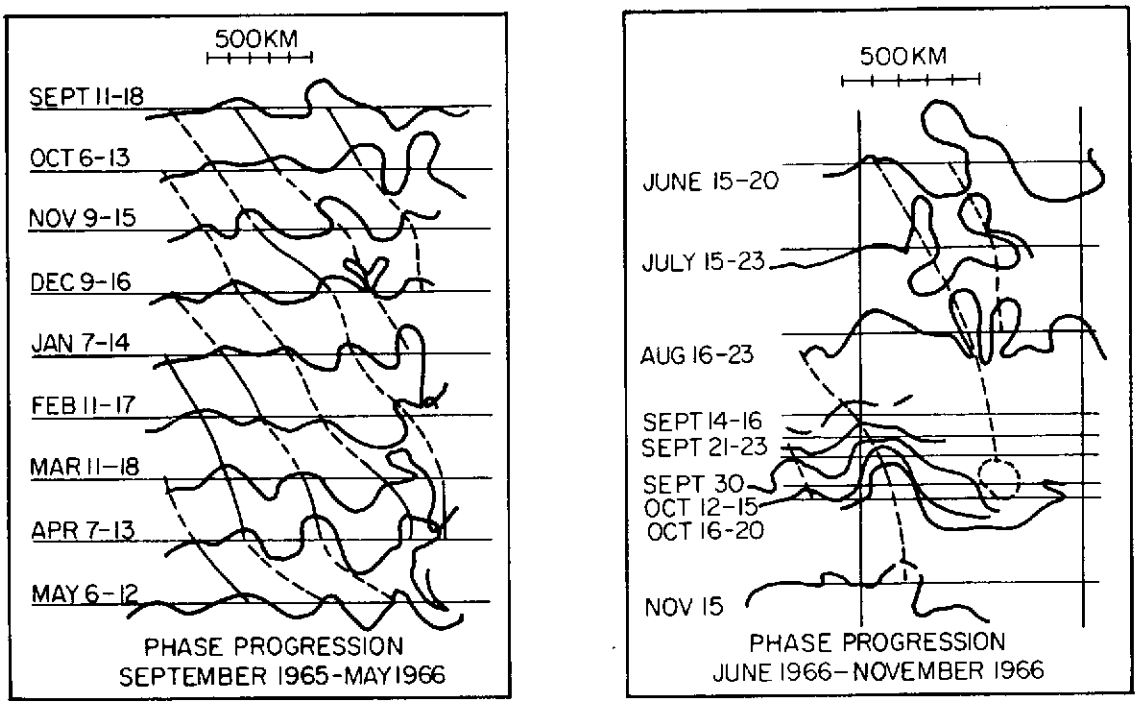

Figure 34.

Altitude variations across much of the Gulf Stream due to the geostrophic effect are of the order of a meter.

Some information about its position will be available from sources other than GEOS-C.

The inclination of 65° also makes it possible to study the antarctic circumpolar current which is of interest for more than one reason. It is the only continuous current which corresponds to a closed circuit or curve on the globe. It is also the strongest current, being equivalent in terms of mass flux to five or six Gulf Streams. The 65° orbit would also provide good geometry for viewing the Gulf Stream. This point is discussed in Section III, 4, C.

v. Sea State

It is expected that the problem of interpreting the range measures in the presence of sea state effects will be attacked by an approach such as the one offered by Pierson and his colleagues[60].

vi. Storm Surges

Storm surges, such as those associated with hurricanes, for example, can have amplitudes of up to a couple of meters and wavelengths of some fifty kilometers. Near coast lines the amplitudes have been known to increase to the order of seven or eight meters.

Phenomena such as storm surges will be represented and/or observed when and where they occur, to the extent that this is practicable.

vii. Tsunamis

Tsunamis are thought to have amplitudes of nearly half a meter and wavelengths of perhaps three hundred kilometers. Detailed theoretical representation of a tsunami involves the representation of the ocean bottom topography and complex ray-tracing calculations to map out the advance of the expanding wave. The occurence of a tsunami in a region and at a time when it might be observed by GEOS-C would be a relatively rare event. It could, however, be modeled and studied in this way.

3. The Calibration of the Altimeter

a. Short-Arc Tracking of GEOS-C in the Caribbean Area

The consideration of short-arc and long-arc tracking error budgets can begin with a look at the overall error problem. A typical error breakdown for the GEOS-C altimeter is indicated in Table XVIII[61]. Quantities associated with factors other than the orbit errors have an rms value of approximately 3 meters. This leaves 4 meters or so which might be assigned to the calibration process if the 5 meter rms overall accuracy goal is to be met. Allowing 1 or 2 meters for uncertainties associated with the geoid means that the uncertainties associated with the orbit determination process should contribute no more than about 3.5 meters.

Table XVIII

GEOS-C Mission Altimeter Evaluation

Satellite Altimeter System Measurement Error Source	Error (m)
Altimeter Instrumentation	2
Refraction	0.2
Reflection from Waves	0.5
Spacecraft Attitude	2
Root Sum Square	2.9
Calibration Error Allocation	4.1
Altimeter System Evaluation Goal	5

If comparable accuracies are to be achieved over extensive areas, the accuracy within a short-arc calibration region such as the one in the Caribbean must be increased still further. This point will be discussed further below.

A detailed analysis of short-arc tracking using lasers and cameras in the Caribbean area has been conducted by Berbert and Loveless[62]. Their analysis of a number of cases involving various combinations of lasers and cameras is summarized in Figure 35. Assumptions underlying these analyses are listed in Table XIX. The other angle measure accuracies of 100" listed there were those assumed for the laser angles used in the analysis indicated by the open circles in Figure 35. In all cases, in addition to the altimeter bias uncertainty, uncertainties in orbital, survey, and range measure parameters were also estimated. The triangle corresponds to a similar analysis of a three-laser-only case made for a much larger triangle based on stations at Antigua, Key West, and Panama. It resulted in a value of 4.1 meters, only slightly higher than that for the smaller triangle. As can be seen, a number of cases meet both the basic 4 meter requirement and the 3.5 meter figure obtained by allowing a couple of meters for uncertainties associated with the geoid.

Berbert and Loveless concluded that the 2-laser, 2-camera combination was probably the most cost effective in terms of the probabilities of obtaining reasonable amounts of data.

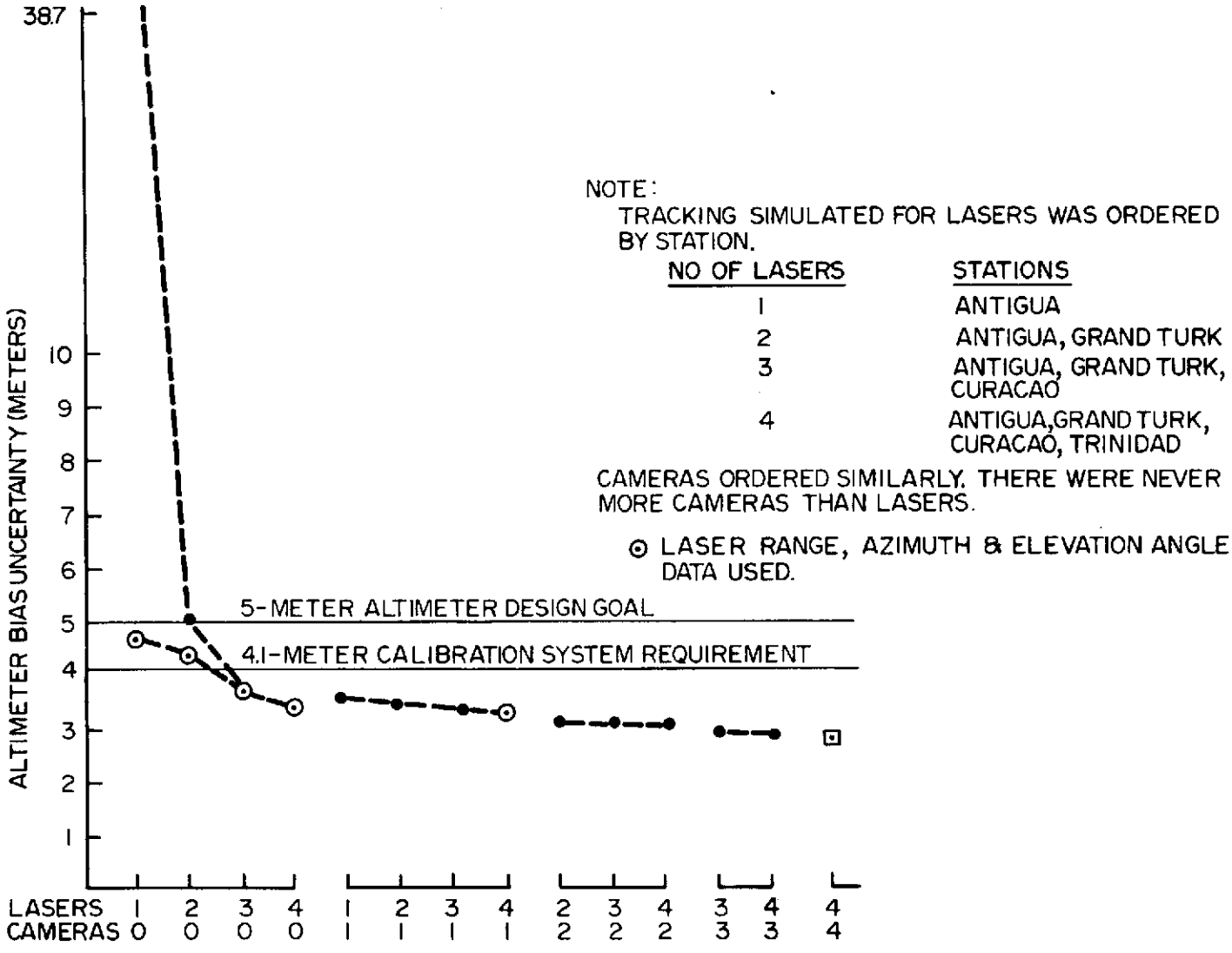
38.7
ALTIMETER BIAS UNCERTAINTY (METERS)
10
9
8
7
6
5
4
3
2
1
5-METER ALTIMETER DESIGN GOAL
4.1-METER CALIBRATION SYSTEM REQUIREMENT
LASERS 1 2 3 4 1 2 3 4 2 3 4 3 4 4
CAMERAS 0 0 0 0 1 1 1 1 2 2 2 3 3 4
NOTE:
TRACKING SIMULATED FOR LASERS WAS ORDERED BY STATION.
NO OF LASERS
STATIONS
1 ANTIGUA
2 ANTIGUA, GRAND TURK
3 ANTIGUA, GRAND TURK, CURACAO
4 ANTIGUA, GRAND TURK, CURACAO, TRINIDAD
CAMERAS ORDERED SIMILARLY. THERE WERE NEVER MORE CAMERAS THAN LASERS.
⊙ LASER RANGE, AZIMUTH & ELEVATION ANGLE DATA USED.

Figure 35.

Table XIX

GEOS-C Mission Altimeter Evaluation Analysis

Assumptions	A Priori Uncertainties	Noise rms
Recovered Quantities		
Range Measures	2 m	2 m
Altimeter Height Measures	100 m	10 m
Orbit – R&V Components	1 km, 1 km/sec	
Station Positions – E, N, V Components	30, 30, 1 m	
Other Quantities		
Camera Angle Measures		1"
Other Angle Measures		100"

Tracking using lasers having ten centimeter accuracies can yield more accurate determinations of the orbit as has been pointed out by Vonbun.[63] Results for 30 cm systems are indicated in Figure 36. This basic tracking system accuracy should give relative altitude accuracies of the order of half a meter. The limiting factor in this case would then appear to be the state of knowledge of the geoid which is thought to be on the order of a meter or two.

b. Long-Arc Tracking of GEOS-C

The surveys of the gravitational field over longer arcs will be greatly facilitated by the long-arc satellite-to-satellite tracking of GEOS-C which can be

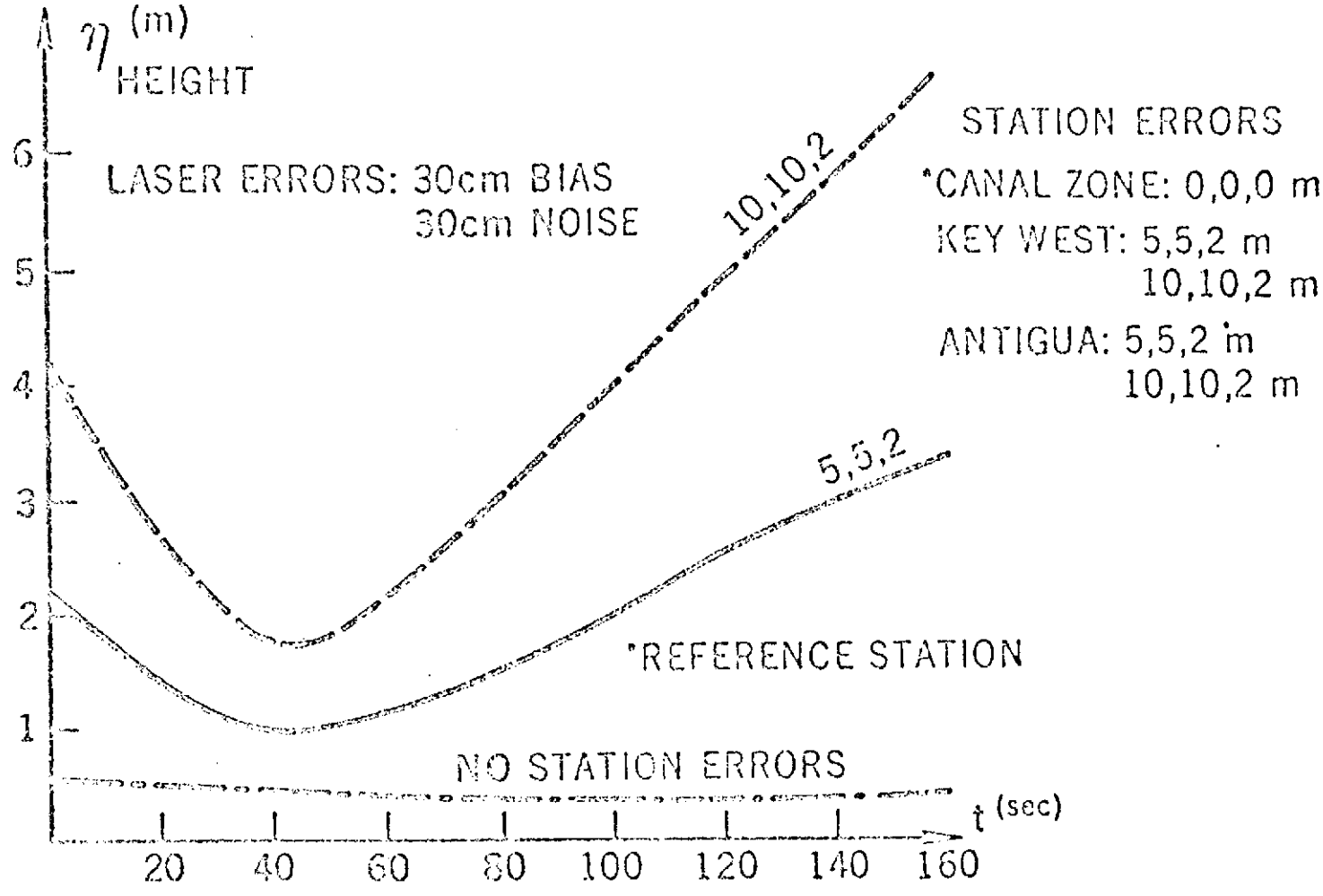

Figure 36. GEOS-C Height Errors Using Laser Tracking

conducted through ATS-F. The accuracy capability of this tracking approach is indicated in Figure 37. In the case looked at here, accuracies of some four meters or better persisted for almost three hours beyond the time interval shown in the Figure before the results deteriorated. Error analysis simulation results thus indicate that altitude accuracies in the three to four meter range can be achieved in this way. This is reasonably comparable to the current estimates of the accuracy of the world-wide geoid obtained from the satellite orbit analyses[18]. Satellite contributions to these have a spatial resolution of the order of 18°, however. Hence, altimeter and satellite-to-satellite tracking surveys even at the 6° resolution level will definitely provide new information. They will of course also provide the extremely valuable independent views which are so important.

4. Ocean Surface Altitude Representation and Analysis Using Altimeter Data

The set of GEOS-C data will itself make possible a better representation of the effects indicated above. More than one kind of study holds promise. Tide can be analyzed on a global basis using all the altimeter data. Information about the geoid and the sea state can be sought everywhere. Current phenomena, such as those associated with the Gulf Stream meanders, will be watched in certain regions of the oceans. Storm surges and Tsunamis will be looked at when and where they occur, insofar as this is feasible.

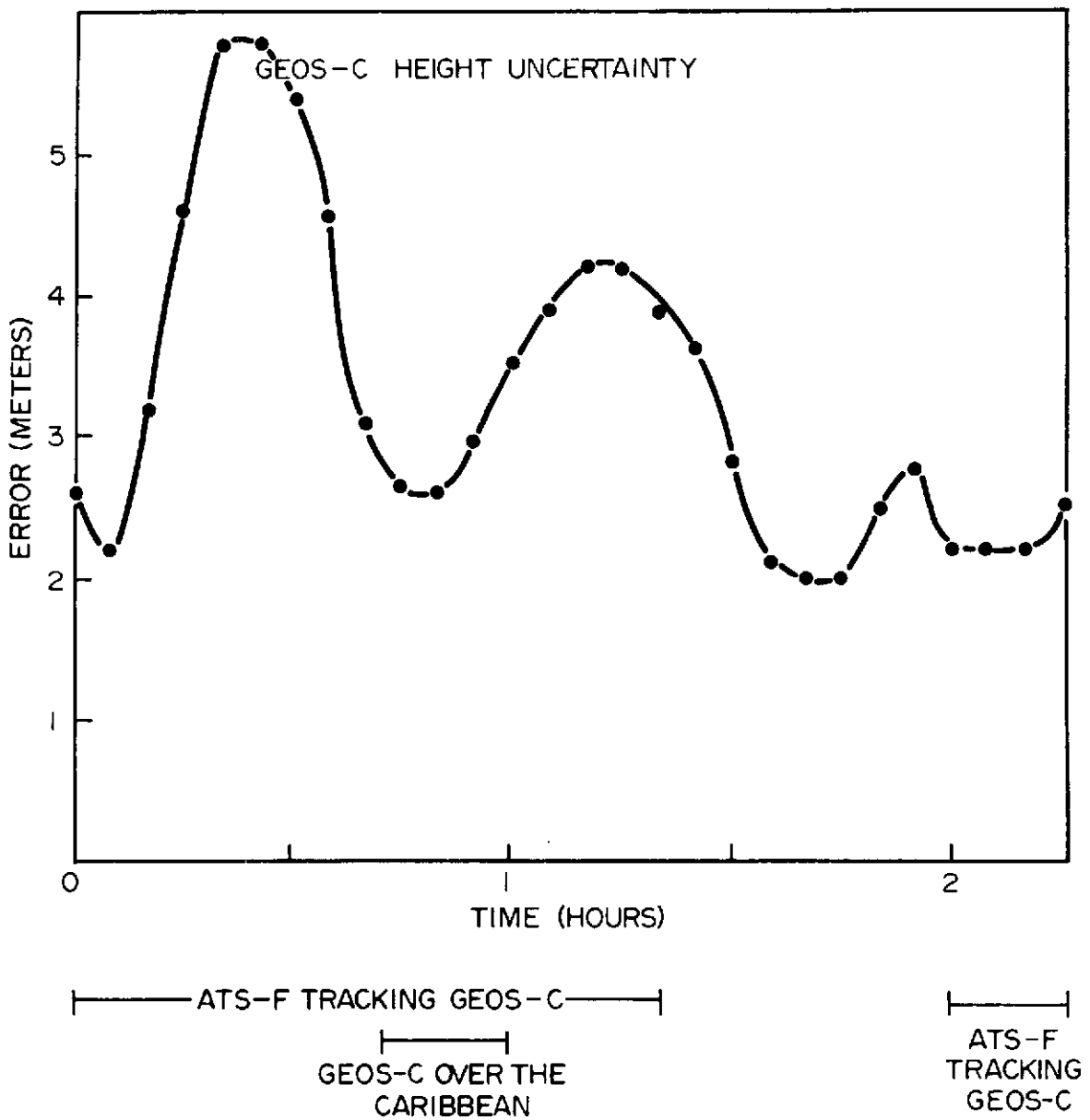
GEOS-C HEIGHT UNCERTAINTY
ERROR (METERS)
5
4
3
2
1
0
1
2
TIME (HOURS)
ATS-F TRACKING GEOS-C
GEOS-C OVER THE CARIBBEAN
ATS-F TRACKING GEOS-C

Figure 37.

a. Gravimetry

Gravimetric investigations by means of a GEOS-C altimeter will include at least three kinds of studies. First, it is anticipated that it should be possible to conduct an altimeter survey having a spatial resolution of about 6 degrees using the orbit ground track pattern which was worked out above in the discussion of the selection of a typical GEOS-C orbit. This will permit a direct inter-comparison with the results of the gravimetric investigation at the 6° resolution level conducted by means of a satellite-to-satellite tracking system. A mutual validation of both the two approaches achieved in this way will increase the confidence of both types of results.

A similar altimeter gravimetric survey could be conducted at a finer resolution, e.g., down to 1°. This can be thought of as the second type of experiment. This could also be conducted through the use of the GEOS-C orbit ground track pattern indicated earlier in the discussion of the GEOS-C orbit selection.

Thirdly, fine structure could be investigated in greater detail in regions of special interest such as those near the East and Gulf coasts of America.

The interesting region in the neighborhood of the Puerto Rican Trench, for example, could be studied with the aid of the Caribbean facilities indicated in the calibration discussion.

Another possible region of this type will be discussed in a later section.

The results of these regional studies, will, it is expected, be correlated closely with the surface gravimetry data discussed above.

b. Tides

Zetler has pointed out, for example, that GEOS-C will, over its lifetime, provide data which can be used as the basis for a global tidal study.[54]

As possible regional tidal study is discussed below in Section III, 4,C,i,B.

c. A Region for Earth and Ocean Dynamics Studies

As has been indicated above, surveys of certain phenonema such as the geoid and tides can be conducted on both global and regional bases. The following discussion deals with an area in which regional investigations of more than one type could be conducted fairly readily from a practical standpoint.

i. Ocean Dynamics

The Atlantic region off the coast of the Northeastern United States is of particular interest from the standpoint of the Gulf Stream meanders as was indicated in Figure 33 which is given by Hansen[59]. These features have amplitudes on the order of a meter. Tidal variations in this same region, while not quite as large as those found elsewhere, are nevertheless of considerable size, i.e., of the order of a meter also. This is indicated in Figures 30 and 31 where certain tidal components are seen[53 & 55].

This region is also a reasonably attractive one from the standpoint of some of the practicalities of short-arc tracking. Good advantage could be taken of lasers which are usually available at Goddard, Wallops Island, and possibly also at SAO. Other possible locations for lasers include Florida, Bermuda, the Canal Zone, and the Antilles, at Antigua and/or Grand Turk. C-band radars are also located at Wallops Island, Cape Kennedy, Bermuda, Antigua and Grand Turk. It would be valuable also to have an additional site near the point on the Bermuda meridian which is as far north of Goddard as Goddard is north of Bermuda. A laser at this location which is near the coast of the Bay of Fundy would be of interest not only from the point of view of oceanographic studies but also for earth dynamics studies, as will be pointed out later in the discussion. A site at this point, which is in Canada, or in nearby Maine would be suitable. It is anticipated that lasers will be located at some of the continental US sites shown in Figure 38, and that at least a couple of portable lasers will be available at times for use at some of the other sites indicated there although no such arrangements have been made at the present time. Three of these lasers in any of the triangular configurations in that map operating at the 10 cm accuracy level would make it possible to determine the altitude of GEOS-C with a relative accuracy of the order of half a meter or better in the neighborhood of the triangle. A fourth laser nearby would provide the important checks on the instrumental biases by furnishing the redundant information. It would also reduce the impact of the cloud cover problem.

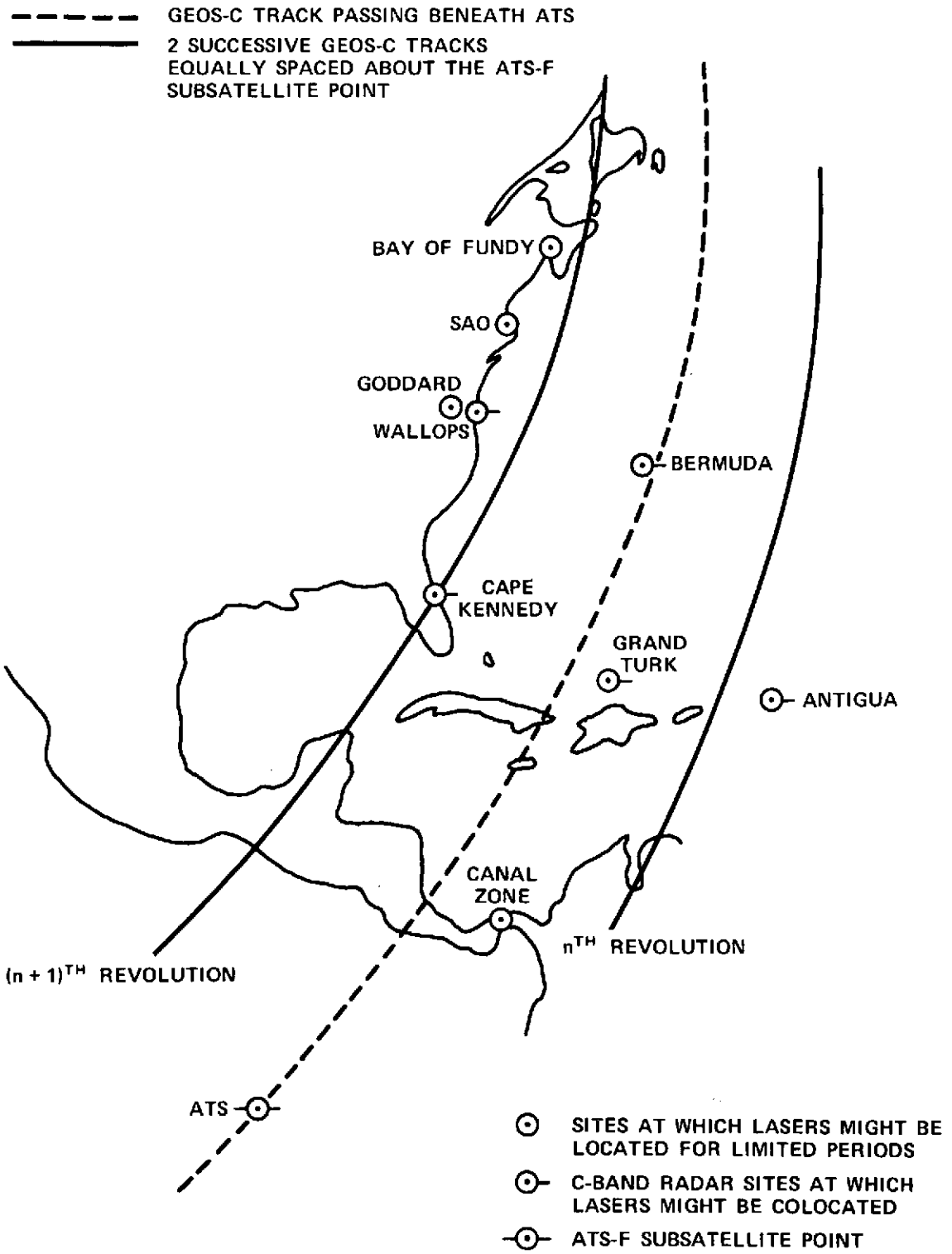
GEOS-C TRACK PASSING BENEATH ATS
2 SUCCESSIVE GEOS-C TRACKS EQUALLY SPACED ABOUT THE ATS-F SUBSATELLITE POINT
BAY OF FUNDY
SAO
GODDARD
WALLOPS
BERMUDA
CAPE KENNEDY
GRAND TURK
ANTIGUA
CANAL ZONE
n^{TH} REVOLUTION
$(n+1)^{TH}$ REVOLUTION
ATS
SITES AT WHICH LASERS MIGHT BE LOCATED FOR LIMITED PERIODS
C-BAND RADAR SITES AT WHICH LASERS MIGHT BE COLOCATED
ATS-F SUBSATELLITE POINT

Figure 38

a. Gulf Stream Meander Studies

The altimeter tracking patterns are also good for observing the Gulf Stream meanders in this region. Shown in Figure 39 are surface tracks of the 65° orbit with 6.3° daily spacing which was obtained in the earlier discussion. It is seen that the northward and sourthward going tracks cross the two principal branches of a typical Gulf Stream meander nearly orthogonally, providing almost ideal geometry for studying the behavior of these interesting features. Each ground track seen in Figure 39 will be followed four days later by one removed just one degree from it, hence it will be possible to observe each feature once every four days. This frequency is well matched to the observational needs of a Gulf Stream meander experiment, as can be seen from inspection of Figures 34 and 39[59]. The mean wave length of a meander is often of the order of 300 kilometers, as was indicated above in the discussion associated with Figures 33 and 34. A typical meander moves a distance equal to its own wave length in about a couple of months. This interval might be thought of as a characteristic time constant which can be associated with the Gulf Stream meanders in this sense. Observations every four days are well suited for a Gulf Stream meander experiment. In fact observations every ten days or so would be most welcome, as Hansen has already pointed out[59]. This also allows a margin for gaps in the observing program which might be due to such things as weather conditions or operational factors.

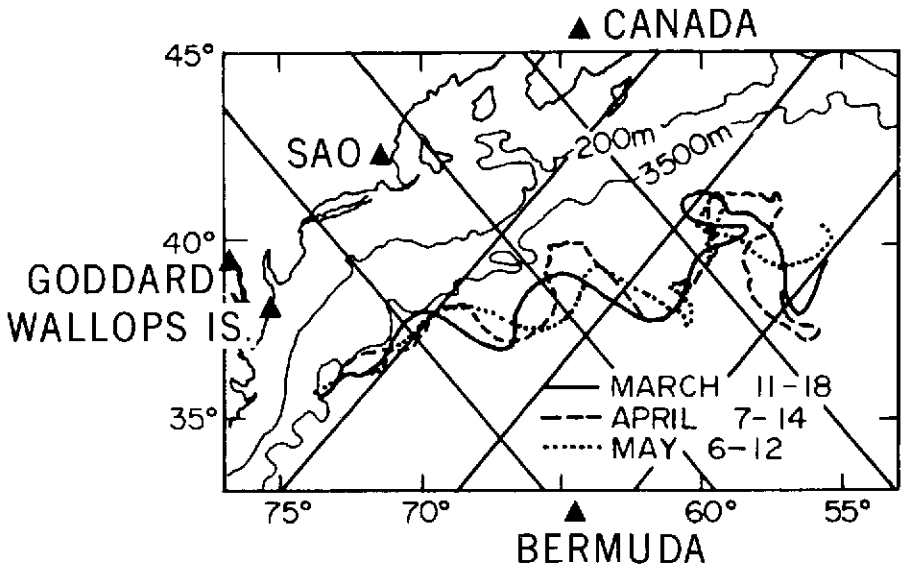

Figure 39.

Similar studies of the Kuroshio current could be conducted by means of lasers similarly placed in Japan and nearby islands such as IWO, Jima, say.

B. Tidal Studies

1. An Anti-Amphidromic Region Tidal Study

A model for the M_2 semi-diurnal component of the tide due to Hendershott appears in Figure 30. Hendershott has pointed out that the regions separating the amphidromic points in which the tidal range is large and the phase is slowly varying are of greater interest than the amphidromes themselves because the tidal potential energy is largely to be found in these anti-amphidromic regions. He suggested that the most important of these regions have their centers at approximately 0°N, 15°W; 15°S, 75°E; 5°N, 135°W; 10°S, 115°W.[78] Zetler has also called attention to the importance of these regions[79].

These locations are indicated in Figure 40. The first of these regions, which is the Sierra Leone Basin Area, is perhaps potentially the most suitable for study by means of the GEOS-C altimeter and orbit determination system since it is adjacent to island and coastal sites at which tracking lasers might be located. A US tracking facility is on Ascension Island. The French already have had a laser at Dakar and operated ground terminal facilities at Quagadougou. The Syncom satellites were tracked by a radio range and range rate system from a ship at anchor in the harbor of Lagos, Nigeria. These would be suitable sites from the scientific standpoint for tracking by means of 10 cm lasers. A set of three lasers at Freetown, Abidjan and Ascension might be even somewhat better from the geometric standpoint. No arrangements have been made at the present time for 10 cm laser tracking from any of these 5 sites. The location in the Lagos/Abidjan area will be referred to simply as the Gulf of Guinea site.

Tracks of GEOS-C in this Sierra Leone Basin anti-amphidrome laser triangle region are seen in Figure 41. Twice each day the ground track passes through or very close to this triangle. At least one northbound track of the type seen, for example, would occur each day in the neighborhood of the triangle. These tracks are seen to be nearly orthogonal to the co-range lines of the semi-diurnal tide. Southbound tracks, nearly parallel to the co-range lines also occur daily in useful locations. The orbit worked out for GEOS-C in the above discussion has the property of moving about 10.5 degrees each day relative to the moon. A complete cycle of the semi-diurnal lunar tide can be observed by

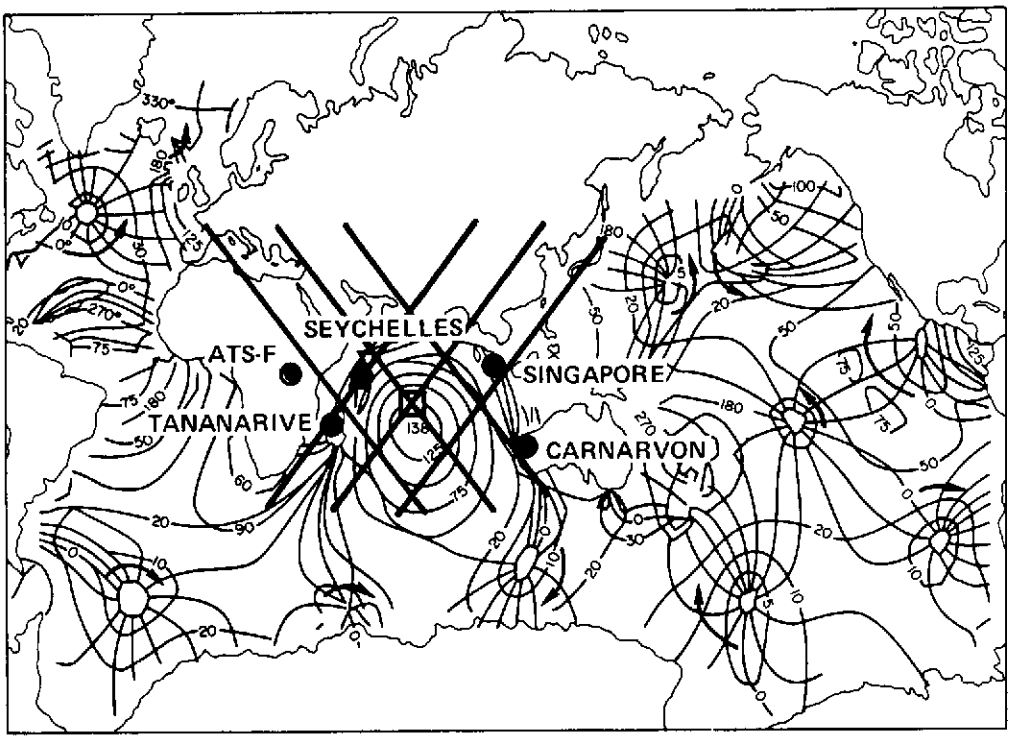

Fig. 40. COTIDAL AND CORANGE LINES FOR THE M_2 TIDE OBTAINED BY SOLVING LTE WITH COASTAL VALUES SPECIFIED. COTIDAL LINES RADIATE FROM AMPHIDROMIC POINTS, CORRESPONDING TO THE PROGRESSION OF TIDAL CRESTS IN THE SENSE INDICATED BY THE HEAVY ARROWS AROUND THESE POINTS OF VANISHING TIDAL RANGE. HIGH TIDE OCCURS ALONG THE COTIDAL LINES LABELED 0° JUST AS THE MOON PASSES OVER GREENWICH MERIDIAN. SUCCESSIVE COTIDAL LINES DELINEATE TIDAL CRESTS AT LUNAR HOURLY INTERVALS. (FOR CLARITY, ONLY SELECTED COTIDAL LINES ARE LABELED,30° CORRESPONDS TO A DELAY OF ONE LUNAR HOUR.) CORANGE LINES (5, 10, 20, 50, 75, 100, 125 cm) CONNECT LOCATIONS OF EQUAL TIDAL AMPLITUDE (NOT DOUBLE AMPLITUDE). THEY SURROUND AMPHIDROMIC POINTS (WHERE RANGE VANISHES AND PHASES VARY RAPIDLY) AND RANGE MAXIMA (WHERE RANGE IS LARGEST AND PHASES NEARLY CONSTANT).

○ SITES AT WHICH LASERS MIGHT BE LOCATED FOR LIMITED PERIODS

● ATS-F SUBSATELLITE POINT

□ APPROXIMATE CENTER OF ANTI-AMPHIDROMIC REGION

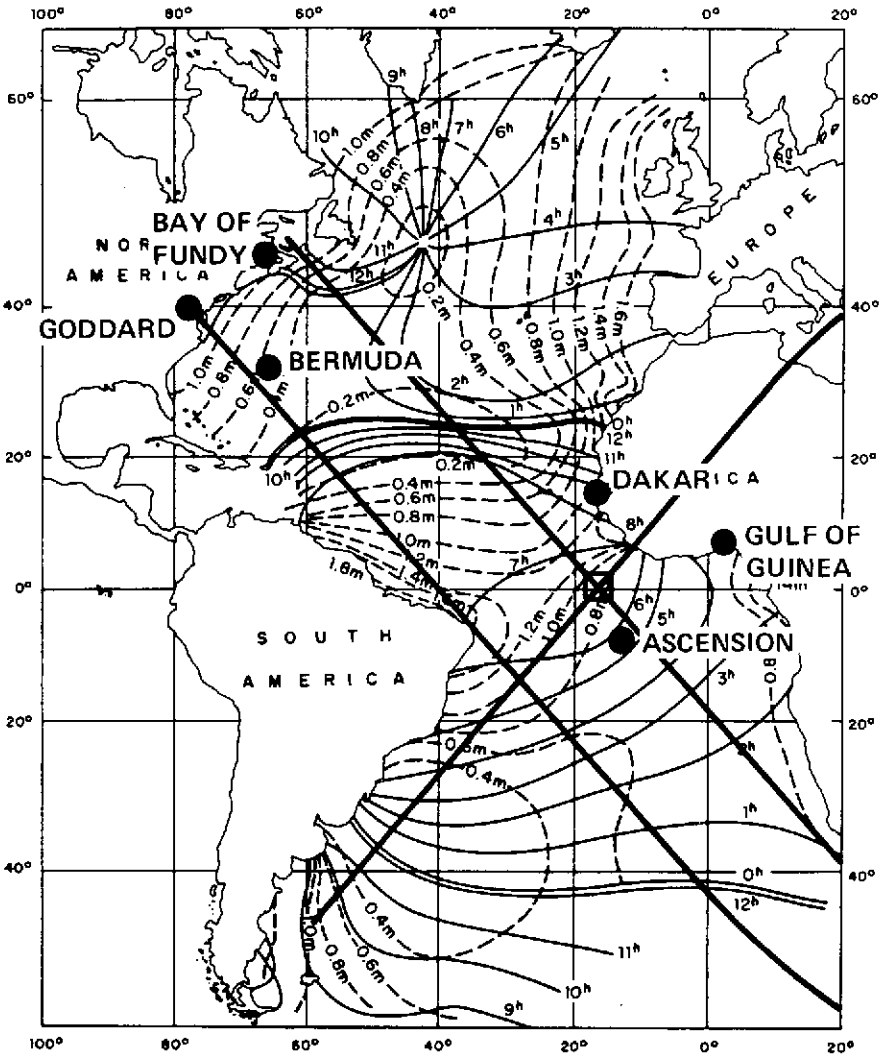

Fig.41 THEORETICAL TIDES OF ATLANTIC OCEAN. FULL LINES: CO-TIDAL LINES REFERRED TO MOON-TRANSITION THROUGH MERIDIAN OF Grw., DASHED LINES: CO-RANGE LINES OF THE SEMI-DIURNAL TIDE M_2 IN m (ACCORDING TO HANSEN).

□ APPROXIMATE CENTER OF ANTI-AMPHIDROMIC REGION

● SITES AT WHICH LASERS MIGHT BE LOCATED FOR LIMITED PERIODS

The ATS-F satellite will pass directly over the Sierra Leone Basin anti-amphidrome region as it moves from 94° west longitude to 34° east longitude. It will be within about 30° of the nominal center of the region on the equator at 15° west longitude for the duration of the 17-day interval in which GEOS-C can sense a complete cycle of the semidiurnal lunar tidal component. Satellite-to-satellite tracking between ATS-F and GEOS-C would certainly augment the laser capability. It may make it possible to conduct a useful investigation with a smaller number of lasers. Its value would be enhanced if it remained within about 13° of the center of the region for the entire 17 day cycle. Such a drift rate in this region, which is about half the one currently planned, would provide an observing interval of some 26°. This is comparable with the characteristic GEOS-C observing span which is associated with the fact that its equator crossings in the neighborhood of a given point from day to day range over a 26° longitude interval.

The GEOS-C altimeter operating in the 0.5 meter accuracy mode with the relative orbital altitude determined to about half a meter should permit tidal observations to about a meter or better. The GEOS-C systems thus offer the possibility of conducting an initial, exploratory tidal experiment in the Sierra Leone Basin anti-amphidrome region.

Satellite-to-satellite tracking from ATS-F at 94° W together with laser tracking from American and Pacific sites would open up the possibility of studying the anti-amphidrome regions in the Pacific as is indicated in Figure 42.

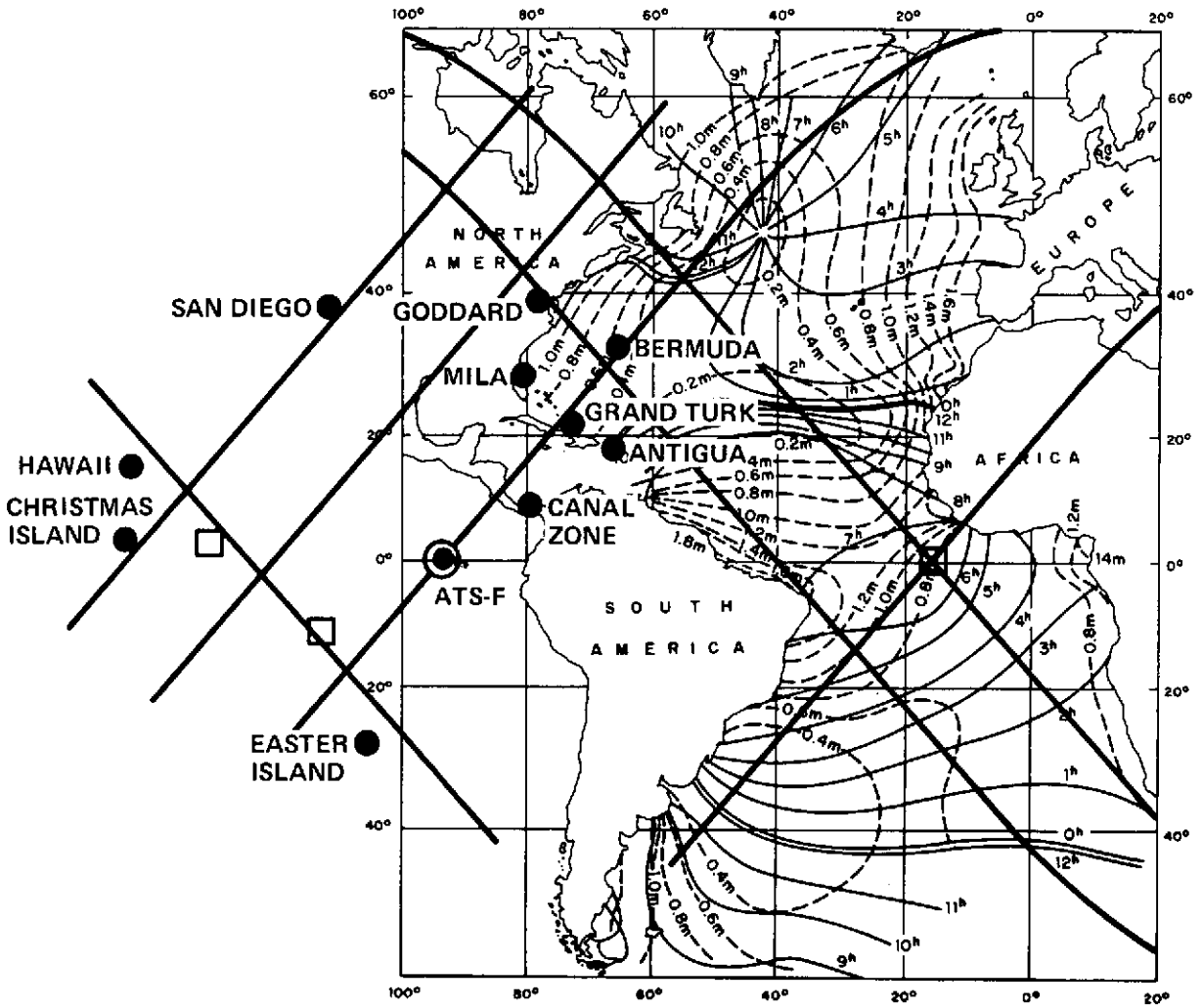

Fig.42. THEORETICAL TIDES OF ATLANTIC OCEAN. FULL LINES: CO-TIDAL LINES REFERRED TO MOON-TRANSITION THROUGH MERIDIAN OF Grw., DASHED LINES: CO-RANGE LINES OF THE SEMI-DIURNAL TIDE M_2 IN m (ACCORDING TO HANSEN).

- SITES AT WHICH LASERS MIGHT BE LOCATED FOR LIMITED PERIODS
- ATS-F SUBSATELLITE POINT
- APPROXIMATE CENTERS OF ANTI-AMPHIDROMIC REGIONS

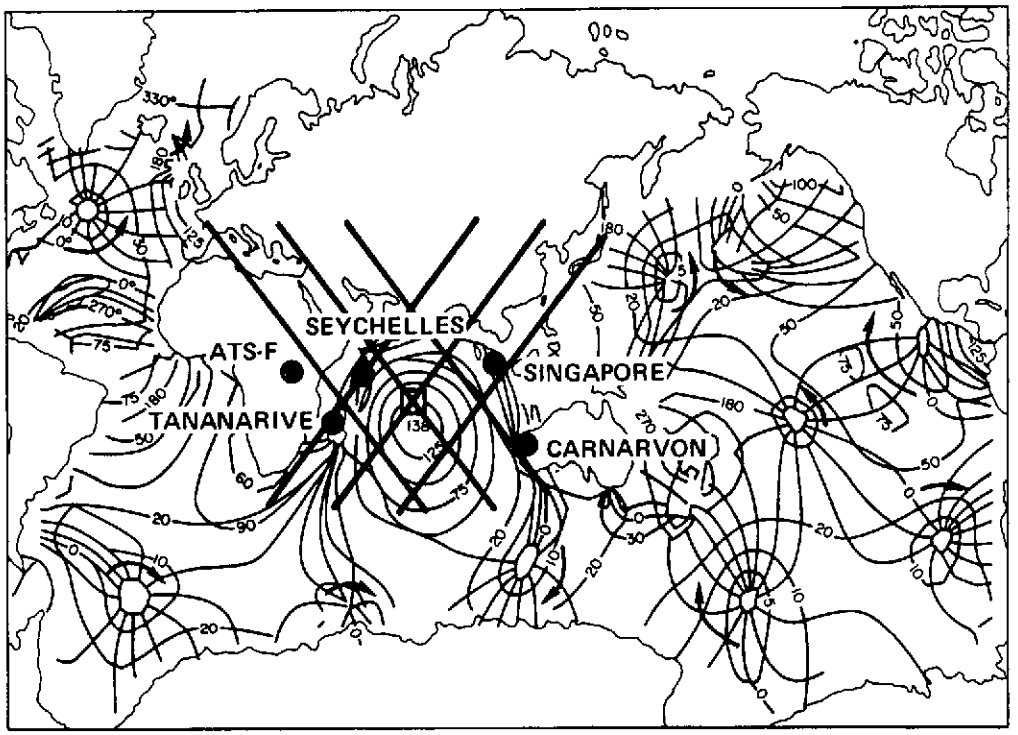

Fig. 42a. COTIDAL AND CORANGE LINES FOR THE M_2 TIDE OBTAINED BY SOLVING LTE WITH COASTAL VALUES SPECIFIED. COTIDAL LINES RADIATE FROM AMPHIDROMIC POINTS, CORRESPONDING TO THE PROGRESSION OF TIDAL CRESTS IN THE SENSE INDICATED BY THE HEAVY ARROWS AROUND THESE POINTS OF VANISHING TIDAL RANGE. HIGH TIDE OCCURS ALONG THE COTIDAL LINES LABELED 0° JUST AS THE MOON PASSES OVER GREENWICH MERIDIAN. SUCCESSIVE COTIDAL LINES DELINEATE TIDAL CRESTS AT LUNAR HOURLY INTERVALS. (FOR CLARITY, ONLY SELECTED COTIDAL LINES ARE LABELED,30° CORRESPONDS TO A DELAY OF ONE LUNAR HOUR.) CORANGE LINES (5, 10, 20, 50, 75, 100, 125 cm) CONNECT LOCATIONS OF EQUAL TIDAL AMPLITUDE (NOT DOUBLE AMPLITUDE). THEY SURROUND AMPHIDROMIC POINTS (WHERE RANGE VANISHES AND PHASES VARY RAPIDLY) AND RANGE MAXIMA (WHERE RANGE IS LARGEST AND PHASES NEARLY CONSTANT).

○ SITES AT WHICH LASERS MIGHT BE LOCATED FOR LIMITED PERIODS

● ATS-F SUBSATELLITE POINT

□ APPROXIMATE CENTER OF ANTI-AMPHIDROMIC REGION

2. A Continental Shelf Tidal Study

A tidal experiment in the neighborhood of a continental shelf could be conducted in the western North Atlantic in the region covered by the tracking sites indicated in Figure 38. Amplitudes of the order of a meter are indicated, for example, in Figures 31 and 42. It is anticipated that lasers having 10 centimeter accuracy will be located at sites in this region in connection with the altimeter calibration and the Gulf Stream studies outlined above. Data taken in connection with these activities would also be useful in connection with such a tidal study. Additional observations specifically designed for the tidal investigation would also be needed. We see from Figure 42, that, again, the GEOS-C altimeter satellite ground track passes through or very close to the laser tracking region once each day. At least one of the northbound tracks of the type seen in Figure 42 for example, would occur every day. These tracks are, again, nearly orthogonal to the co-range lines of the semi-diurnal tide as is also apparent from the figure. Southbound tracks, nearly parallel to the co-range lines, also occur daily in useful locations in similar fashion. The GEOS-C orbit will, again, sample a whole semi-diurnal cycle in about two and a half weeks.

3. A Bay of Fundy Tidal Study

Tidal amplitudes in the Bay of Fundy region are the largest on earth. Ranges as high as fifteen meters are found. They should be amendable to direct measurement by the GEOS-C altimeter system. They should provide what may well be the first opportunity for an actual tidal observation by the GEOS-C. They

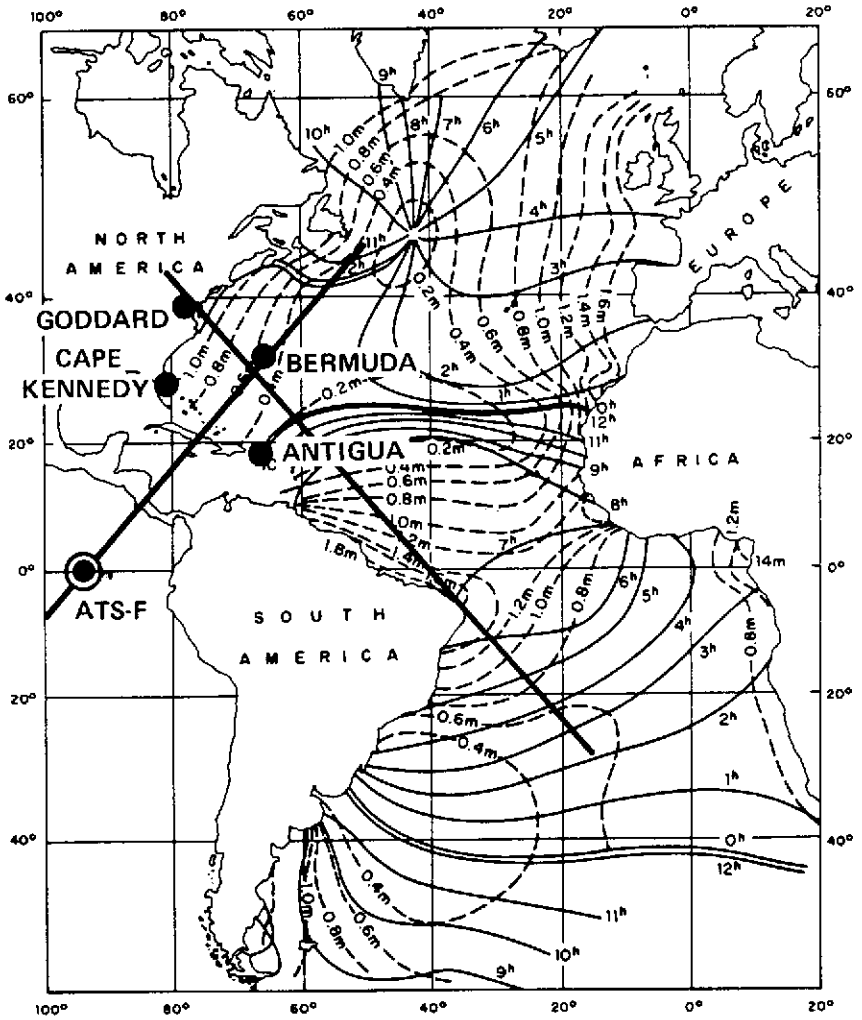

Fig. 42b. THEORETICAL TIDES OF ATLANTIC OCEAN. FULL LINES: CO-TIDAL LINES REFERRED TO MOON-TRANSITION THROUGH MERIDIAN OF Grw., DASHED LINES: CO-RANGE LINES OF THE SEMI-DIURNAL TIDE M_2 IN m (ACCORDING TO HANSEN).

● SITES AT WHICH LASERS MIGHT BE LOCATED FOR LIMITED PERIODS

◉ ATS-F SUBSATELLITE POINT

4. Global Tidal Studies

The use of altimeter data gathered over extended periods of time has been studied by Zetler[52]. He finds the prospects to be promising.

ii. Earth Dynamics

The laser tracking regions of Figures 38 and 41 also would have other uses in connection with the Earth Dynamics side of the Earth and Ocean Dynamic Satellite Applications program[4].

a. Gravimetric Fine Structure

Fine structure in the gravity field should be deducible from observations made in the general area covered in Figure 38, but perhaps somewhat away from the immediate neighborhood of the Gulf Stream meanders.

b. Polar Motions and Earth's Rotational Rate Variations

The leg from Bermuda to the Bay of Fundy area would be suitable for observing polar motion in the manner of the experiment conducted by Smith[64]. The links from Goddard to such a pair of sites taken together would also be useful for a companion experiment to observe the variations of the earth's rotational rate. Similar remarks apply to other sets of lines in Figure 38 which are roughly in latitude directions.

The Sierra Leone Basin laser triangle would also be ideal for monitoring variations in the earth's rotation rate since it is astride the equator.

5. Altimeter Data Requirements

a. Gravitational Field Surveys

The altimeter survey conducted at the 6° resolution level would involve, as indicated above, portions of the equivalent of some 4 days of orbit tracks. Roughly speaking, some three days of "sea tracks" will occur, since the altimeter will be over land about a quarter of the time. Again, from the standpoint of 6 degree coverage, redundant information will be obtained near the maximum latitudes. As before, however, continuous coverage will be useful, at least to begin with. Accordingly, about 75 hours of altimeter observing would be required for the 6° survey, and some 450 hours for the one degree survey.

Such a set of observing programs would provide the basic data for gravimetric geodesy studies leading to the shape of the geoid, for example.

b. Tidal Analyses

These data will also be of real value in connection with a variety of oceanographic investigations including global tidal studies.

Additional types of observational data sets which would be useful for tidal studies can be considered in terms of the earlier discussion associated with Figures 41 and 42 say, and the thinking about the GEOS-C orbit.

As pointed out there, the moon moves some 10.5 degrees per day relative to the GEOS-C orbit of the type contemplated, and hence a cycle of the semi-diurnal lunar tidal component could be observed in about 17 days.

The durations of the northbound and southbound tracks of interest here would each be in the 10-minute range. Hence, about twenty minutes a day of observing, or a total of some six hours in all would give data for a tidal study of this type. Repetitions of this type of study in different regions such as the Pacific and Indian Oceans and at different times would be valuable. In other situations, as many as five passes per day might prove to be useful. In such cases a total of about fifteen hours would be required for a study. Some half dozen such tidal experiments would involve approximately a hundred hours of altimeter observing time. Much of this might be in addition to the 75 or so hours for the 6° geoid survey. It would be included in the 450 hours or so needed for the 1° geodetic altimeter survey.

c. Gulf Stream Studies

The altimeter observation tracks described above in connection with the regional tidal study in the Western Atlantic would also serve as the basis for a study of the Gulf Stream meanders.

From the standpoint of the geoid study, the 6° and 1° resolution observations could be obtained anytime, in the sense that the gravity field is invariant over

the lifetime, and to within the accuracy, of the GEOS-C experiment. Studies of tides and the Gulf Stream meanders require observations made in specific sequences as indicated in the above discussion. Hence, these should be given first priority in the scheduling except, of course, for observations of short-lived phenomena such as those associated with tsunamis and storm surges. Observations designed to fill in the remaining regions required to complete the gravity surveys could then be scheduled so as to utilize the next increment of spacecraft capability.

d. Calibration

The altimeter calibration, which would precede studies discussed above, could also be conducted in the laser tracking region of Figure 38 in areas away from the meanders, near the coasts where ground truth is available. The calibration passes might in time be combined with the program to observe tides and meanders. Calibration and validation may thus involve only a small utilization of the GEOS-C resources relative to that which is envisioned for the scientific investigations, per se.

Satellite-to-satellite tracking may also be useful when combined with precision laser tracking in the laser tracking region of Figure 38 in making observations in the neighborhood of the amphidromic point in the North Atlantic seen in Figures 30 and 31. Such a region could also be a good one in which to make the cross over point checks which have been proposed by Stanley[61].

IV. A SET OF SATELLITE-TO-SATELLITE TRACKING STUDIES

A. Introduction

It is presently planned to conduct satellite-to-satellite tracking experiments with GEOS-C and ATS-F and with NIMBUS-E and ATS-F. Thought is also being given to the possibility of equipping Atmosphere Explorer and Small Astronomy Satellite (SAS-C) spacecraft with the capability for conducting satellite-to-satellite tracking operations with ATS-F. Such capabilities would be of value from the standpoint of the gravimetric geodesy studies, and, in the case of the Atmosphere Explorer spacecraft, for example, for operational reasons as well as is indicated in references 65 through 67. The present discussion will consider in more detail the aspects having to do with the gravitational field studies. These possibilities are only in the thinking stage at the moment and in fact, it appears as this material goes to press that, for practical reasons, it may not be feasible to equip the AE-C spacecraft with satellite-to-satellite tracking capability. The discussion of these cases involving AE and SAS spacecraft is included here, though, for the purpose of illustrating the possibilities inherent in orbits such as these.

It is presently estimated that the ATS-GEOS and ATS-NIMBUS tracking systems will have accuracies of about 7 meters in range and 0.07 centimeters per second in range rate for a ten second integration interval. It will be assumed for the purposes of this discussion that the links between AE and ATS and SAS-C

and ATS would have similar characteristics. The AE and SAS-C systems may turn out to be slightly less accurate, perhaps by a factor of two, than the NIMBUS and GEOS systems for tracking through ATS. For this discussion however, it is convenient to assume that all these tracking systems will be similar, since this facilitates the understanding and comparison of the potential contributions of the different missions.

Estimated orbital parameters of the low altitude satellites involved are given in Table XX. The values shown for the altitudes of Atmosphere Explorers when they are in their nearly-circular, low-altitude orbits are used for planning purposes. Decisions will probably be made during each flight mission concerning the different height ranges which will actually be surveyed from the circular orbits in the 700 to 250 kilometer altitude range toward the end of the spacecraft's active lifetime. Nevertheless certain kinds of observations can be made about an ensemble of orbits of the types seen in Table XX.

First, the array of different inclinations should be of real value. For example, range rate data will be taken over a given feature by satellites traversing at different angles in the orbits having different inclinations. It is anticipated that observable effects will frequently occur in two such distinct orbital paths when they pass over a given geographical region. Evidence of this type will be helpful in sorting out real physical effects from others which may be associated in some way with the measurement and analytical processes. This point is discussed in reference 68, and in reference 44 in connection with Figure 20. It is

Table XX

Orbit Parameters Planned or Considered for Spacecraft Proposed for Satellite-to-Satellite Tracking Experiments

Spacecraft	Altitude (kilometers)	Inclination (degrees)
NIMBUS-E	1110, circular	100
GEOS-C	1000, circular	115
SAS-C	550, circular	3
AE-C	700, circular	65
	600, circular	65
	500, circular	65
	400, circular	65
	300, circular	65
	250, circular	65
	150, elliptical*	65
	120, elliptical*	65
AE-D	700, circular	100
	600, circular	100
	500, circular	100
	400, circular	100
	300, circular	100
	250, circular	100
	150, elliptical*	100
	120, elliptical*	100
AE-E	700, circular	20
	600, circular	20
	500, circular	20
	400, circular	20
	300, circular	20
	250, circular	20
	150, elliptical*	20
	120, elliptical*	20

*Perigee altitude,
Apogee altitude ~4000 km

seen that a variety of inclinations will be available ranging from within 3° of the equator to within 10° of the pole.

When satellites pass over regions having the same ground track but at different altitudes, it may be possible to learn more about the anomalous regions. For example, information may be obtained about the horizontal extent and/or the depth of the features involved. This point is discussed further in reference 44 in connection with Figure 20.

One case is of special interest here. NIMBUS-E and the second Atmosphere Explorer, AE-D, will both have the 100° inclination, but will orbit at widely different altitudes.

The spatial resolutions obtainable with these spacecraft in the sense of the discussion of Section III, A, 1, associated with Figure 21 are indicated in Table XXI. Also shown there are the values for the resolution nodal longitude interval, λ, i.e., the spacing between equator crossings which corresponds to the spatial resolution, r, and the inclination, i, in the manner indicated in Section III, A, 2, i.e., $\lambda = r \csc i$. For a satellite orbit at a 40° inclination, but otherwise having the same characteristics as those indicated for the GEOS-C call in the Table, the resolution nodal longitude interval would be about 8.9° for example.

Gravitational fields which have been derived recently on the basis of a combination of satellite data and gravimetry have spatial resolutions of 11° or

Table XXI

Orbit and Gravimetric Geodesy Experiment Parameters for Spacecraft Proposed for Satellite-to-Satellite Tracking

Spacecraft	Altitude (kilometers)	Inclination (degrees)	Spatial Resolution (degrees)	Resolution Nodal Longitude Interval (degrees)
NIMBUS-E	1110	100	6.2	6.3
GEOS-C	1000	115	5.7	6.3
SAS-C	550	3	4.0	90.0
AE-C	700	65	4.5	5.0
	600	65	4.0	4.5
	500	65	3.5	4.0
	400	65	3.0	3.4
	300	65	2.5	2.7
	250	65	2.0	2.4
	150*	65	1.5	1.6
	120*	65	1.2	1.4
AE-D	700	100	4.5	4.6
	600	100	4.0	4.2
	500	100	3.5	3.6
	400	100	3.0	3.1
	300	100	2.5	2.6
	250	100	2.0	2.2
	150*	100	1.5	1.5
	120*	100	1.2	1.3
AE-E	700	20	4.5	13.2
	600	20	4.0	12.0
	500	20	3.5	10.2
	400	20	3.0	9.0
	300	20	2.5	7.3
	250	20	2.0	6.3
	150*	20	1.5	4.3
	120*	20	1.2	3.6

*Perigee Altitude

so, or about 1200 kilometers near the equator. The geoids associated with them are considered to be reliable to about three meters. It is estimated that the information content of these fields which corresponds to spatial resolutions finer than about 18°, or about 2000 kilometers near the equator, is derived largely from the surface gravity data. (Cf. reference 18.)

It is seen from Table XXI that the satellite-to-satellite tracking experiments which are contemplated offer the prospect of improving the spatial resolution by factors in the range from about half to one order of magnitude.

The geoids associated with fields such as 1 through 5 in Table I have been estimated to have accuracies on the order of 15 meters[69].

The SAO 69 (II) solution in Table I, when truncated as 8, 8 does not represent an improvement over its predecessor, the SAO M-1 field. Except for resonant terms, the improvement due to the added satellite data in the latest solution is thus probably to be found chiefly in the terms of the 9th and 10th degrees, some of which are poorly determined[18]. The geoid associated with the general portion of that solution, as it reflects satellite data, is estimated to be somewhat better than fifteen meters but perhaps not greatly so.

Comparisons of this field with results obtained using recent gravimetric data indicate that geoid uncertainties of five to seven meters are to be expected

when the gravimetric data are moderately dense and accurate.[70] This field as it reflects satellite data per se, is probably still less accurate.

It is estimated, thus, that the contribution of the satellite data to this field corresponds to a geoid accuracy on the order of ten meters, say, which in turn corresponds to some two and a half milligals. Accuracies comparable to this should be obtainable from 700 kilometer altitude orbits with the ATS satellite-to-satellite tracking system using 45-second integration times to achieve accuracies of the order of 0.15 to 0.2 millimeters per second. (Cf. Figure 22 and Reference 45.) A one-minute integration time would give a tracking capability on the order of 0.1 millimeters per second which corresponds to an acceleration resolution capability of the order of 1.5 milligals in terms of sensing mean anomalies in squares about 5° on a side for a satellite at an altitude of 700 kilometers.[45] In a sense, the ultimate range rate integration interval would correspond to the time required to pass over or traverse the square. A further improvement in tracking accuracy and the corresponding sensing capability might be achieved in this way. On this basis, the Atmosphere Explorer, in an orbit at about 250 kilometers altitude, would have an acceleration resolution capability of the order of a milligal. This may be somewhat optimistic, hence it will be assumed, more conservatively, that the acceleration resolution capability of the Atmosphere Explorer in a 250 kilometer orbit will be on the order of a couple of milligals. The acceleration resolution capability of GEOS-C and NIMBUS-E is estimated to be on the order of four milligals, and the acceleration resolution

of SAS-C is estimated to be on the order of three milligals. In making these various estimates, it was assumed in accordance with Schwarz's finding that the sensitivities vary roughly as the reciprocal of the altitude in this general range.[45, 71]

The estimates of the acceleration resolutions to be derivable from satellite-to-satellite tracking appear to be comparable with the estimates of the accuracies we have now from satellites, however, the differences between these two kinds of estimates may be no more than their uncertainties.

Certain additional features of interest which are associated with these different contemplated experiments are indicated in the following discussion.

B. NIMBUS-E

The NIMBUS-E/ATS-F experiment is expected to be the first of the satellite-to-satellite tracking experiments. As was indicated in the above discussion, it will provide us with an improvement of nearly a factor of three in spatial resolution. It will also, of course, give us our first experience with this new type of data and technique.

The 6.6 bidaily nodal longitude interval which is indicated in Table XXII implies that some 27 orbital arcs of interest will be trackable from ATS-F in a given position. There is both a northbound and a southbound pass associated with each interval hence some 54 arcs will be of interest. The total tracking

interval would thus be approximately 54 hours. ATS will at first be at 94° west longitude and later at 35° east longitude. A second survey centered at the eastern longitude would involve another 54 arcs and another fifty-four hours. Some fifteen hours would involve overlapping coverage which should be useful for correlative and corroborative purposes. In addition, as ATS moves from one location to another, satellite-to-satellite tracking could provide additional data having different geometrical characteristics. In all some three such surveys, centered at about 94° west, 35° east, and 30° west, would be very valuable.

Table XXII

Gravimetric Geodesy Experiment Parameters and Observation Requirements for Certain Spacecraft Proposed for Satellite-to-Satellite Tracking

Spacecraft	Altitude (kilometers)	Resolution Nodal Longitude Interval (degrees)	Daily or Bidaily Nodal Longitude Interval (degrees)	Number of Arcs Per Survey	Number of Hours Per Survey
NIMBUS-E	1110	6.3	6.6*	54	54
GEOS-C	1000	6.3	6.3	57	56
SAS-C	550	90.0	—	4	3

*Bidaily

C. GEOS-C

The GEOS-C satellite orbit is presently envisioned to be somewhat lower than the NIMBUS-E orbit. This will offer a corresponding increase in resolution. Also the GEOS-C orbit will not be subject to perturbations by control jets. In addition, the orbit of GEOS-C will be known much more accurately, independently of the satellite-to-satellite tracking, through the use of the very accurate geodetic tracking systems which it will employ. Hence, it is the ideal satellite on which to really evaluate the satellite-to-satellite tracking system as was pointed out in reference 72 in which this experiment was first proposed. The GEOS-C satellite will, in addition, as was pointed out above, also provide data at another inclination. Observational requirements worked out along the lines indicated in the discussion of the NIMBUS-E case are indicated in Table XXII.

D. SAS-C

The SAS-C spacecraft, orbiting at a relatively low altitude, would afford a still further increase in spatial resolution and a gain of nearly a factor of two in acceleration resolution. SAS-C would also add data at still another inclination. Again, typical observational requirements are listed in Table XXII.

E. The Atmosphere Explorers

The Atmosphere Explorers would provide a marked increase in the capabilities for both spatial resolution and acceleration resolution. They would also, as was pointed above, provide data at different inclinations, and at a number of

heights for each of the inclinations. This would enhance considerably the value of such a gravimetric geodesy investigation.

Gravimetric geodesy investigations which could be performed with Atmosphere Explorer by means of satellite-to-satellite tracking are of two types, those associated with the elliptic orbits and those associated with the circular orbits. Present tentative plans call for an elliptic orbit for AE-C having an inclination of 65°, an apogee height of about 4000 km, and a perigee height which will usually be about 150 km, and which will be lowered to about 120 km periodically. The circular orbits will be at several heights in the range from about 250 to 700 km.

For the elliptic case the orbit having a perigee of about 150 km would be in existence long enough to permit a survey to be made. The altitude of about 150 km corresponds to a spatial resolution of 1.5 degrees in the sense of the discussion of Section III, A, 1, which is associated with Figure 21. The planned orbit is close to one which will have a daily nodal separation of 1.6 degrees. This would be the appropriate spacing for the case in which the perigee is near the equator, which is one of the possibilities now under consideration. If the perigee is far from the equator, the survey could be completed with a correspondingly larger nodal spacing and with a correspondingly smaller number of passes than is indicated here.

A slight increase in the period of the orbit, of the order of a minute, and a corresponding increase in apogee height, of the order of a 100 km, would give a daily nodal spacing of 1.6 degrees. This orbit, then, would permit the making of a survey which would provide the coverage to correspond to the lowest altitude reached by the AE-C spacecraft in such a case. The altitude region between 150 and 1110 km would be of interest. This would permit correlation of results with those obtained from all the satellites to be tracked from ATS, i.e., NIMBUS-E, GEOS-C, and possibly SAS-C. The Atmosphere Explorer will be below 1110 km over a true anomaly range of about 142° , or for about 34 minutes per revolution. Some 100 arcs under ATS when it is at a given location would suffice to complete a survey at the 1.5 degree resolution level. Roughly speaking, one pass every other day during the eight months or so at AE-C is in the elliptical orbit would be sufficient. An additional eighty passes would complete the survey if ATS would move between 94° west and 35° east during this period. Thus a total of some 180 passes, or less than one pass per day on the average, would suffice for the entire longitude history of ATS-F. The corresponding tracking time requirements are about 57 hours for the 100 passes and 105 hours for the 180 passes.

If the perigee is at the equator, each arc which is of interest could be observed from ATS during one continuous interval. If the perigee is at the pole, the arcs of interest would be observed in two equal portions, when the ATS is on either side of the AE-C orbit. When perigee occurs in an intermediate

position the arcs of interest would be observed from ATS in two unequal time intervals occurring when ATS is on either side of the AE orbit. The total observing time would be about the same for all these cases, i.e., about 105 hours.

The dipping down of the perigee to 120 km altitude provides a spatial resolution that is even finer, i.e., about 1.2°. In view of the limited time during which the perigee will be at these low altitudes, however, a complete survey would probably not be practical. Nevertheless the observation of portions of the orbit at this height from ATS at different longitudes would be of great interest.

The circular orbits planned for the AE missions would also be of great value from the gravimetric geodesy standpoint. There is interest in matching the nodal spacing at the equator to the spatial resolution capability associated with the altitude. It is seen from Table XXIII that the desired resolution nodal longitude intervals do not correspond too well with the daily or bidaily nodal longitude intervals associated with the orbits at the nominal altitudes at the 100 kilometer intervals.

The nodal spacing could be matched to the desired spacings more closely by modifying somewhat the periods and altitudes listed in Table XXIII. The orbital altitude parameters in or near the range from 250 to 700 km which are close to those considered for the Atmosphere Explorer C and which would also yield the nodal separations that could form the basis for good gravimetric

geodesy experiments are indicated in Table XXIV. It is seen that only relatively small changes from the nominal orbits would suffice in most cases.

Table XXIII

Gravimetric Geodesy Experiment Parameters for Certain Possible Atmosphere Explorer-C Orbits

Altitude (kilometers)	Resolution Nodal Longitude Interval (degrees)	Daily or Bidaily Nodal Longitude Interval (degrees)
700	5.0	1.2*
600	4.5	6.9
500	4.0	0.8
400	3.4	2.9*
300	2.7	6.9
250	2.4	2.9

*Bidaily

The approximate values shown in Table XXIV are suggested for illustrative purposes. It is anticipated that further study of the matter of orbit selection from the standpoint of the atmospheric research requirements and the gravimetric geodesy criteria could reveal orbit parameters which would meet the atmospheric experimenters needs and at the same time make it possible to conduct valuable gravimetric geodesy experiments.

Table XXIV

Experiment Parameters and Observation Requirements for Certain Possible Atmosphere Explorer-C Orbits Which Would Be Valuable for the Gravimetric Geodesy Investigation

Altitude (kilometers)	Resolution Nodal Longitude Interval (degrees)	Daily or Bidaily Nodal Longitude Interval (degrees)	Number of Arcs per Survey	Number of Hours per Survey	Number of Arcs per 45° Survey	Number of Hours per 45° Survey
725	5.1	5.1*	63	45	35	17
570	4.4	4.4	73	50	41	19
460	3.7	3.7	87	58	49	22
405	3.4	3.4*	94	62	53	23
240	2.3	2.3	139	88	78	33
150-4100	1.6	1.6	100	57		

*Bidaily

It is seen from Table XXIV that on the order of 60 to 140 passes of nearly half an orbit in length would be of interest at the heights shown there. The AE satellite will probably spend only some 10 or 30 days at each of these altitudes, however. Thus, from two to fourteen passes per day would be required, which may be beyond the resources available. In such a case, a more limited survey could be attempted.

A useful survey could be conducted over the region lying within about 45° of the sub-ATS region. This would involve only a much smaller number of arcs, and each one would not be nearly so long as in the case of the complete survey. Hence only a fraction of the observing time would be required for such a limited survey. Such a survey would correspond reasonably well to the type of experiment which was conducted in connection with the discovery of the lunar mascons.

The satellite-to-satellite tracking system of the type which might be used between AE and ATS will have an accuracy of about 0.07 cm per second for a ten second integration interval. This corresponds to an acceleration of about seven milligals. It is planned that the accelerometer to be used in connection with the atmospheric density experiments will operate over two resolution ranges while the experiment is in progress. These extend, respectively, from 5×10^{-4} to 10^{-6} g, and from 10^{-5} to 2×10^{-8} g. It appears, then, that the accelerometer resolution would be adequate for the needs of such a gravimetric geodesy investigation.

Some of the parameters of geodetic interest associated with the spacecraft discussed here are summarized in Table XXV.

V. COMPANION EARTH AND OCEAN PHYSICS STUDIES

Precise laser tracking of the type contemplated in connection with the discussion associated with Figures 38 and 41 has also yielded interesting new

Table XXV

Spacecraft	Inclination (degrees)	Altitude (kilometers)	Approximate Spatial Resolution (degrees)	Order of Acceleration Resolution (milligals)
Existing set of Spacecraft			18.0	2.5
NIMBUS-E	100	1111	6.2	2.0
GEOS-C	115	1000	5.7	2.0
AE-C	65	725	4.6	1.5
SAS-C	3	550	4.0	1.5
AE-C	65	240	2.0	1.0

results which have exciting implications for the emerging Earth and Ocean Physics Applications Program (EOPAP) now in the planning stages at NASA.[4]

A. Polar Motion

The Preliminary Polar Motion Experiment, has, for example, yielded one component of the motion of the pole which agrees with the BIH smoothed curve to within a meter over a five-month period.[73] These results appear in Figure 43. The basic data were obtained by tracking the BE-C spacecraft with an accurate laser located at the Goddard Space Flight Center. The significance of this result lies in the fact that the laser values for the latitude were obtained with six-hour data spans from a single observing station, whereas the BIH curve

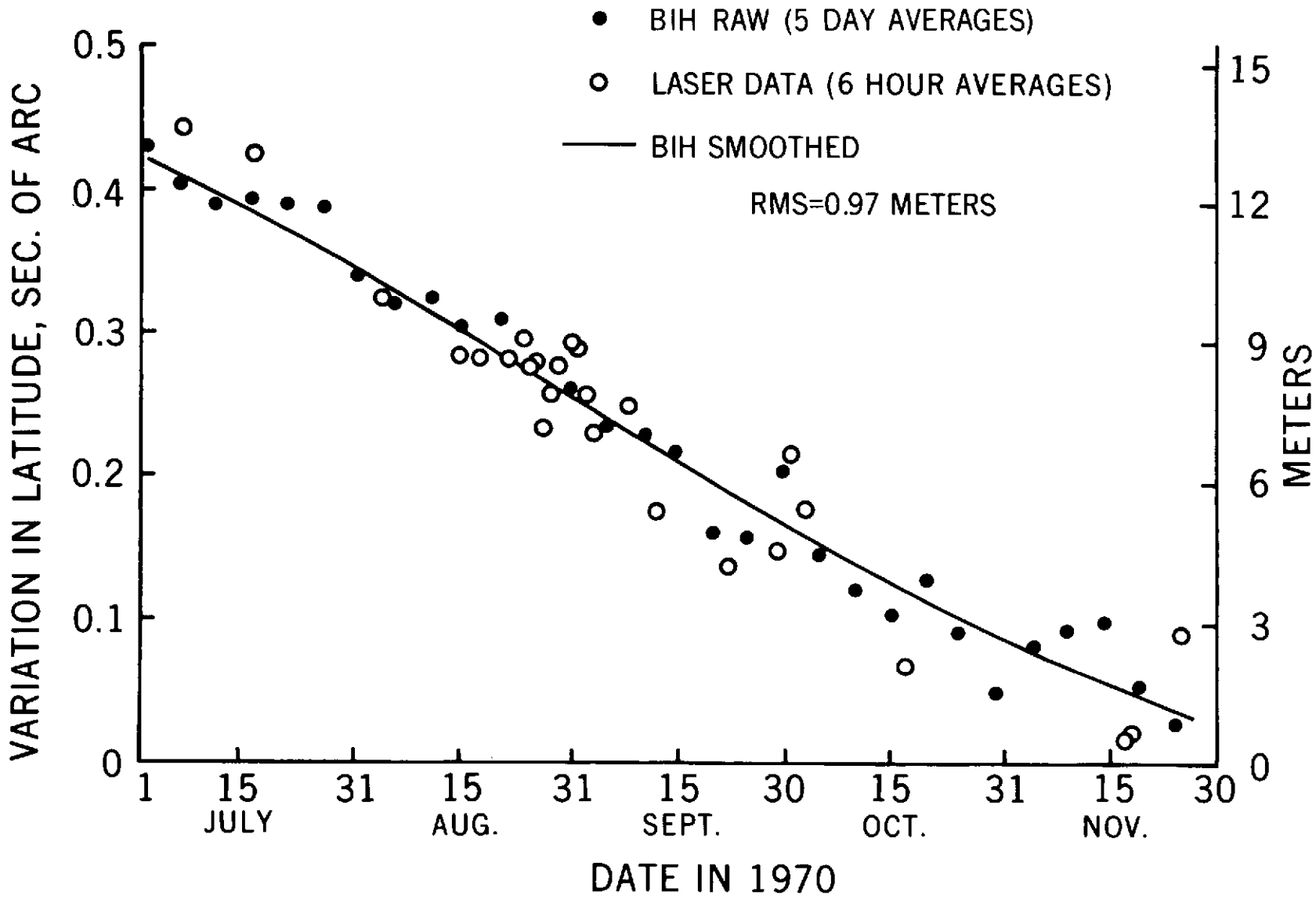

Figure 43. Variation in Latitude of Goddard Laser

is derived from the smoothing of five day averages of data obtained from some 40 stations around the world.

The Preliminary Polar Motion Experiment configuration actually involved a pair of lasers, the one at Goddard and a second one located on the same meridian about 400 kilometers to the north, at Seneca Lake, New York.

B. Baseline Determination

1. A Laser Measurement

The data from these two lasers were used to measure the distance between them. Results of several determinations of this intersite baseline involving data spans ranging from about a week to a couple of months are indicated in Table XXVI. It is seen that a repeatability about 30 centimeters was obtained.

Table XXVI

Godlas-Senlas Chord Distance

Solution		Survey Difference
1	408699.20 m	+ 43 cm
2	408698.87 m	+ 10 cm
3	408699.33 m	+ 56 cm
4	408699.44 m	+ 67 cm
5	408698.91 m	+ 14 cm
Ground Survey	408698.77 m	

The same observational material was used in still another way to determine a value for Love's tidal number, k_2.

2. VLBI Measurements

Very Long Baseline Interferometry (VLBI) has also yielded baseline determination results with accuracies of the order of a meter or two. [74, 75] More recent results indicate that higher precision can be expected in the measurement of baselines by means of VLBI.[75]

C. The San Andreas Fault Experiment (SAFE)

The baseline determination results indicated in Table XXVI were obtained with lasers having a 50 centimeter noise figure. It is planned to utilize better lasers, having accuracies of the order of 5 to 10 centimeters, to study the motion of the tectonic plates at the San Andreas Fault. It is hoped that this San Andreas Fault Experiment (SAFE) will result in the determination of the baseline length with a precision of 10 centimeters.[76]

VI. THE GEOPAUSE SATELLITE SYSTEM CONCEPT

The GEOPAUSE satellite system concept offers promising possibilities for conducting Earth and Ocean Physics Applications investigations of several types at and below the decimeter level. These include a set of earthquake-related studies of fault motions and the earth's tidal, polar and rotational motions, as well as studies of the gravity field and the sea surface topography which should furnish basic information about mass and heat flow in the oceans.

The state of the orbit analysis art is presently at about the 10 meter level, or about two orders of magnitude away from the 10 cm range accuracy capability expected in the next couple of years or so. The realization of a 10 cm orbit analysis capability awaits the solution of four kinds of problems, namely, those involving orbit determination and the lack of sufficient knowledge of tracking system biases, the gravity field, and tracking system biases, the gravity field, and tracking station locations.

The GEOPAUSE satellite system concept provides promising approaches in connection with all of these areas. A typical GEOPAUSE statellite orbit has a 14 hour period, a mean height of about 4.6 earth radii, and is nearly circular, polar, and normal to the ecliptic. At this height only a relatively few gravity terms have uncertainties corresponding to orbital perturbations above the decimeter level. The orbit is, in this sense, at the geopotential boundary, i.e., the geopause. The few remaining environmental quantities which may be significant can be determined by means of orbit analyses and accelerometers. The GEOPAUSE satellite system also provides the tracking geometry and coverage needed for determining the orbit, the tracking system biases and the station locations. (Cf. Figures 44 and 45.) Studies indicate that the GEOPAUSE satellite, tracked with a 2 cm ranging system from nine NASA affiliated sites, can yield decimeter station location accuracies. Five or more fundamental stations well distributed in longitude can view GEOPAUSE over the North Pole as is indicated in Figure 46. This means not only that redundant data are available

~10m ⟶ ~0.1m FOR: EARTH DYNAMICS | FIELDS | OCEAN DYNAMICS

STATE OF ORBIT ANALYSIS ART NOW

RANGE TRACKING PRECISION BY 1973

EARTHQUAKE STUDIES
FAULT MOTIONS
POLAR MOTIONS
ROTATION RATES
SOLID EARTH TIDES

GRAVITY
GEOID
MAGNETIC

OCEAN TOPOGRAPHY
GENERAL CIRCULATION & CURRENTS
MASS & HEAT FLOW
TIDES, TSUNAMIS
STORM SURGES

PROBLEM AREAS

ORBIT DETERMINATION

TRACKER BIASES

ENVIRONMENT

STATION POSITIONS

GRAVITY FIELD

GEOPAUSE APPROACHES

GEOPAUSE ORBIT:

PERIOD~14^h, a~4.6 e.r., NEARLY CIRCULAR, POLAR, NORMAL TO ECLIPTIC

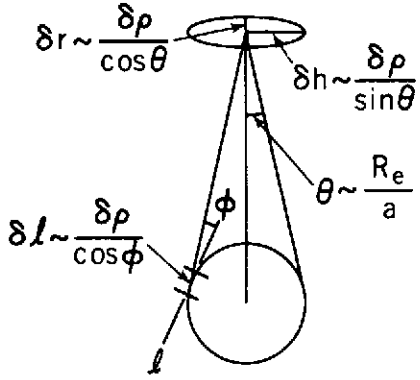

ACCURACIES OF ORBIT RADIUS AND LINE OF SIGHT COORDINATES ARE CLOSE TO RANGE TRACKING ACCURACIES

TRACKER BIASES DETERMINED BY MEANS OF CONTINUAL REDUNDANT DATA

ORBIT	5 cm GRAVITY ERROR TERMS
GEOS	~1000
GEOPAUSE	~6

THUS AT THE GEOPOTENTIAL BOUNDARY i.e., THE GEOPAUSE REMAINING ENVIRONMENT QUANTITIES FROM ORBIT ANALYSIS & ACCELEROMETERS

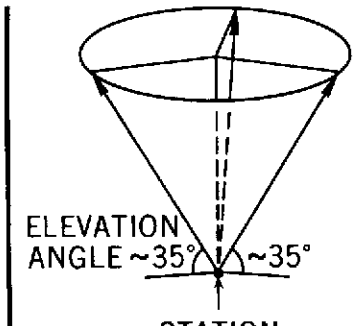

AZIMUTHS 120° APART ORBIT YIELDS ORTHOGONAL GEOMETRY FOR STATION POSITIONING

Figure 44. Earth Physics Program Goals

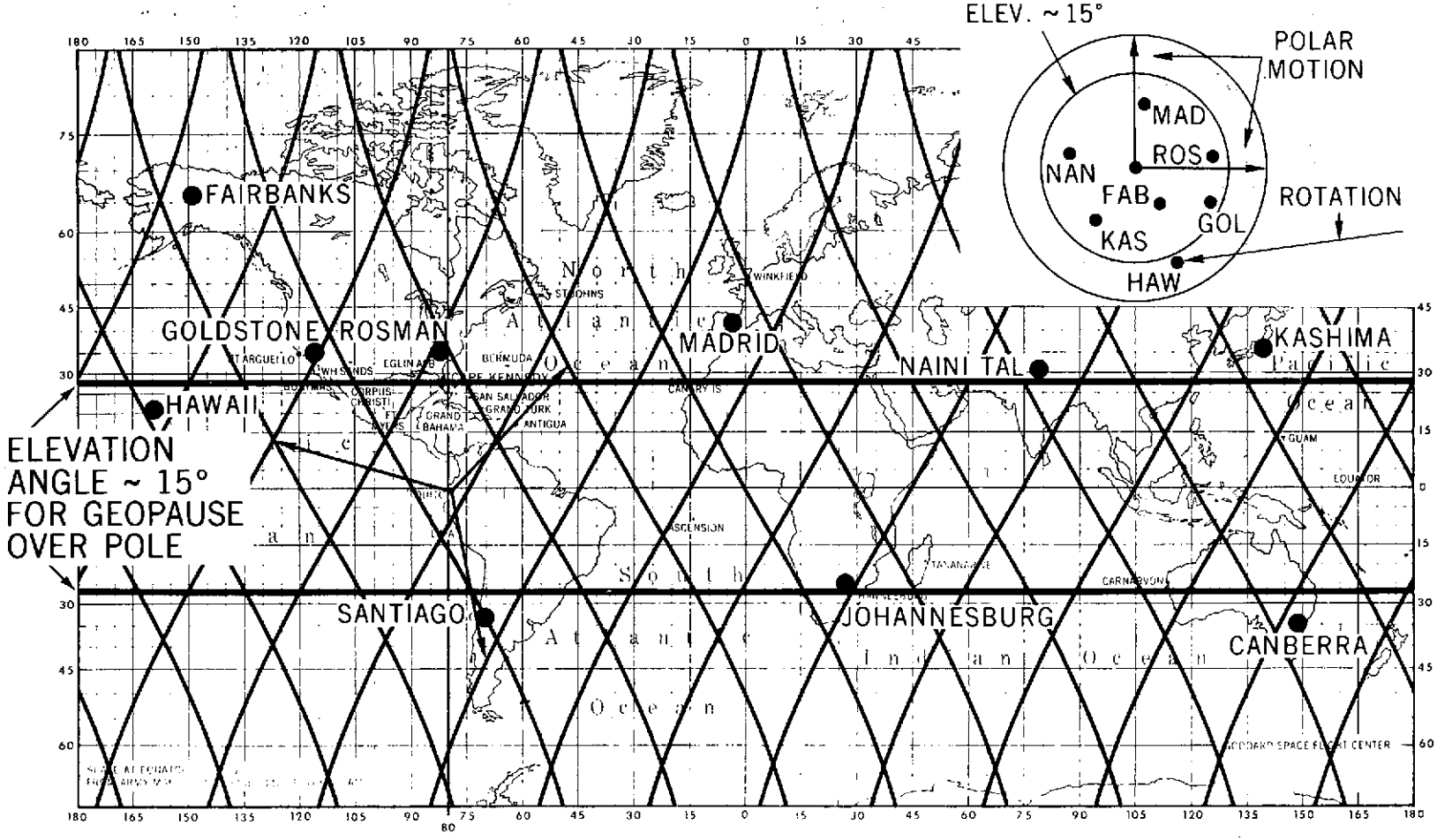

GEOPAUSE SUBSATELLITE TRACKS DURING ONE WEEK

● TYPICAL FUNDAMENTAL STATIONS

GEOPAUSE WITH 2cm RANGE TRACKING DATA YIELDS DECIMETER STATION LOCATIONS AND FAULT MOTIONS

Figure 45. Geopause Orbit Yields the Geometry for Determination of Orbit, Tracker Biases, GM, Station Locations, Fault Motions, Polar Motions, Rotation Rates, Tides

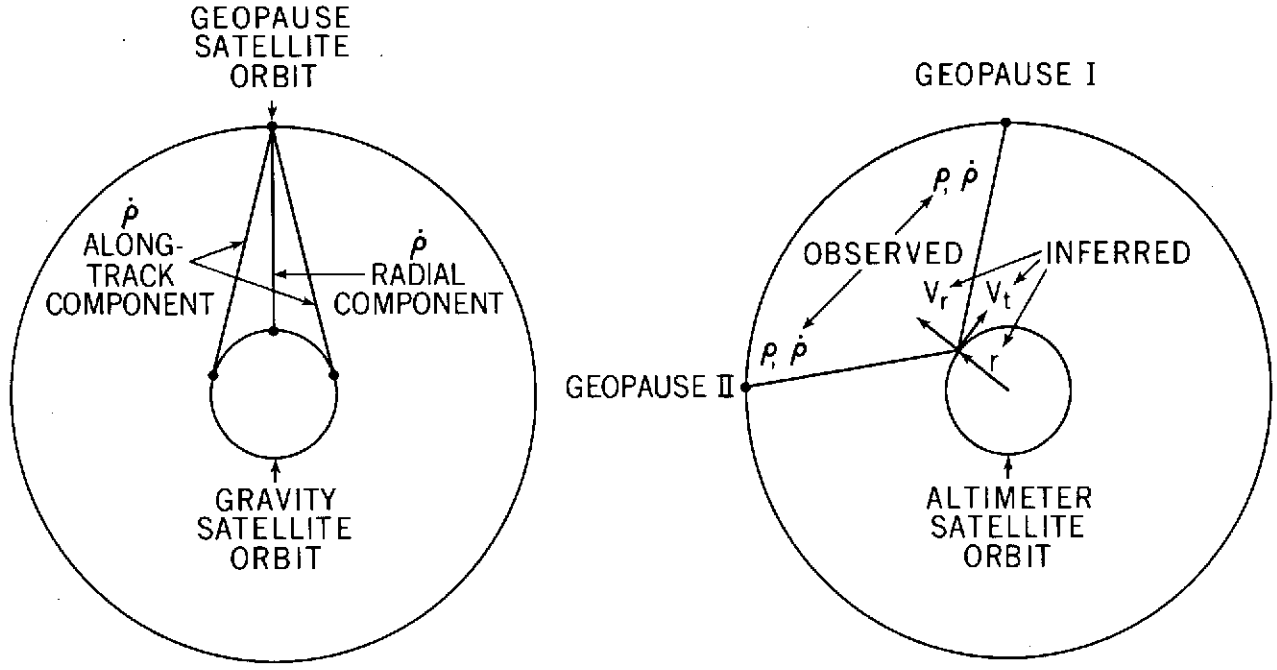

GEOPAUSE TRACKING COPLANAR DRAG-FREE GRAVITY SATELLITE TO 0.03 mm/sec YIELDS DECIMETER GEOID WITH 2.5° RESOLUTION IN 2 MONTHS

2 GEOPAUSE SATELLITES & COPLANAR ALTIMETER SATELLITE YIELD OCEAN SURFACE HEIGHT ABOVE GEOID WITH 7° RESOLUTION IN 2 WEEKS

OCEAN SURFACE

TIDES, TSUNAMIS, STORM SURGES ⟷ CURRENTS, GENERAL CIRCULATION &

GEOID

BOUNDARY CONDITIONS FOR MASS & HEAT FLOW

Figure 46. Geopause for Global Surveys and Reference Coordinate Systems

for determining tracking system biases, but also that both components of the polar motion can be observed frequently. When tracking GEOPAUSE, the NASA Goddard network sites become a two-hemisphere configuration which is ideal for a number of earth physics applications such as the observation of the polar motion with a time resolution of a fraction of a day.

GEOPAUSE also provides the basic capability for satellite-to-satellite tracking of drag-free satellites for mapping the gravity field and altimeter satellites for surveying the sea surface topography. Geometries are indicated in Figure 46. It has been estimated that satellite-to-satellite tracking at the 0.03 mm per second level can yield 10 cm accuracy in the determination of the geoid.[3] GEOPAUSE tracking a coplanar, drag-free satellite for two months to 0.03 mm per second accuracy should yield the geoid over the entire earth to decimeter accuracy with 2.5° spatial resolution. Two GEOPAUSE satellites tracking a coplanar altimeter satellite can then yield ocean surface heights above the geoid with 7° spatial resolution every two weeks. These data will furnish basic boundary condition information about mass and heat flows in the oceans which are important in shaping weather and climate.

The GEOPAUSE satellite system thus offers the promise of making key contributions to the study of the major areas of earth and ocean dynamics.

ACKNOWLEDGMENTS

It is a pleasure to acknowledge many helpful discussions with a number of individuals at Goddard and other institutions including many in connection with satellite geodesy whose works are cited in the references and a number in connection with oceanographic studies including Drs. W. S. Von Arx, C. Bowen, and K. Hasselmann of the Woods Hole Oceanographic Institution, Dr. K. Bryan of the NOAA Laboratory, Princeton, Drs. J. R. Apel, B. D. Zetler, and D. V. Hansen of the NOAA Atlantic Oceanographic and Meteorological Laboratories, Drs. W. H. Munk and M. C. Hendershott of the Scripps Institution of Oceanography, La Jolla, California, Dr. W. J. Pierson, Jr. of the New York University, Dr. W. Sturges of the University of Rhode Island, Dr. M. Talwani of the Lamont-Doherty Geological Observatory, and Dr. B. Yaplee of the Naval Research Laboratory.

REFERENCES

1. GEOS-A Mission Plan, National Geodetic Satellite Program Office, NASA, September 16, 1965.

2. Project Plan For the Geodetic Earth Orbiting Satellite (GEOS-C), Review Draft, NASA Wallops Station, September, 1971.

3. NASA, "The Terrestrial Environment: Solid Earth and Ocean Physics" Prepared by MIT for NASA, ERC, April, 1970.

4. "Earth and Ocean Dynamics Satellite Applications Program," NASA, Washington, D. C., April 1, 1971 (Preliminary Issue).

5. Anderle, R. G., "Observations of Resonance Effects on Satellite Orbits Arising from the Thirteenth and Fourteenth-order Tesseral Gravitational Coefficients," Journal of Geophysical Research, Volume 70, No. 10, May, 1965.

6. Guier, W. H., and Newton, R. R., "The Earth's Gravitational Field as Deduced from the Doppler Tracking of Five Satellites" Journal of Geophysical Research, Volume 70, No. 18, September 1965.

7. Lundquist, C. A., and Veis, G., "Geodetic Parameters for a 1966 Smithsonian Institution Standard Earth," Smithsonian Astrophysical Observatory Special Report No. 200, 1966.

8. Kaula, W. M., Journal of Geophysical Research, Volume 71, No. 22, pages 5303-5314, 1966.

9. Rapp, R. H., "The Geopotential to (14,14) from a Combination of Satellite and Gravimetric Data," presented at the XIV General Assembly International Union of Geodesy and Geophysics, International Association of Geodesy, Lucerne, Switzerland, October 1967.

10. Köhnlein, W., "The Earth's Gravitational Field as Derived from a Combination of Satellite Data with Gravity Anomalies," Smithsonian Astrophysical Observatory Special Report No. 264, pages 57-72, December 1967.

11. Kaula, W. M., Publication No. 656, Institute of Geophysics and Planetary Physics, University of California, Los Angles, December 1967.

12. Rapp, R. H., "A Global 5° x 5° Anomaly Field," Presented at the 49th Annual American Geophysical Union Meeting, April 1968.

13. Gaposchkin, E. M., "Improved Values for the Tesseral Harmonics of the Geopotential and Station Coordinates," presented at the XII COSPAR Meeting, Prague, May 1969, Smithsonian Astrophysical Observatory.

14. Gaposchkin, E. M., Private Communication, U.S. Gov't. Memorandum, July 22, 1969.

15. Gaposchkin, E. M., Private Communication, U.S. Gov't. Memorandum, October 7, 1969.

16. Gaposchkin, E. M. and Lambeck, K., "New Geodetic Parameters for a Standard Earth," presented at the Fall Meeting of the American Geophysical Union, San Francisco, California, December 1969.

17. Murphy, James P. and Marsh, J. G., "Derivation and Tests of the Goddard Combined Geopotential Field (GSFC 1.70-C," Goddard Space Flight Center Report No. X-552-70-104, January 1970.

18. Gaposchkin, E. M. and Lambeck, K., "1969 Smithsonian Standard Earth (II)," SAO Special Report 315, May 18, 1970.

19. Wagner, C. A., "Resonant Gravity Harmonics from 3-1/2 Years of Tracking Data on Three 24-Hour Satellites," Goddard Space Flight Center Report No. X-643-67-535, November 1967.

20. Gaposchkin, E. M. and Veis, G., "Comparisons of Observing Systems and the Results Obtained from Them," presented at the COSPAR meeting, London, July 1967.

21. Murphy, J. and Victor, E. L., "A Determination of the Second and Fourth Order Sectorial Harmonics in the Geopotential From the Motion of 12-Hr. Satellites," Planetary and Space Science Vol. 16, pp. 195-204, 1968.

22. Yionoulis, S. M., "Improved Coefficients of the Thirteenth-Order Harmonics of the Geopotential Derived from Satellite Doppler Data at Three Different Orbital Inclinations," Johns Hopkins/Applied Physics Laboratory Report TG-1003, May 1968.

23. Wagner, C. A., "Determination of Low-Order Resonant Gravity Harmonics from the Drift of Two Russian 12-Hour Satellites," Journal of Geophysical Research, Vol. 73, No. 14, July 1968.

24. Murphy, J. P. and Cole, I. J., "Gravity Harmonics from a Resonant Two-Hour Satellite," GSFC X-552-68-493, December 1968.

25. Wagner, C. A., "Combined Solution for Low Degree Longitude Harmonics of Gravity from 12- and 24-Hour Satellites," Journal of Geophysical Research, Vol. 73, No. 24, December 1968.

26. Douglas, B. C. and Marsh, J. G., "GEOS-II and 13th Order Terms of the Geopotential," Celestial Mechanics 1 (1970) 479-490, August 1969.

27. Wagner, C. A. and Fisher, E. R., "Geopotential Coefficient Recovery from Very Long Arcs of Resonant Orbits," GSFC X-552-69-498, November 1969.

28. Siry, Joseph W., "Geodetic and Orbital Research at the NASA Goddard Space Flight Center," presented at the Conference on Scientific Research Using Observations of Artificial Satellites of the Earth, Bucharest, June 1970.

29. Siry, Joseph W., "Astronomic and Geodynamic Parameters," Goddard Space Flight Center Report No. X-550-70-481, November 1970.

30. Lerch, Francis J., Wagner, Carl A., Smith, David E., Sandson, Mark L., Brownd, Joseph E. and Richardson, James A., "Gravitational Field Models for the Earth," presented at COSPAR, Working Group 1, Madrid, May 1972.

31. Velez, C. E. and Brodsky, G. P., "Geostar I, A Geopotential and Station Position Recovery System," GSFC Report No. X-553-69-544, November 1969.

32. Kozai, Y., "Revised Zonal Harmonics in the Geopotential," Smithsonian Astrophysical Observatory Special Report No. 295, Cambridge, Mass., February 1969.

33. Cazenave, A., Forestier, F. Nourel, and Pieplu, J. L., "Improvement of Zonal Harmonics Using Observations of Low Inclination Satellites, DIAL, SAS, and PEOLE," presented at: American Geophysical Union Annual Meeting, Washington, D. C., April 1971.

34. Wagner, Carl A., "Earth Zonal Harmonics from Rapid Numerical Analysis of Long Satellite Arcs," GSFC Report No. X-553-72-341, August 1972.

34A. Wagner, C. A., "Low Degree Resonant Geopotential Coefficients from Eight 24-Hour Satellites," GSFC Report No. X-552-70-402, October 1970.

35. Murphy, J. P. and Felsentreger, T. L., "Analysis of Lunar and Solar Effects on the Motion of Close Earth Satellites," NASA TN D-3559, August 1966.

36. Brouwer, D., "Solution of the Problem of Artificial Satellite Theory Without Drag," A. J., 64, 378-397, 1959.

37. Siry, J. W., Murphy, J. P. and Cole, I. J., "The Goddard General Orbit Determination System" Goddard Space Flight Center Report No. X-550-68-218, May 1968.

38. Lerch, F. J., Marsh, J. G., D'Aria, M. D. and Brooks, R. L., "GEOS-I Tracking Station Positions on the SAO Standard Earth (C-5), "NASA TN D-5034, June 1969.

39. Berbert, J. H., Loveless, F. and Lynn, J. J., "GEOS Station Position Solution Comparisons," Trans. Am. Geophys. Un. 50, 602, 1969.

40. Marsh, J. G., Douglas, B. C. and Klosko, S. M., "A Unified Set of Tracking Station Coordinates from Geodetic Satellite Results," Goddard Space Flight Center Report No. X-552-70-479, November 1970.

41. Marsh, J. G., Douglas, B. C. and Klosko, S. M., "A Unified Set of Tracking Station Coordinates Derived From Geodetic Satellite Tracking Data," GSFC Report No. X-553-71-370, July 1971.

42. Vincent, Samir, Strange, William E. and Marsh, James G., "A Detailed Gravimetric Geoid from North America to Eurasia," GSFC Report No. X-553-72-94, March 1972.

43. Felsentreger, T. L., Murphy, J. P., Ryan, J. W. and Salter, L. M., "Lunar Gravity Fields Determined from Apollo 8 Tracking Data, NASA TMX 63666, July 1969.

44. Murphy, J. P. and Siry, J. W., "Lunar Mascon Evidence from Apollo Orbits," Planetary and Space Science, Vol. 18, pp. 1137 to 1141, 1970.

45. Schwarz, Charles R., "Gravity Field Refinement by Satellite to Satellite Doppler Tracking," Department of Geodetic Science Report No. 147, Ohio State University Research Foundation, December 1970.

46. Siry, Joseph W., "Satellite Altitude Determination Uncertainties," presented at the NOAA, NASA, NAVY Sea Surface Topography Conference, Key Biscayne, Florida, October 6, 1971.

47. Von Arx, W. S. (1966) Level-Surface profiles across the Puerto Rico Trench, SCIENCE, 154 (3757), 1651-1654.

48. Talwani, M., "The Ocean Geoid," presented at the NOAA, NASA, NAVY Sea Surface Topography Conference, Key Biscayne, Florida, October 6, 1971.

49. Uotila, U. A., Rapp, R. H. and Karki, P. A., "The Collection, Evaluation and Reduction of Gravity Data," Report No. 78, Department of Geodetic Science, The Ohio State University Research Foundation, Columbus, Ohio, October 1966.

50. Rapp, R. H., "Accuracy of Potential Coefficients Obtained From Present and Future Gravity Data," presented at the Symposium on Geodetic Uses of Artificial Satellites, Washington, D. C., April 1971.

51. Strange, W. E., Vincent, S. F., Berry, R. H. and Marsh, J. G., "A Detailed Gravimetric Geoid For the United States," Goddard Space Flight Center Report No. X-552-71-219, June 1971.

52. Strange, W. E., Private Communication.

53. Hendershott, Myrl, and Munk, Walter, "Tides," Annual Review of Fluid Mechanics, Vol. 2, pp. 205-224, 1970.

54. Zetler, B. and Maul, G. A., "Precision Requirements for a Spacecraft Tide Program," Journal of Geophysical Research, 76, 6601-6605, 1971.

55. Hansen, W., "Die halbtagigen Gezeiten im Nordatlantischen Ozean," Dtsch. Hydr. Z. 2, 44-51 (1949).

56. Hendershott, Myrl, Private Communication.

57. Stommel, Henry, "Summary Charts of the Mean Dynamic Topography and Current Field at the Surface of the Ocean, and Related Functions of the Mean Wind-Stress," Studies on Oceanography, 53-58, 1964.

58. Bryan, K., Private Communication.

See also, "Numerical Models: A Tool for the Prediction of Ocean Climates and Circulation," Transactions of the American Geophysical Union, Vol. 51, No. 4, p. 259, April 1970.

59. Hansen, Donald V., "Gulf Stream Meanders Between Cape Hatteras and the Grand Banks," Deep Sea Research, 17, 495-511, 1970.

60. Pierson, Willard J., Jr. and Mehr, Emanuel, "The Effects of Wind Waves and Swell on the Ranging Accuracy of a Radar Altimeter," New York University Report, January 1970.

61. Stanley, H. Ray, Private Communication.

62. Berbert, John H. and Loveless, Fred M., "A Satellite Altimeter Bias Recovery Simulation," GSFC X-550-71-224, May 1971.

63. Vonbun, F. O., "Satellite-to-Satellite Tracking and Its Contribution to Spacecraft Altimetry," presented at the NOAA, NASA, NAVY Sea Surface Topography Conference, Key Biscayne, Florida, October 6, 1971.

64. Smith, D. E., Kolenkiewicz, R. and Dunn, P. J., "Geodetic Studies by Laser Ranging to Satellites," presented at the Third International Symposium on the Use of Artificial Satellites For Geodesy," Washington, D. C., April 1971.

65. Siry, J. W., "Atmosphere Explorer Design Review," Memorandum, April 3, 1970.

66. Siry, J. W., "An Atmosphere Explorer/ATS Satellite-to-Satellite Tracking, Orbit Determination and Data Transmission Capability" Memorandum to D. W. Grimes, February 24, 1971.

67. Siry, J. W., "Earth and Ocean Dynamics Satellite Applications Program; Satellite-to-Satellite Tracking Between Atmosphere Explorer and ATS, and Between SAS and ATS," Memorandum to Chairman, Earth Physics Working Group, June 2, 1971.

68. Muller, P. M. and Sjogren, W. L., "Mascons: Lunar Mass Concentrations," Science, 161, 680-684 (1968).

69. Kaula, W. M., "The Appropriate Representation of the Gravity Field for Satellite Geodesy," Proceedings of the IV Symposium on Mathematical Geodesy, Trieste, 57-65, 1969.

70. Marsh, J. G., Private Communication.

71. Schwarz, C., Private Communication.

72. Siry, J. W., "Proposed Earth Physics and Geodesy Programs Including an ATS-GEOS Tracking and Orbit Determination Experiment" letter to NASA Headquarters, J. Naugle and J. Rosenberg with enclosure, August 27, 1969.

73. Smith, D. E., Kolenkiewicz, R., Dunn, P., Plotkin, H. and Johnson, T., "Polar Motion from Laser Tracking of Artificial Satellites," Science, Vol. 178, 405, 1972.

74. Hinterreger, H., Shapiro, I., Robertson, D., Knight, C., Ergas, R., Whitney, A., Rogers, A., Moran, J., Clark, T. and Burke, B., "Precision Geodesy via Radio Interferometry," Science, 178, pp. 396-398, 1972.

75. Ramasastry, J., Rosenbaum, B. and Midelini, R., "Precision Baseline Determination Using Very Long Baseline Interferometry (VLBI)," Trans. A.G.U., Vol. 53, 349, 1972.

76. Smith, D. E., Savage, J., Tocher, D. and Scholz, C., "The San Andreas Fault Experiment," Trans. A.G.U., 53, 349, 1972.

77. Holland, W. R., "On the Enhanced Transport in the Gulf Stream," Transactions of the American Geophysical Union, Vol. 53, No. 4, p. 415, 1972.

78. Hendershott, M., "Three Contemporary Notes on Deep Sea Tide Problems," Report of IAPSO, SCOR, UNESCO Working Group No. 27 Meeting on "Tides of the Open Sea," Venice, 18-19, October 1971.

79. Zetler, B., Personal Communication.